

IOW, Seestraße 15, 18119 Rostock

Dr. Thomas Neumann

Senior Scientist

Rostock, 10.09.2022

Andrew Yool
Topical Editor
GMD

Seestraße 15
D-18119 Rostock
phone: +49 381 51 97 130
fax: +49 381 51 97 440
www.io-warnemuende.de
thomas.neumann@io-warnemuende.de

Revision gmd-2022-79

Dear Andrew Yool (GM editor)

Hereby, I submit the revised version of the manuscript gmd-2022-79

Non-Redfield carbon model for the Baltic Sea (ERGOM version 1.2) -- Implementation and Budget estimates

Thomas Neumann, Hagen Radtke, Bronwyn Cahill, Martin Schmidt, and Gregor Rehder

First of all, we would like to thank the two referees and you for the careful consideration of the manuscript and many helpful comments. We followed the referees' suggestions and think that the manuscript has improved considerably. However, we do not agree with referee's #1 decision and attempt to rebut it with a detailed response to his comments and two additional sections.

We included Gregor Rehder in the list of co-authors, who was mentioned in the acknowledgement before, because of his contributions for the revised version.

An appendix with our detailed response to the referees' comments together with a marked-up manuscript is attached at the end of the letter. Thank you for time and effort to consider the submitted manuscript.

A request from the technical evaluation was to ensure that the used color schemes allow readers with color vision deficiencies to correctly interpret figures. We use different line styles and checked the figures with the Color Blindness Simulator.

With best regards, Thomas Neumann

Appendix



First of all, we would like to thank two referees for the thorough reviews of our manuscript. We followed the suggestions and think that the manuscript has improved considerably.

In the following, we respond to the referee's remarks. Remarks are shown in blue and our response in black.

Referee #1

While I believe that the authors evaluated important issues for the modeling carbon cycle in the Baltic Sea, the study suffers from significant technical and model experimental design flaws. In particular, the assumption that cellular C:N:P of healthy phytoplankton is fixed at the Redfield ratio is not supported by either observation or previous modeling studies. Furthermore, almost identical issues in the Baltic Sea (underestimation of model pCO₂) have been previously resolved by the model study (Fransner et al., 2018). It is not clear how the current study is a major improvement over the study by Fransner et al. and other numerous modeling studies (Kuznetsov et al., 2008; Kreuz et al., 2015; Wan et al., 2011) that introduced non-Redfieldian stoichiometry to improve carbon cycle, nitrogen, phosphorus, and oxygen dynamics in the Baltic.

We disagree that the described changes of ERGOM are not a major step forward in the description of the C-cycle of the Baltic Sea. However, we are thankful for the comments, as it clearly shows that we fell short in explaining why the model set up was chosen, and what is different - and progress - in comparison to earlier approaches. In the revised version, we provide an additional section ("Differences to earlier Approaches") which is drafted below:

The study Fransner et al. (2018) is limited to the northern Baltic (Gulf of Bothnia). Therefore, it has not been shown that the model works reasonably for the whole Baltic Sea. The simulation period in Fransner et al. is 21 years which may be sufficient for the Gulf of Bothnia (GoB) but is much too short for the whole Baltic Sea. Radtke et al. (2012) show a residence time for phosphorus of more than 35 years.

Fransner et al. use both, non-Redfield phytoplankton biomass and extracellular release of DOC. They found that for the GoB "A substantial part of the fixed carbon is directly exuded as semilabile extracellular DOC" (26%-52%). In order to keep the model as simple as possible and with it the computational effort as low as possible, we decided to include extracellular release of carbon only. We see this fact as an advantage over Fransner et al., especially for ensemble simulations on climate scales. Unfortunately, the authors do not show any deep water properties like oxygen which may be impacted by the increased downward carbon flux.

For Kuznetsov et al. (2008), a follow up study Kuznetsov et al. (2011), demonstrate that non-Redfield biomass, at least during summer since cyanobacteria only are considered, is by far not sufficient to reproduce observed pCO₂. We use this result also as an argument to focus on extracellular release.

The model used in Kreuz et al. (2015) is applied at a station in the central Baltic Sea. Thus, it is not shown that the model gives reasonable results in a 3D environment. It uses a similar approach as in Fransner et al. with a flexible elemental ratio in phytoplankton and extracellular release of DOM. From our point of

view, it involves the same disadvantage concerning the computational effort and do not proof that cell quotas improve the carbon cycle dynamics.

Wan et al. (2011) changed N/P uptake and mineralization ratios but did not introduce a flexible elemental uptake ratio. This approach implies violation of mass conservation.

We think that the question to what extent the elemental ratio (C/N/P) in healthy phytoplankton cells can deviate from Redfield is not answered yet. There are some studies claiming that the elemental ratio remains close to Redfield which we refer to in the introduction. On the other hand, some studies report strong deviations in POM. However, in most studies no separation of living cells and other particles have been performed (e.g. Nausch et al., 2009). Therefore, we make the alternative proposal to realize a non-Redfield uptake by introducing extracellular release. The advantage is a simpler model with less computational demands.

General Comments:

1. The assumption about fixed C/N/P of phytoplankton cells: the authors assume that “the stoichiometry of healthy phytoplankton cells follow the Redfield ratio.” (line 45). However, this is likely not the case for phytoplankton in the Baltic, especially diazotrophs that thrive over summer following spring bloom (Larsson et al., 2001).

This comment is also related to the above raised concern by the referee #1. We address the rationale for the way we chose our parameterization in an additional section "Rationale for model setup" in the revised version with the below drafted content:

We do not doubt flexibility in phytoplankton stoichiometry. However, from a modeler's point of view, we consider a fixed elemental ratio in phytoplankton as a reasonable simplification with the advantage of less model complexity. We proved this concept by the application for the Baltic Sea. Measurable state variables agree well with the model data. Especially for surface pCO₂, we achieved a considerable improvement. Improvement of the carbon cycle mass balances was the main focus of our model development since it plays a vital role in the energy cascade of the marine ecosystem.

For this reason, we decided to transfer the intracellular deviation from a fixed elemental ratio into dissolved organic matter with a flexible ratio as extracellular release. We justify this assumption by the little effect of intracellular flexibility on the carbon uptake which is a focus of our model development. Furthermore, observations of C/N/P ratios which distinguish between living cells and POM are still missing in the Baltic Sea area. In the following, we review literature supporting our assumptions.

In Kuznetsov et al. (2008 and 2011), we applied the Larsson et al. findings for diazotrophs. However, these elemental ratios do not explain observed pCO₂, although the C/P ratio in diazotrophs increase up to fourfold and an additional, artificial, in spring blooming, diazotrophs species was introduced.

Larsson et al. did their study with filamentous cyanobacteria. Filaments consist not only of vegetative cells but also of akinetes, heterocysts, and vacuoles which in sum not necessarily are composed according the Redfield ratio. Especially, vacuoles develop in a later state of the bloom and may explain

an increasing C:P ratio. These mechanisms are not explicitly formulated in our model and parametrized instead by extracellular release.

Nausch et al. (2009) show that the elemental C:P ratio (up to 400) is elevated especially in cyanobacteria (their Fig. 7) similar to Larsson et al. However, the C:P ratio (100-200) in POM at the same stations is much lower (same Fig.). Taking the high C:P ratio of cyanobacteria into account, the C:P ratio of the remaining POM is close to the Redfield ratio (~100). In their Tab. 2, C:N ratios in POM are given (7-9) which appear close to Redfield. The slight C enrichment in POM cannot explain observed pCO₂ (see also Kuznetsov, 2011).

Kreus et al. (2015) introduce extracellular release and cell quota into their model and run it in 1D environment in the central Baltic Sea. Two experiments have been performed (a) variable quotas, and (b) fixed quotas. POC:PON ratios are virtually the same for both experiments while POC:POP ratios show a different seasonality. However, they conclude that fueling the summer cyanobacteria bloom controlling the carbon cycle and nitrogen dynamics is determined by DOM which is also part of our model. The shortcoming in the DIP cycle in experiment (b) of Kreis et al. has been solved with our approach. In summary, one can conclude that cell quotas do not have an impact on the nitrogen and carbon cycle (their Fig. 5).

2. No rigorous assessment of how the model improved from the Redfield model: The authors do not fully quantitatively assess how incorporating non-Redfield C:N:P improves modeling nutrients and oxygen dynamics.

We do not claim to improve nutrient and oxygen dynamics but the carbon dynamics, clearly shown in Figs. 1 and 14. For nutrients and oxygen, we show that the concentrations almost match with observations at selected stations.

In addition, a poor model fit of Alkalinity to observation by almost 200-300 μM raises concern about whether the carbon cycle model is correctly configured and parameters are tuned.

We can dispel the referee's doubts: Alkalinity is a largely conservative tracer and its concentration is the result of boundary fluxes and mixing of water masses. That is, there is no freedom for model tuning. The underestimated alkalinity concentration is a well-known issue in Baltic Sea models (see discussion and references in our manuscript) and hypotheses to additional alkalinity sources exist but are lacking a proof by observations so far.

Other Comments:

1. L16: It may be more appropriate to call it "non-Redfieldian," not "non-Redfieldish" throughout the text.

We followed the referee's suggestion.

2. L46: What is the justification that phytoplankton are healthy in the study area? Does healthy imply nutrient-replete? If so, please justify.

No. Healthy cells are able to divide (grow) if conditions allow.

3. L47-48: The study by Martiny et al. (2013) clearly demonstrates significant deviation in C:N:P of suspended POM in the nutrient-deplete and nutrient-replete regions.

Variations may be significant in a statistical sense but in our opinion moderate in terms of absolute values. Their Fig. 2 gives for POC:PON = ~5-9, and for POC:POP = ~80-150 neglecting the last 3 month (out of 32). The POC:POP increase at the end of the time series cannot be attributed to a phosphate limitation (their Fig. 1) as a quota model would suggest. Furthermore, the authors note in their discussion section the analyzed POM constitutes not solely of phytoplankton.

4. L56 “Strong observational evidence for evidence for an ER of DOM”: Please provide ER evidence in Baltic.

Evidence is given e.g. in Hoikkala et al. (2015) and references therein, now in the list of references.

5. Figure 3 and L 123-125: What exactly are these relationships between DIN/DIP and C:N:P in terms of equations? How are they derived?

We use eq. 1-4 as stated in L 124. The paragraph has been re-phrased.

6. Figure 4: Where are the heterotrophic bacteria that feed on DOM?

Bacteria are not explicitly simulated but are parameterized by the degradation rates, as many models do. As already discussed above, we follow the principle to keep the model as simple as possible. This is necessary to handle large simulations in a 3D environment. Complexity of a model depends on the research question and if bacteria are in the focus, of course they have to be considered explicitly.

7. Figure 6: Please define what “organic matter” means? Is it DOM + POM or POM only?

It is DOM+POM. See line 189 in the revised version or 180 in the initial version.

8. L187-L188: “We have to note that our model approach does not allow for C:N and C:P ratio below Redfield ratios in the DOM and POM fractions.” What is the justification for this? C:N and C:P in nutrient-rich regions such as the Southern Ocean are below Redfield ratios of 106 and 6.625 (Martiny et al., 2013).

This is a simplification of the nature in our model approach avoiding computationally expensive cell quotas. A justification is *inter alia* the moderate deviations shown in Martiny et al. (2013). The impact on the carbon cycle is negligible as demonstrated in e.g. Kreuz et al. (2015).

9. Figure 13: It would be helpful to plot the Redfield case as a control.

Fig. 1

Referee #2

Specific comments:

1. The introduction needs to be reorganized:

The first paragraph put to the end of the introduction part

This is a request by the editor. We have a first paper on ERGOM 1.2 and were asked to make a note in the very beginning that it is the same model with a focus on a different part of the model.

The paragraph stating from line 45 move to the beginning of the intro, which is followed by the paragraph starting from line 20.

We re-organized the introduction as the referee recommended.

2. Line 47: (Martiny et ., 2016) change to Martiny et ., (2016)

Done.

3. Line 52: 'a variation between adapted.... a global scale' does this mean that different groups has different N:P ratio?

Yes, this is how we understand the study. The four phytoplankton groups have fixed but slightly different elemental ratios. This setup gives best accordance with observed POM ratios due to different composition of the model groups.

4. Line 53, state to stated

We used recommendations in <https://www.languageediting.com/verb-tenses-in-scientific-writing/>.

Done.

5. Line 73-81, 'A prominent...mixing occurs.' This is not model description, consider to move them to the introduction or discussion part.

The referee is right, this is not pure model description. Thus, we integrated the paragraph in the introduction section.

6. Line 82, in situ conditions (Fig.1)

Done.

7. Line 82-84, 'The missing organic carbon concentrations'. This is not model description, consider to move them to the introduction or discussion part.

We like to thank the referee for this hint. Same as for #5.

8. Line 84: 'decided to' deleted, 'extend' to 'extended'

Done.

9. Line 85: 'an' to 'a', 'not limited' change to 'allow extra'

Done.

10. Line 86: 'ultimately by' to 'beyond the part limited by'

Done.

11. Line 101-102, 'When nutrients..... biomass', Does that mean in this case, equation 1 does not take place?

That is true. Instead, eq. 2-4 become "active". However, there is a smooth transition from eq. 1 to eqs. 2-4 controlled by the limitation functions I_N and I_P . See also our comment to #13.

12. Line 103-104, 'if both N produced', how to define both N and P are limiting? Could you give an explicit definition of N limitation/P limitation and N,P limitation since those terms are pretty important throughout the paper.

The referee is right. Our formulation was a bit sloppy. We re-phrased the sentence to: "If both N and P become exhausted, the fraction of produced DOC increases." In addition, we introduced a figure demonstrating the succession of production rates for phytoplankton, DON, DOP, and DOC. See also our comment to #14.

13. Figure 2, for nutrient rich conditions, Does that mean only when $\min(I_N, I_P, I_L) = I_L$ in equation 1, the phytoplankton growth takes place?

Nutrient limitations are formulated as a Michaelis-Menten or Monod kinetic. $I_N = N/(N_h + N)$. Depending on the half saturation constant N_h and the ambient nutrient concentration N , growth rate gradually decreases with decreasing N . According to Liebig's law, we use the minimum of all limitation functions. It gives a value between 0 and unity and is then multiplied with the maximum growth. If I_N becomes lower, then $(1 - I_N)$ in eq. 3 increases and DOP production starts. Back to your question, as long as $\min(I_N, I_P, I_L) > 0$, phytoplankton growth and the minimum value of the limitation functions control the uptake. However, simultaneous respiration and mortality decrease phytoplankton.

14. Figure 3, So the production of DOP/DON/DOC can not happen at the same time? if so, how could that condition with N,P limitation happen (DOC production)? Or how to define N limitation/P limitation and N,P limitation? And DOC change to DOM (DOC)

Production of phytoplankton, DOC, PON, and DON is simultaneous and controlled by the limitation functions. That is, the actual production rate of each OM compartment is variable and depends on nutrient concentrations. If e.g. N decreases DOP production increases (if P is sufficiently available) and phytoplankton growth decreases. We included an additional figure (4) demonstrating the production rates of PY, DON, DOP, and DOC.

15. Line 113: 'a doubling of rates within' to 'doubling of growth rate with'

Done.

16. Line 119: 'we divide the nutrient ...carbon assimilation'. This is quite misleading. If the value is one as shown in Fig.3, which means only equation 1 takes place. We take P: C uptake ratio as example, it is $1 \text{ P} \cdot 106 / \text{C} = 1$. When goes to the extreme cases when there is no Nitrogen in the system and very high P concentrations ($l_p=1, l_n=0$), then equation 3 and 4 take place if I'm correct? If yes, then in equation 3, $d\text{DOP}/dt = r_0 \cdot \text{PY} \cdot \text{IL} \cdot \text{IT}$ (in P unit as shown in Table 1) in equation 4, $d\text{DOC}/dt = r_0 \cdot \text{PY} \cdot \text{IL} \cdot \text{IT}$ (in C unit) then further $d\text{DOP}/dt = d\text{DOC}/dt$. we assume $d\text{DOP}/dt = d\text{DOC}/dt = 1$, which means by producing 1 DOP, 1P and 106 C are assimilated, and by producing 1 DOC, only 1 DOC is assimilated, then the P:C uptake ratio is $1 \text{ P} \cdot 106 / (106 + 1) \Rightarrow$ it is not 0.5. Is my understanding wrong? could you please correct me?

Eqs. 1-4 show relative rates, which are independent on OM stoichiometry. Building biomass (OM), the elemental composition has to be considered. That is, P, N, and C are taken up with different speeds. This is part of the uptake processes in the model as a factor.

Assuming, the model "currency" is phosphorus and 1 mol P is taken up for OM building, then e.g. 16 mol N and 106 mol C are take up as well. In the example you raised, where $d/dt(\text{DOP}) = d/dt(\text{DOC}) = r_0$, DOP will increase by r_0 moles P and $106 \cdot r_0$ moles C per time unit while DOC will increase by $106 \cdot r_0$ mol C. This will give for the uptake ratio: $r_0 \cdot \text{P}(\text{DOP}) / (r_0 \cdot 106 \text{C}(\text{DOP}) + r_0 \cdot 106 \text{C}(\text{DOC})) = 1 \text{ P} / 212 \text{C}$, and normalized by $1 \text{ P} / 106 \text{C}$ yields 0.5. We get the same result from the relative rates. Therefore, we will stick to the relative rates, normalized with the uptake stoichiometry.

17. Line 120: equations '1 to 4' change to '2 to 4'

Done.

18. Figure 3: 'Nutrients (N,P) to carbon uptake ratios', This is also quite misleading. When talking about N (or P) to C uptake ratio, one always tends to think about the comparison with the Redfield numbers. So can you give it a more accurate definition?

We think all information is given in the figure's caption. Nutrient concentrations are normalized with their half saturation constant, that is, a concentration of one gives a limitation of 0.5. The N/C and P/C ratios are normalized by the classical Redfield numbers 16/106 and 1/106, respectively. Thus, a ratio of one refers to the Redfield ratio.

19. Line 125: transparent exopolymer particle (TEP) to TEP

Changed

20. Line 137, any reference?

There is no reference for our model because we introduced it in the presented development step.

21. Figure 4: What's the mean by $f(\text{R}, \text{N}, \text{P})$

We are thankful for the hint. It should be $f(\text{N}, \text{P})$. We modified the figure.

22. Figure 4: arrows: respiration \rightarrow no-Redfield assimilation and O_2 , why? What process is this standing for? I did not get it from the process description in appendix.

Many thanks for discovering this bug. The arrow should end in the nutrient pool and of course oxygen or other electron acceptors are used. However, for clarity of the schematic, we decided not to draw arrows for all oxygen demanding processes. We made a note in the figure's caption.

23. Figure 5: Could you give the colorbar for the bathymetry?

Done.

24. Table 2: Can you illuminate these region divisions in Figure 5?

Done.

25. Line 254-255: 'the closed budget ... should be zero': In Fig.15a, how is the sum of fluxes calculated? is it $\text{sum}(\text{Riverine load} + \text{air} \rightarrow \text{sea flux} + \text{transport from north sea} + \text{burial} + \text{ocean change} + \text{sediment change})$ or $\text{sum}(\text{Riverine load} + \text{air} \rightarrow \text{sea flux} + \text{transport from north sea} + \text{burial})$? If the former, then the term 'sum of fluxes' is rather misleading especially without any explicit expression (change of inventory is not flux). If the later, why it is necessarily zero? Is there any net gain due to anthropogenic influence?

Thanks for the hint. Term "sum of fluxes" is too sloppy. We changed it into sum of boundary fluxes and inventory changes. We did the correction throughout the text.

26. Line 260: 'In the water column... 70s': I can not see an obvious increase of nutrient loads in the 1960s and 1970s (especially compared with 1980s). Instead, the increase of water column carbon inventory is more coincident with the change of transport from North Sea (Fig.15a, see for example the sharp increase in 1963-1965).

Loads are shown in Figs 18 and 19. They show a clear increase between 1960 until 1980. We refer now to the figures showing loads in the discussion of the increased carbon inventory. We think that nutrient loading is the main reason for carbon increase in the Baltic. The increase continues until about 1980 together with the loads and decreases with decreasing loads afterwards. However, it is still on a high level mirroring the eutrophic state.

Another questions, over the time 1963-1975, the total inventory (water+sediment) shows a constant increase, which means there should be a net carbon flux into the system, but why this is not reflected from the sum of fluxes in Fig.15c, which instead shows a constant slight decrease?

Thanks for pointing at this issue. It is because of our (sloppy) use of fluxes which lumps together boundary fluxes and inventory changes. This should be zero in a mass conserving system. We corrected the terms fluxes and inventory changes.

The inventory increase is due to higher carbon fixation initiated by increased nutrient loads. It becomes not obvious in the air-sea fluxes because changes in the inventory are very small compared to the air-sea fluxes.

Could you also re-plot the Fig.15a so that the fluxes are not shielded by the legends?

Done.

27. Line 264-265: 'The increasing sum.... source': I can not understand this sentence even though I agree an internal source. If the sum of fluxes (river and transport) is zero, while there are changes in inventory, it indicates an internal source. But as stated here, the increase of fluxes and inventory change is not necessary an internal source. Please re-write this sentence to give a clear argument about the implication of internal source, for instance, smaller riverine load compared with transport but a long-term constant inventory. Probably an additional plot of the sum of river and transport in Fig.16b, which facilitate the comparison with the yellow line.

We re-phrased the paragraph and modified figure 17.

28. Line 266: ??--> Appendix B4?

Done.

29. Line 270-271: denitrification.... Cyanobacteria (denitrification.... Cyanobacteria)

Done.

30. Figure 6: c) residual of the budget which can be attributed to alkalinity generation: How was this calculated? And is this a cumulated result?

Yes, it is a cumulated result, now noted in the figure. The alkalinity generation is calculated indirectly as the sum of boundary fluxes and inventory changes. In a mass conserving system it should be zero like it is for carbon. This deviation from zero, the residual, we attribute to alkalinity generation. We think this is better explained now by more carefully using the terms fluxes and inventory change.

31. Line 276: boundary fluxes: what do 'boundary fluxes' constitute of? likely redundant here, can it be deleted? the same for nitrogen budget.

We think "boundary fluxes" is the more precise term which is different from "internal fluxes" describing e.g. phosphorus fluxes between model state variables.

32. Figure 17: b) legend of 'Denit Ocean' is wrong (line type)

Corrected.

c) Suggest to make the line type (and legend) of 'Denit Ocean' identical with the other two plots (a and b)

Corrected

33. Line 345: 'reasonable' to 'reasonably'

Corrected.

Technical evaluation

A request from the technical evaluation was to ensure that the used color schemes allow readers with color vision deficiencies to correctly interpret figures. We use different line styles and checked the figures with the Color Blindness Simulator.

Literature:

L. Hoikkala, P. Kortelainen, H. Soinne, H. Kuosa, Dissolved organic matter in the Baltic Sea: Journal of Marine Systems, Volume 142, 2015, Pages 47-61, <https://doi.org/10.1016/j.jmarsys.2014.10.005>.

Kuznetsov, Ivan; Neumann, Thomas; Schneider, Bernd; Yakushev, Evgeny: Processes regulating pCO₂ in the surface waters of the central eastern Gotland Sea: a model study. Oceanologia, Volume 53, Issue 3, 2011, Pages 745-770, <https://doi.org/10.5697/oc.53-3.745>.
(<https://www.sciencedirect.com/science/article/pii/S0078323411500223>)

Markus Kreuz, Markus Schartau, Anja Engel, Monika Nausch, Maren Voss: Variations in the elemental ratio of organic matter in the central Baltic Sea: Part I—Linking primary production to remineralization, Continental Shelf Research, Volume 100, 2015, Pages 25-45, <https://doi.org/10.1016/j.csr.2014.06.015>.

Monika Nauscha, Günther Nausch, Hans Ulrich Lass, Volker Mohrholz, Klaus Nagel, Herbert Siegel, Norbert Wasmund: Phosphorus input by upwelling in the eastern Gotland Basin (Baltic Sea) in summer and its effects on filamentous cyanobacteria. Estuarine, Coastal and Shelf Science 83 (2009) 434–442, <https://doi.org/10.1016/j.ecss.2009.04.031>

Radtke, H., Neumann, T., Voss, M., and Fennel, W. (2012), Modeling pathways of riverine nitrogen and phosphorus in the Baltic Sea, J. Geophys. Res., 117, C09024, doi:10.1029/2012JC008119.

Non-Redfield carbon model for the Baltic Sea (ERGOM version 1.2) – Implementation and Budget estimates

Thomas Neumann¹, Hagen Radtke¹, Bronwyn Cahill¹, Martin Schmidt¹, and Gregor Rehder¹

¹Leibniz Institute for Baltic Sea Research Warnemünde, Seestr. 15, 18119 Rostock, German

Correspondence: Thomas Neumann (thomas.neumann@io-warnemuende.de)

Abstract. Redfield stoichiometry based marine biogeochemical models suffer from underestimating carbon fixation by primary production. Most pronounced indication of this is the overestimation of the dissolved inorganic carbon concentration and, consequently, the partial pressure of carbon dioxide in surface waters. The reduced production of organic carbon will impact most biogeochemical processes.

5 We propose a marine biogeochemical model allowing for a **non-Redfield non-Redfieldian** carbon fixation. The updated model is able to reproduce observed partial pressure of carbon dioxide and other variables of the ecosystem, like nutrients and oxygen, reasonably well. The additional carbon uptake is realized in the model by an extracellular release of dissolved organic matter from phytoplankton. Dissolved organic matter is subject to flocculation and the sinking particles remove carbon from surface waters. This approach is mechanistically different from existing
10 **non-Redfield non-Redfieldian** models, which allow for flexible element ratios for the living cells of the phytoplankton itself. The performance of the model is demonstrated as an example for the Baltic Sea. **We have chosen this approach because of a reduced computational effort, which is beneficial for large scale and long-term model simulations.**

Budget estimates for carbon illustrate that the Baltic Sea acts as a carbon sink. For alkalinity, the Baltic Sea is a source due to internal alkalinity generation by denitrification. Owing to the underestimated model alkalinity, there
15 exists still an unknown alkalinity source or underestimated land based fluxes.

1 Introduction

We introduce the **non-Redfieldish non-Redfieldian** carbon uptake implemented in the biogeochemical model ERGOM 1.2. In a previous publication (Neumann et al., 2021), the optical model of ERGOM 1.2 is described. In this paper, we focus on the **non-Redfieldish non-Redfieldian** carbon uptake in ERGOM 1.2. We decided to split the description of
20 ERGOM 1.2 into two parts because we think both parts could be used separately in other models as well.

Models for the marine carbon cycle often fail if carbon fixation by autotrophs is restricted to the elemental Redfield ratio (Redfield et al., 1963). As an example, the surface CO₂ partial pressure (*sp*CO₂) for the Baltic Sea can hardly be represented correctly (Omstedt et al., 2014). This is especially obvious by an elevated simulated (Omstedt et al., 2009, 2014). A prominent disagreement is the overestimated *sp*CO₂ in Redfield ratio based models (e.g. Kuznetsov et al., 2011). In
25 Fig. 1, we show the *sp*CO₂ compared to observations during summer, climatology in the central Baltic Sea from observations

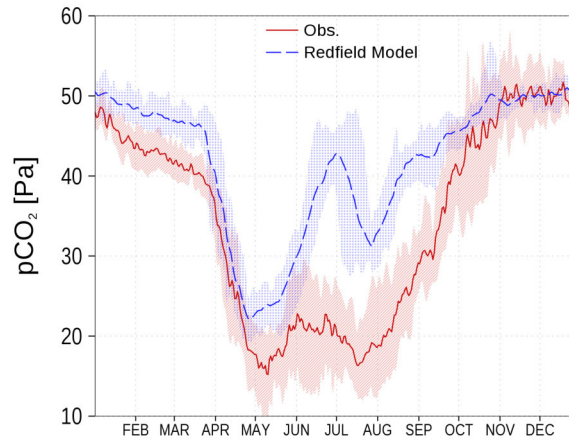


Figure 1. $spCO_2$ in the central Baltic Sea from a previous, Redfield stoichiometry version of ERGOM (blue) and observations (red) as climatology (2003–2016) at station BY15 (Fig.6). Shaded areas show the range between 10th and 90th percentile. Observations are available from SOCAT (see *code and data availability*).

and from a previous, Redfield version of our model ERGOM. There is clear observational evidence that carbon fixation continues after the depletion of nitrate during the spring bloom period, which has been termed post-nitrate production (Schneider and Müller, 2018). As this production cannot be sustained in a strictly Redfield-defined parameterization, the simulated $spCO_2$ strongly deviates from the onset of nitrate-depletion, which in the central Gotland Sea usually starts by mid-April (Fig. 1, see also Schneider and Müller (2018), their Figure 5.13). The $spCO_2$ overestimation vanishes in fall when primary production is limited by depleted nutrients, subsides and deeper mixing occurs. Consequently, the model primary production fixes considerably less carbon compared to *in situ* conditions (Fig. 1). The missing organic carbon impacts all biogeochemical processes of the ecosystem. However, the relatively large freedom in calibration allows one to tune the models to match observed variables like nutrient concentrations.

Fransner et al. (2018) demonstrated the considerable improvement by introducing non-Redfieldish dynamics non-Redfieldian dynamics, which allow for an excess carbon uptake. Established methods for implementing a non-Redfieldish non-Redfieldian carbon fixation in ecosystem models are the cell quota model by Droop (1973) and/or additional carbon uptake due to dissolved organic matter (DOM) production (Fransner et al., 2018).

Several studies prove that the stoichiometry of healthy phytoplankton cells do not considerably deviate from the Redfield ratio. Ho et al. (2003) showed in an experimental setup for marine phytoplankton that the biomass composition is generally close to the Redfield ratio. In situ data of particulate organic matter (POM) by Martiny et al. (2016) display only moderate deviations from Redfield ratio. Considering that POM constitutes not only of phytoplankton, other particles like heterotrophs or detritus may impact the observed ratios. Sharoni and Halevy (2020) showed with the aid of model experiments that variations in POM stoichiometry are best explained by taxonomic composition of phytoplankton

45 compared to phenotypic plasticity. That is, phytoplankton with a minimum flexibility of the nutrient cell quota, but a variation between adapted groups, fits best the observed elemental ratio variations on a global scale. Engel (2002) stated that "the fundamental need for N and P for biomass synthesis does not allow large deviations from Redfield".

DOM in the ocean is one of Earth's major carbon reservoirs (Hansell et al., 2009). Many production, degradation and consumption processes control its dynamics. An excellent review of DOM dynamics is given by Carlson and Hansell (2015). We will summarize some facts from this review which we think are important to guide our model development: Main The main producer of DOM is phytoplankton within the euphotic zone due to extracellular release (ER). Two common models exist to explain mechanisms for ER: (i) The overflow model and (ii) the passive diffusion model. The overflow model assumes an active DOM release by healthy cells. This process is directly coupled to primary production (PP) and regulates the frequently mismatching availability of irradiation and nutrients. The active ER will be used to dissipate energy from the photosynthetic machinery and protect it from damage. In the passive diffusion model, ER is controlled by different concentrations of DOM inside and outside of the cell. The concentration gradient forces an ER across the cell membrane. This process is stronger more strongly coupled to phytoplankton biomass instead of primary production. For both models, experimental evidence exists and it is possible that both are valid and depending on environmental conditions, one or the other process is more active.

60 Although ER is coupled to PP in the overflow model, there is not a constant fraction of produced DOM. In fact, fractionation depends on nutrient availability and phytoplankton composition (Carlson et al., 1998). Phytoplankton ER consists to up to 80% of carbohydrates which are important precursors for the formation of transparent exopolymer particles (TEP). TEP are sticky and aggregate into larger particles which may sink down (Engel et al., 2004) and are methodically often be counted as particulate organic carbon (POC) (Carlson and Hansell, 2015). Therefore, not considering TEP production results in underestimating ER (Wetz and Wheeler, 2007).

Several studies prove that the stoichiometry of healthy phytoplankton cells follow the Redfield ratio. Ho et al. (2003) show in an experimental setup for marine phytoplankton that the biomass composition is generally close to the Redfield ratio. In situ data of particulate organic matter (POM) by (Martiny et al., 2016) show only moderate deviations from Redfield ratio. Considering that POM constitutes not only of phytoplankton, other particles like heterotrophs or detritus may impact the observed ratios. Sharoni and Halevy (2020) show with the aid of model experiments that variations in POM stoichiometry are best explained by taxonomic composition of phytoplankton compared to phenotypic plasticity. That is, phytoplankton with a minimum flexibility of the nutrient cell quota, but a variation between adapted groups, fits best the observed elemental ratio variations on a global scale. Engel (2002) state that "the fundamental need for N and P for biomass synthesis does not allow large deviations from Redfield".

70 Considering the Considering the fact that biogeochemical models for the Baltic Sea with a Redfieldish Redfield carbon fixation are not able to reproduce the observed carbon cycle (see also Fig 1) and a strong observational evidence for an ER of DOM (Hoikkala et al., 2015), we develop a model able to fix carbon beyond the classical Redfield ratio. In this study, we introduce a non-Redfieldish non-Redfieldian carbon uptake by maintaining Redfieldish Redfield composition of living biomass, but allowing ER of highly carbon-enriched DOM in the model ERGOM 1.2 and show selected budgets derived from the model simulations.

2.1 Biogeochemical model

We start with explaining the biogeochemical model ERGOM (Leibniz Institute for Baltic Sea Research, 2015), which describes cycles of the elements nitrogen, phosphorus, carbon, oxygen, and partly sulfur.

Primary production, forced by photosynthetically active radiation (PAR), is provided by three functional phytoplankton groups (large cells, small cells, and cyanobacteria). The chlorophyll concentration used in the optical model is estimated from the phytoplankton groups (Neumann et al., 2021). Dead particles accumulate in the detritus state variable. A bulk zooplankton grazes on phytoplankton and is the highest trophic level considered in the model. Phytoplankton and detritus can sink down in the water column and accumulate in a sediment layer. In the water column and in the sediment, detritus is mineralized into dissolved inorganic nitrogen and phosphorus. Mineralization is controlled by water temperature and oxygen concentration. Oxygen is produced by primary production and consumed due to all other processes, e.g., metabolism and mineralization.

The stoichiometry in all organic carbon components of the model is confined to the classical Redfield ratio (Redfield et al., 1963). The advantage of this approach is the model’s simplicity. However, observations of the carbon cycle in the Baltic Sea reveal the shortcomings of this kind of models (Fransner et al., 2018). A prominent disagreement is the overestimated $spCO_2$ in Redfield ratio based models (e.g. Kuznetsov et al., 2011). $spCO_2$ in the central Baltic Sea from a previous, Redfield stoichiometry version of ERGOM (blue) and observations (red) as climatology (2003–2016) at station BY15 (Fig.6). Shaded areas show the range between 10th and 90th percentile. Observations are available from SOCAT (see *code and data availability*). We show in Fig. 1 the $spCO_2$ climatology in the central Baltic Sea from observations and from a previous, Redfield version of the model ERGOM. There is clear observational evidence that carbon fixation continues after the depletion of nitrate during the spring bloom period, which has been termed post-nitrate production (Schneider and Müller, 2018). As this production cannot be sustained in a strictly Redfield-defined parameterization, the simulated $spCO_2$ strongly deviates from the onset of nitrate-depletion, which in the central Gotland Sea usually starts by mid-April (Fig. 1, see also Schneider and Müller (2018), their Figure 5.13). The $spCO_2$ overestimation vanishes in fall when primary production subsides and deeper mixing occurs. Consequently, the model primary production fixes considerably less carbon compared to *in situ* conditions. The missing organic carbon impacts all biogeochemical processes of the ecosystem. However, the relatively large freedom in calibration allows to tune the models to match observed variables like nutrient concentrations. Based on these findings, model (e.g. Fransner et al., 2018). Based on the findings presented in Sec. 1, specifically the underestimation of carbon fixation, we decided to extend our model by introducing a non-Redfield stoichiometry in a non-Redfieldian stoichiometry into carbon fixation. The aim of this extension is to not limit carbon fixation ultimately allow for carbon fixation beyond the part limited by the availability of nutrients.

Our basic idea is that the element composition in vegetative phytoplankton cells remains at the Redfield ratio and under certain circumstances, extracellular dissolved organic matter (DOM) is produced. This extracellular DOM has a fairly flexible elemental ratio. The produced DOM is subject to flocculation (TEP formation) with a certain rate and eventually sinks down as particulate organic matter (POM). In order to realize the elemental flexibility in DOM, we introduce three different DOM state variables together with the POM counterparts. We call the DOM

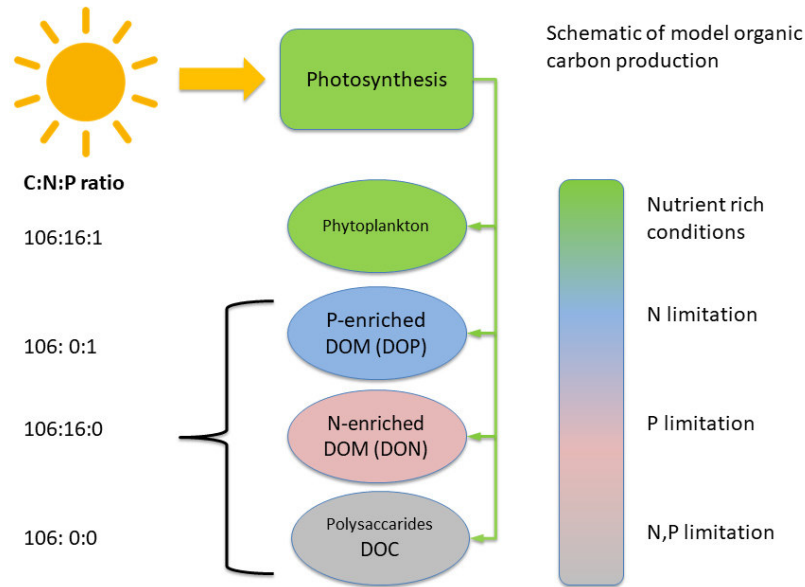


Figure 2. Schematic of DOM production. In case of sufficient nutrients nitrogen (N) and phosphorus (P), phytoplankton biomass is produced. If N becomes exhausted, DOP is produced and by depleted P, DON is produced. If both N and P are depleted, DOC is produced.

state variables dissolved organic carbon (DOC), dissolved organic nitrogen (DON), and dissolved organic phosphorus (DOP). The model considers DOC as polysaccharides (COH_2), and DON and DOP as DOC with additional nitrogen (N) and phosphorus (P), respectively. In DON and DOP the elemental ratio is fixed to the Redfield ratio and they are counted in units of N and P: $\text{DON} - (\text{COH}_2)_{106/16}\text{N}$ and $\text{DOP} - (\text{COH}_2)_{106}\text{P}$. Altogether, model DOM has a flexible elemental ratio with the restriction that the carbon fraction **never is is never** below the Redfield ratio. That is, DOM **usually is is usually** enriched by carbon compared to the Redfield ratio. One could also have used one DOM state variable with a completely free elemental ratio. However, we used the different DOM compartments because we may consider a different fate for DOC, DON, and DOP later.

The production of DOC, DON, and DOP by phytoplankton is controlled by light availability and nutrient concentrations. Under optimal conditions, primary production increases phytoplankton biomass. When nutrients become limiting, DOM **will be produced by photosynthesis instead production increases while the production** of phytoplankton biomass **decreases**. A schematic is shown in Figure 2. In case of N limitation, DOP is produced and under P limitation, DON is produced. If both N and P **are limiting, DOC is produced becoming exhausted, the fraction of produced DOC increases**. We have to note that only phytoplankton is able to produce DOM. That means, if phytoplankton biomass decreases because a net growth is not possible due to e.g. nutrient limitation, the DOM production will decrease as well. In

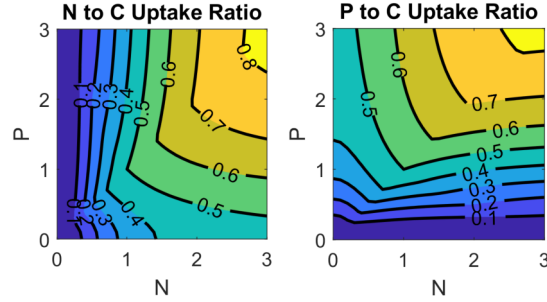


Figure 3. Nutrients (N, P) to carbon uptake ratios in dependence as a function of nutrient concentrations. Nutrient concentrations are normalized by the half saturation constant in the limitation function and the uptake is normalized by the Redfield ratio. A ratio of one means uptake in the classical Redfield ratio and values less than one describe an excess carbon uptake.

particular, the DOM production is controlled by a reversal of the phytoplankton nutrient limitation. The phytoplankton

130 gross growths Gross phytoplankton growth in our model is:

$$\frac{dPY}{dt} = r_0 \cdot PY \cdot \min(l_N, l_P, l_L) \cdot l_T \quad (1)$$

PY is the phytoplankton biomass, r_0 the maximum uptake rate, and l_n are limitation functions ranging between zero and one. Subscripts N , P , and L are for nitrogen, phosphorus, and light. l_T is a (possible) temperature impact on uptake. For nutrient limitation (l_N , l_P), we use a squared Monod kinetic (Monod, 1949; Neumann et al., 2002).

135 Light limitation (l_L) follows Steele (1974) and for temperature control (l_T), a Q10 rule is applied (Eppley, 1972) meaning a doubling of rates within doubling of growth rates with a 10 Kelvin temperature increase. For the temporal development of the DOM compartments we formulate:

$$\frac{dDON}{dt} = r_0 \cdot PY \cdot \min(1 - l_P, l_N, l_L) l_T \quad (2)$$

$$\frac{dDOP}{dt} = r_0 \cdot PY \cdot \min(l_P, 1 - l_N, l_L) l_T \quad (3)$$

140
$$\frac{dDOC}{dt} = r_0 \cdot PY \cdot \min(\max(1 - l_P, 1 - l_N), l_L) l_T \quad (4)$$

The dependence of nutrients uptake in relation to carbon uptake on nutrient concentrations is shown in Fig. 3. For this purpose, we divide the nutrient assimilation for nutrients N and P by the carbon assimilation. The assimilation consists of phytoplankton growth (Redfield ratio) and ER defined in equations 1 to 4 equation 1 and equations 2 to 4, respectively. The nutrient concentrations are normalized by the half saturation constant from the Monod kinetics. A

145 value of one in Fig. 3 denotes a carbon uptake in the Redfield ratio while smaller values is an excess carbon uptake.

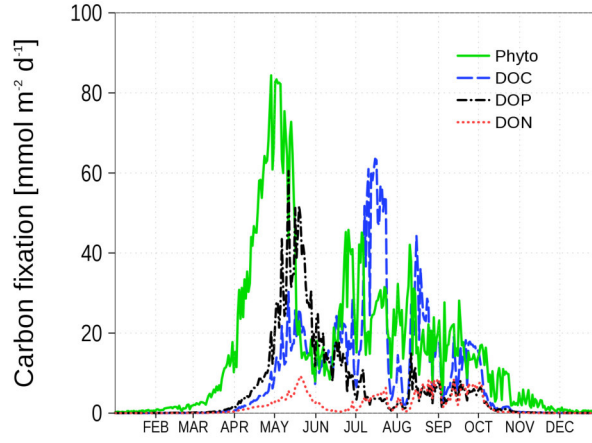


Figure 4. Vertically integrated carbon uptake rates at station BY15 (Fig. 6) in 2015. Shown are production rates for different organic matter compartments phytoplankton, DOC, DOP, and DON.

In case of low N concentrations, the N:C uptake ratio declines to zero. The P:C uptake ratio in this case depends on P concentrations and asymptotically approaches 0.5 for high P concentrations. That is, ER consists of DOC and DOP in equal shares. Figure 4 demonstrates the different carbon uptake rates with a realistic example from our model simulations for station BY15 (Fig. 6) in 2015. In spring, when nutrients are available in high concentrations, phytoplankton biomass production dominates. Later in spring, N becomes exhausted and the fraction of DOP production increases. DOC production dominates in summer when both N and P are at low concentrations. DON production is always at a low level at this stations because the winter concentration of P is in excess to the N concentration with respect to the Redfield ratio. Altogether, carbon fixation is solely mediated by phytoplankton. Depending on the nutrient concentrations, organic carbon production ends up in phytoplankton, DOC, DON, and DOP. The fractionation is controlled by the limitation functions which ensure a smooth transition and co-existence of the different carbon fixation pathways.

Extracellular DOM eventually forms particles (POC, PON, POP) which constitutes transparent exopolymer particles (TEP). Engel (2002) shows a linear relation between dissolved inorganic carbon (DIC) uptake and TEP production implying a direct transfer from DOM to TEP. Therefore, we chose a simple rate equation for DOC flocculation:

$$\frac{dPOC}{dt} = rf \cdot DOC \quad (5)$$

rf is a constant rate for POC formation. The same equation applies for DON and DOP forming their counterparts PON and POP.

Table 1. State variables of the biogeochemical model ERGOM shown in Fig. 5.

Symbol	State Variable	Units <element> [mol kg ⁻¹]
O ₂	dissolved oxygen	dioxygen
N ₂	dissolved nitrogen	dinitrogen
CDOM	colored dissolved organic matter	carbon
DIC	dissolved inorganic carbon	carbon
TA	total alkalinity	molar equivalent
NH ₄	ammonium	nitrogen
NO ₃	nitrate	nitrogen
PO ₄	phosphate	phosphorus
SO ₄	sulfate	sulfur
S	sulfur	sulfur
H ₂ S	hydrogen sulfide	sulfur
large cells	large cell phytoplankton	nitrogen
small cells	small cell phytoplankton	nitrogen
cyanobacteria	cyanobacteria	nitrogen
zooplankton	bulk zooplankton	nitrogen
detritus	detritus	nitrogen
DOC	dissolved organic carbon	carbon
DON	DOC with additional nitrogen	nitrogen
DOP	DOC with additional phosphorus	phosphorus
POC	particulate organic carbon	carbon
PON	POC with additional nitrogen	nitrogen
POP	POC with additional phosphorus	phosphorus
sediment detritus	detritus accumulated in the sediment layer	nitrogen [mol m ⁻²]
Fe(III) – PO ₄	phosphate adsorbed to iron-3 minerals in the sediment	phosphorus [mol m ⁻²]

Sediment state variable units are mol m⁻².

2.2 Rationale for model design

The model design was guided by the main principle keeping the model as simple as possible. This is especially important for model applications in a 3D environment and at long time scales like climate change as well as in ensemble approaches because we want to keep the computational effort at a feasible level. Therefore, we decided to implement ER which allows a flexible nutrients to carbon uptake ratio. A cell quota approach was not implemented since it requires a number of additional state variables.

We do not doubt the flexibility in phytoplankton stoichiometry. However, from a modeler's point of view, we consider a fixed elemental ratio in phytoplankton as a reasonable simplification with the advantage of less model complexity. We proved this concept by the application for the Baltic Sea. Measurable state variables agree well with the model data. Especially for $spCO_2$, we achieved a considerable improvement. Improvement of the carbon cycle mass balances was the main focus of our model development since it plays a vital role in the energy cascade of the marine ecosystem.

For this reason, we decided to transfer the intracellular deviation from a fixed elemental ratio into dissolved organic matter with a flexible ratio as extracellular release. We justify this assumption by the little effect of intracellular flexibility on the carbon uptake (see also Sec. 2.3) which is a focus of our model development. Furthermore, observations of C/N/P ratios which distinguish between living cells and POM are still missing in the Baltic Sea area. In the following, we review literature supporting our assumptions.

In Kuznetsov et al. (2011, 2008), we applied the Larsson et al. (2001) findings for diazotrophs. However, these elemental ratios do not explain observed $spCO_2$, although the C/P ratio in diazotrophs increase up to fourfold and an additional, artificial, in spring blooming, species of diazotrophs was introduced. Larsson et al. (2001) did their study with filamentous cyanobacteria. Filaments consist not only of vegetative cells but also of akinetes, heterocysts, and vacuoles which in sum not necessarily are composed according the Redfield ratio. Especially, vacuoles develop in a later state of the bloom and may explain an increasing C/P ratio. These mechanisms are not explicitly formulated in our model and parameterized instead by extracellular release.

Nausch et al. (2009) showed that the elemental C/P ratio (up to 400) is elevated especially in cyanobacteria (their Fig. 7) similar to Larsson et al. (2001). However, the C/P ratio (100-200) in POM at the same stations is much lower (same Fig.). Taking the high C/P ratio of cyanobacteria into account, the C/P ratio of the remaining POM is close to the Redfield ratio (~ 100). In their Tab. 2, C/N ratios in POM are given (7-9) which appear close to Redfield. The slight C enrichment in POM cannot explain observed $spCO_2$ (Kuznetsov et al., 2011).

Kreus et al. (2015) introduced extracellular release and cell quota into their model and run it in an 1D environment in the central Baltic Sea. Two experiments have been performed (a) variable quotas, and (b) fixed quotas. POC/PON ratios are virtually the same for both experiments while POC/POP ratios show a different seasonality. However, they conclude that fueling the summer cyanobacteria bloom controlling the carbon cycle and nitrogen dynamics is determined by DOM which is also part of our model. The shortcoming in the DIP cycle in experiment (b) of Kreuz et al. (2015) has been solved with our approach. In summary, one can conclude that cell quotas do not have an impact on the nitrogen and carbon cycle (their Fig. 5).

2.3 Differences to earlier approaches

Omstedt et al. (2009) inferred that the carbon dynamics in the Baltic Sea cannot be correctly represented with a strict Redfield based model. Since this time, several carbon cycle models have been proposed for the Baltic Sea. We will review a few of them and highlight the differences to our approach.

Kuznetsov et al. (2008, 2011) used an elevated C/P ratio in cyanobacteria. However, they demonstrated that non-Redfieldian biomass, at least during summer since only cyanobacteria are considered, is by far not sufficient to reproduce observed $spCO_2$. We use this result also as an argument to focus on extracellular release.

Wan et al. (2011) changed the N/P uptake and mineralization ratios but did not introduce a flexible elemental uptake ratio. This approach may violate the mass conservation.

Fransner et al. (2018) introduced both non-Redfieldian phytoplankton biomass and extracellular release of DOC. They found that for the Gulf of Bothnia “A substantial part of the fixed carbon is directly exuded as semilabile extracellular DOC” (26%-52%). Their study is limited to the northern Baltic. Therefore, it has not been shown that the model works reasonably for the whole Baltic Sea. Unfortunately, the authors do not show any deep water properties like oxygen which may be impacted by the increased downward carbon flux.

The model used in Kreuz et al. (2015) was applied at a station in the central Baltic Sea. Thus, it is not shown that the model gives reasonable results in a 3D environment. It uses a similar approach as in Fransner et al. (2018) with a flexible elemental ratio in phytoplankton and ER of DOM. From our point of view, it involves the disadvantage of enhanced computational effort and do not proof that cell quotas improve the carbon cycle dynamics (Sec. 2.2).

2.4 Model setup and simulations

For model testing, we use a coupled system of circulation and biogeochemical model similar to that in Neumann et al. (2021). The circulation model is MOM5.1 (Griffies, 2004) adapted for the Baltic Sea. The horizontal resolution is 3 nautical miles. Vertically, the model is resolved into 152 layers with a layer thickness of 0.5m at the surface and gradually increasing with depth up to 2 m. The circulation model is coupled with a sea ice model Winton (2000) accounting for ice formation and drift. The biogeochemical model ERGOM, described in Sec. 2.1, is coupled with the circulation model via the tracer module which is part of the MOM5.1 code.

The code for the biogeochemical model is generated automatically. Fundamentals are a set of text files describing the biogeochemistry independently of programming language and the host system. Code templates describe physical and numerical aspects and are specific for a certain host, e.g., a circulation model. All necessary ingredients (the code generation tool, text files, and templates for several systems) can be downloaded from Leibniz Institute for Baltic Sea Research (2015). The same technique is used for example in Neumann et al. (2021).

We run the model for about 70 years (1948–2019) after a spin-up of 50 years. The long simulation time allows for assessing us to assess the model performance under different forcing conditions, as for example the eutrophication of the Baltic Sea in the 1970s and the nutrient load reduction beginning in 1990.

2.5 Data

The model has been forced by meteorological data from the coastDat-2 dataset (Geyer and Rockel, 2013). Nutrient loads to the Baltic Sea due to riverine discharge and atmospheric deposition have been compiled based on data from HELCOM assessments (e.g. HELCOM, 2018). Riverine alkalinity follows data provided in Hjalmarsson et al.

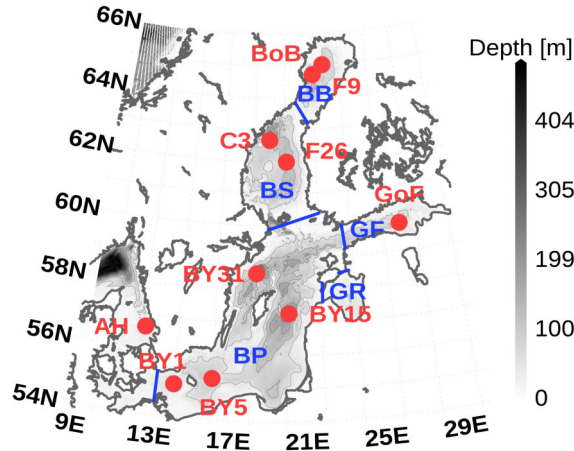


Figure 6. Model domain and bathymetry used for this model study. Red dots denotes stations to which we will refer later in the text. Bathymetry contour lines have a distance of 50 m. Boundaries of regions are in blue with Bay of Bothnia (BB), Bothnian Sea (BS), Gulf of Finland (GF), Gulf Of Riga (GF), and Baltic Proper (BP). The map was created using the software package GrADS 2.1.1.b0 (<http://cola.gmu.edu/grads/>, last access: 14 December 2021), using published bathymetry data (Seifert et al., 2008).

Table 2. Average alkalinity concentration and loads in runoff for different Baltic Sea basins and from different authors. BP: Baltic Proper, GR: Gulf of Riga, GF: Gulf of Finland, BS: Bothnian Sea, BB: Bay of Bothnia (6). HS: Hjalmarsson et al. (2008), GS: Gustafsson et al. (2014b), NM: this study.

Basin	Concentration			Load	
	HS	GS	NM	GS	NM
BP	3244	1910	3156	203	340
GR	3117	3140	3638	92	117
GF	835	689	786	73	89
BS	467	271	240	27	17
BB	136	164	174	19	20
total		904	1165	453	606

Alkalinity concentration in $\mu\text{mol kg}^{-1}$ and loads in Gmol a^{-1} .

(2008). In Tab. 2, we compare riverine alkalinity concentration and loads with published data from Hjalmarsson et al. (2008) and Gustafsson et al. (2014b). The data are relatively similar with the exception of the Baltic Proper. Gustafsson et al. (2014b) use considerably lower values, which impacts the total load. Our mean concentrations differ slightly from Hjalmarsson et al. (2008). We use the basin-wide and constant concentration values given in

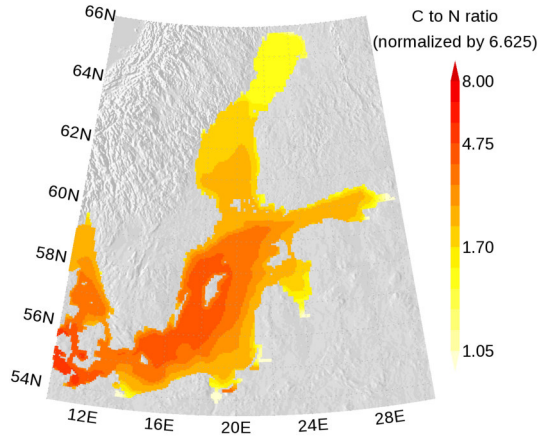


Figure 7. Mean Annual mean elemental carbon to nitrogen ratio in surface organic matter. The ratio is normalized and a ratio of one refers to the classical Redfield ratio. The map was created using the software package GrADS 2.1.1.b0 (<http://cola.gmu.edu/grads/>, last access: 14 December 2021), using published topography data (Seifert et al., 2008).

Hjalmarsson et al. (2008) and assigned the data to our model rivers which show inter annual runoff variability. This results in mean concentration deviations. Loads given in Tab. 2 result from runoff and river specific concentrations.

255 $spCO_2$ for model validation have been extracted from the SOCAT (Surface Ocean CO_2 Atlas) data base (<https://www.socat.info/>). The majority of data are from the voluntary observing ship (VOS) Finnmaid between Lübeck-Travemünde and Helsinki. VOS Finnmaid is a component of the European ICOS (Integrated Carbon Observation System) research infrastructure. Data processing and quality control follow the SOCAT guidelines (Bakker et al., 2016; Pfeil et al., 2013). Additional observation data used for comparison with model results are available from
260 public data bases. Details are given in section *code and data availability*.

3 Results

3.1 How the non-Redfieldish non-Redfieldian approach works

In this section, we demonstrate how a non-Redfieldish non-Redfieldian elemental ratio in organic matter (OM) develops due to the above described model extensions. OM involves all forms of model DOM and POM including model
265 phytoplankton, zooplankton, and detritus. We show data averaged over the whole simulation period and seasonal climatologies. The elemental ratios are based on molar concentrations.

In Figs. 7 and 8, the carbon (C) to nitrogen (N) and carbon to phosphorus (P) ratios in organic matter in surface water are shown. In both figures, the elemental ratios are normalized so that a ratio of one is for the classical Redfield ratio. The figures highlight the different nutrient limitation provinces in the Baltic Sea. The C:N ratio is high in

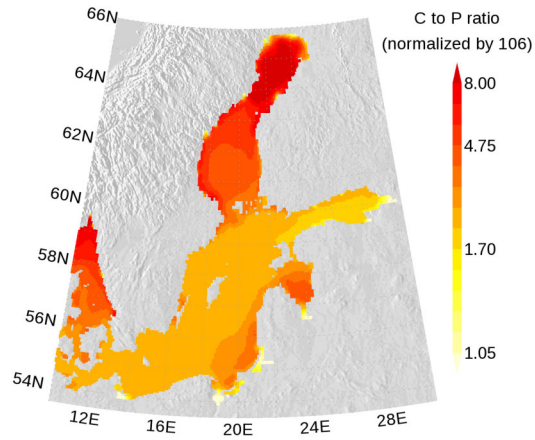


Figure 8. Mean Annual mean elemental carbon to phosphorus ratio in surface organic matter. The ratio is normalized and a ratio of one refers to the classical Redfield ratio. The map was created using the software package GrADS 2.1.1.b0 (<http://cola.gmu.edu/grads/>, last access: 14 December 2021), using published topography data (Seifert et al., 2008).

the central Baltic Sea where N is a limiting nutrient and consequently the C:P ratio is low. The opposite is in the northern Baltic Sea where P is the limiting nutrient. We have to note that our model approach does not allow for C:N and C:P ratio below Redfield ratios in the DOM and POM fractions. Hence, the elemental ratios in OM are always above one. An exception are river mouths where almost no nutrient limitation keeps the C:N and C:P ratios close to one.

We show the N:P ratio in OM and its seasonality in Fig. 9. Again, the figure shows the separation between the nutrient limitation provinces. N limitation is denoted by a low N:P ratio in the central Baltic Sea and a high N:P ratio shows P limitation in the northern Baltic Sea. During the course of the year, the N:P ratio in the central Baltic Sea increases due to nitrogen fixation by cyanobacteria. The temporal development of the DOM fractions can be seen in Fig. 10. In the N-limited Gotland Sea (Fig. 10a), surplus phosphate is transferred into DOP after depleted N starts limiting phytoplankton growth. With intensified nutrient limitation also DON and DOC will be produced by phytoplankton. In summer, with a higher demand of phosphorus by cyanobacteria, the DOP pool is depleted. In contrast, in the northern part of the Baltic Sea, the Bothnian Bay, surplus nitrogen is transferred into DON (Fig. 10b). Almost no DOP develops. In Fig. 11, we show the surface climatology of simulated DOC_{obs} (eq. 7) at station BY15 together with observations. Observed DOC concentrations constitute to a large extent of refractory fractions. In contrast, in the model we only consider the labile, autochthonous part of DOC. Therefore, we subtracted $305 \mu\text{mol kg}^{-1}$ from the observations which is the mean winter concentration. The annual DOC cycle in the observed data appears less pronounced compared to the modeled DOC_{obs} cycle.

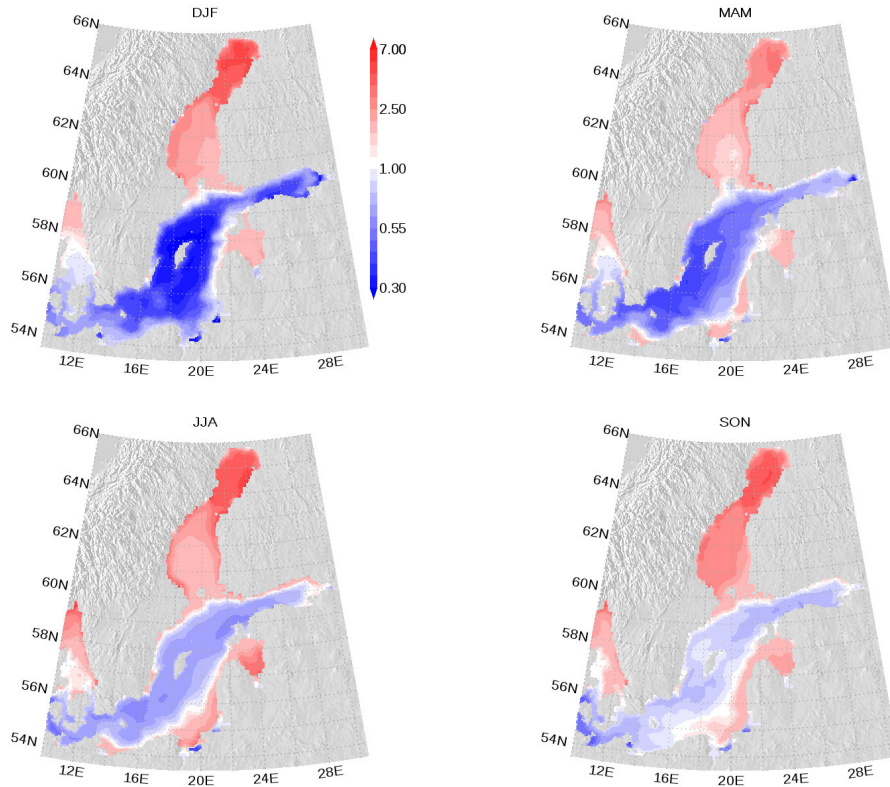


Figure 9. Mean Seasonal mean elemental nitrogen to phosphorus ratio climatology in surface organic matter. The ratio is normalized and a ratio of one refers to the classical Redfield ratio. The map was created using the software package GrADS 2.1.1.b0 (<http://cola.gmu.edu/grads/>, last access: 14 December 2021), using published topography data (Seifert et al., 2008).

3.2 Primary production and extracellular production

We consider primary production (PP) as carbon fixation contributing to phytoplankton biomass while extracellular
 290 production (EP) is the carbon fixation resulting in DOM (DOC, DON, and DOP state variables). Figure 12 shows
 time series and climatology of PP and EP as mean of the whole model domain. The carbon fixation is dominated by
 EP. With increasing nutrient availability beginning in the 1960s, the fraction of PP increases (Fig. 12a). The PP and
 EP climatology in Fig. 12b shows that PP dominates in spring and fall, and EP dominates in summer. Figure 12c
 shows PP of the model phytoplankton groups. Most PP occurs in spring mediated by the large cell phytoplankton
 295 group LPP. In contrast, the most EP is mediated by the small cell phytoplankton group SPP in summer (Fig. 12d).

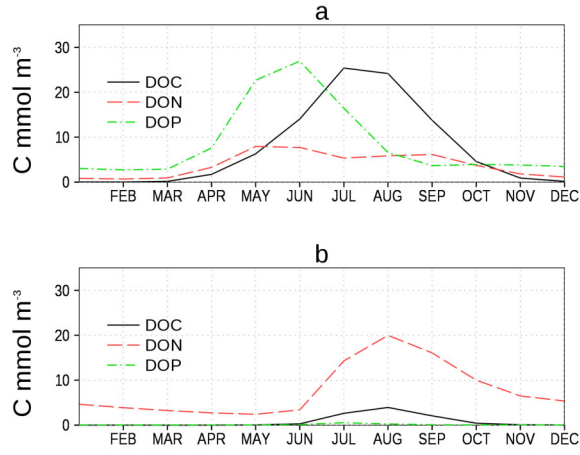


Figure 10. Climatology of surface model DOC, DON, and DOP (in carbon units, Tab. 1 and Eq. 7) at two stations. a) Central station in the Eastern Gotland Sea (BY15), and b) Central Station in the Bothnian Bay (BoB, Fig. 6). Model DON and DOP are converted into carbon units to show all variables in a comparable level.

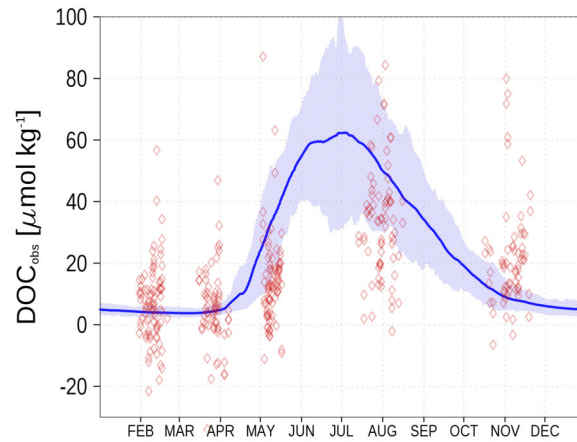


Figure 11. Climatology (1995-2019) of simulated surface DOC_{obs} (eq. 7) at station BY15 (blue line) and observed DOC (red diamonds). The diamond's opacity reflects frequency of observations. The shaded area shows the range between 10th and 90th percentile. From observations, $305 \mu\text{mol kg}^{-1}$ have been subtracted. Observed DOC data are available from IOW ODIN database (see *code and data availability*).

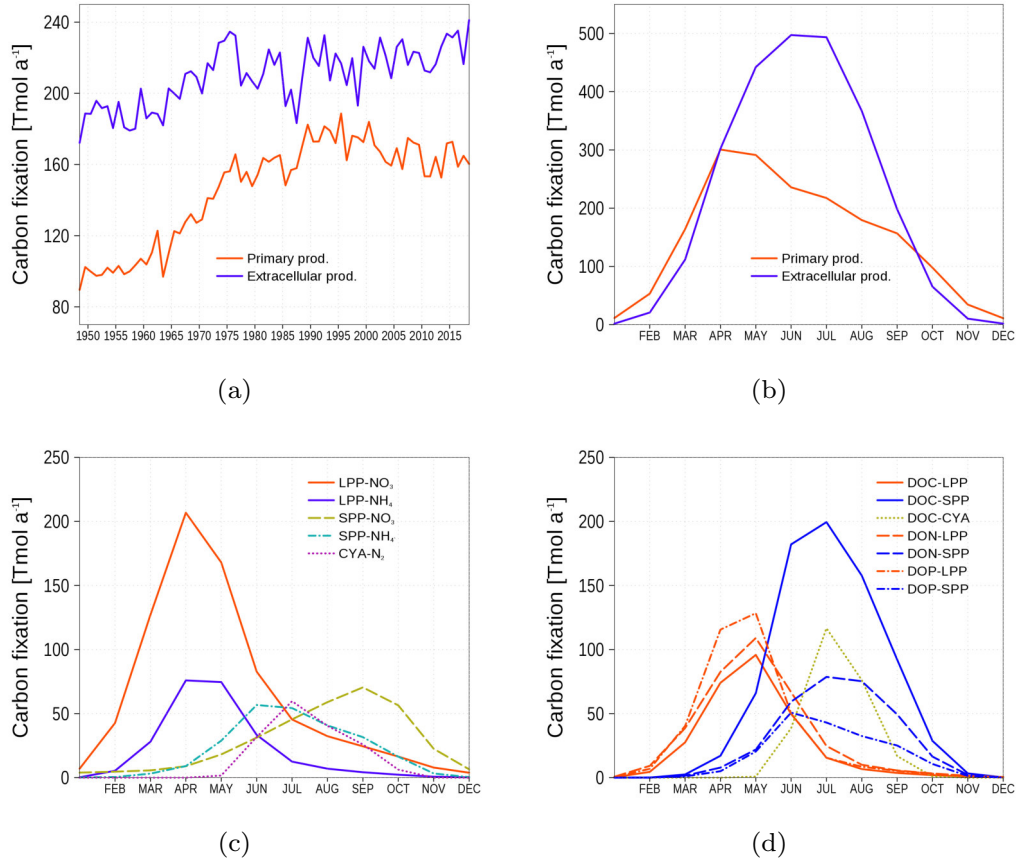


Figure 12. Temporal and spatial mean primary and extracellular carbon fixation by model phytoplankton. a) Time series of annual carbon fixation. b) Climatology of carbon fixation. c) Climatology of primary production related to different uptake processes. LPP- NO_3 and LPP- NH_4 : Carbon fixation by the large cell phytoplankton group related to NO_3 and NH_4 uptake, respectively. SPP- NO_3 and SPP- NH_4 : The same as for LPP but for the small cell phytoplankton group. CYA-N: Carbon fixation by cyanobacteria related to nitrogen fixation. d) Climatology of extracellular production related to different phytoplankton groups: Red lines are uptake by LPP, blue lines by SPP, and green line by cyanobacteria. Different line styles refer DOC, DON, and DOP. All model variables have been converted into carbon units (Eq. 7).

3.3 Assessment of biogeochemical variables

We especially show model data and observations for sea surface carbon dioxide pressure and alkalinity. Other biogeochemical variables are shown in App. A.

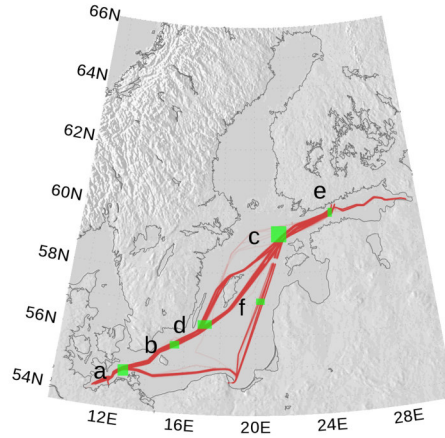


Figure 13. $spCO_2$ observations by VOS Finnmaid between 2003 and 2018 used for model analysis (red line). Opacity refers to frequency of observations. a–f denote regions selected (green rectangles) for comparison with model data. The map was created using the software package GrADS 2.1.1.b0 (<http://cola.gmu.edu/grads/>, last access: 14 December 2021), using published topography data (Seifert et al., 2008).

3.3.1 Sea surface pressure of carbon dioxide ($spCO_2$)

One motivation to introduce a **non-Redfieldish non-Redfieldian** carbon fixation into the ecosystem model ERGOM was the mismatch in observed and simulated $spCO_2$ (Kuznetsov et al., 2011, see also Fig. 1). Redfield models are not able to explain the low observed $spCO_2$ during summer. Temperature increase and ongoing mineralization in the surface layer increase the $spCO_2$ to unrealistic values in the simulations. One conclusion was that still after nutrient limitation, a substantial carbon fixation goes on. Consequently, the carbon fixation is not restricted to the classical Redfield ratio.

For the $spCO_2$ benchmark, we use data taken underway from the voluntary observing ship (VOS) Finnmaid regularly traveling between Lübeck-Travemünde and Helsinki. For more details see section 2.5 and Schneider and Müller (2018). **Pathway** The pathway and $spCO_2$ observations taken by VOS Finnmaid and used in this study are shown in Fig. 13. From the regions denoted by green rectangles, we have selected data to compare with our model simulation. As can be seen from the pathway’s opacity, region f was crossed less frequently than the other regions. The $spCO_2$ climatology is shown in Fig. 14. The **non-Redfieldish non-Redfieldian** carbon fixation keeps the $spCO_2$ low during summer as seen in the observations. In the northern regions c and e, the spring bloom seems to be delayed in the model. However, the general picture is a strongly improved $spCO_2$ in the model compared to earlier model versions (e.g. Kuznetsov et al., 2011), as can be seen by comparing to Fig. 1.

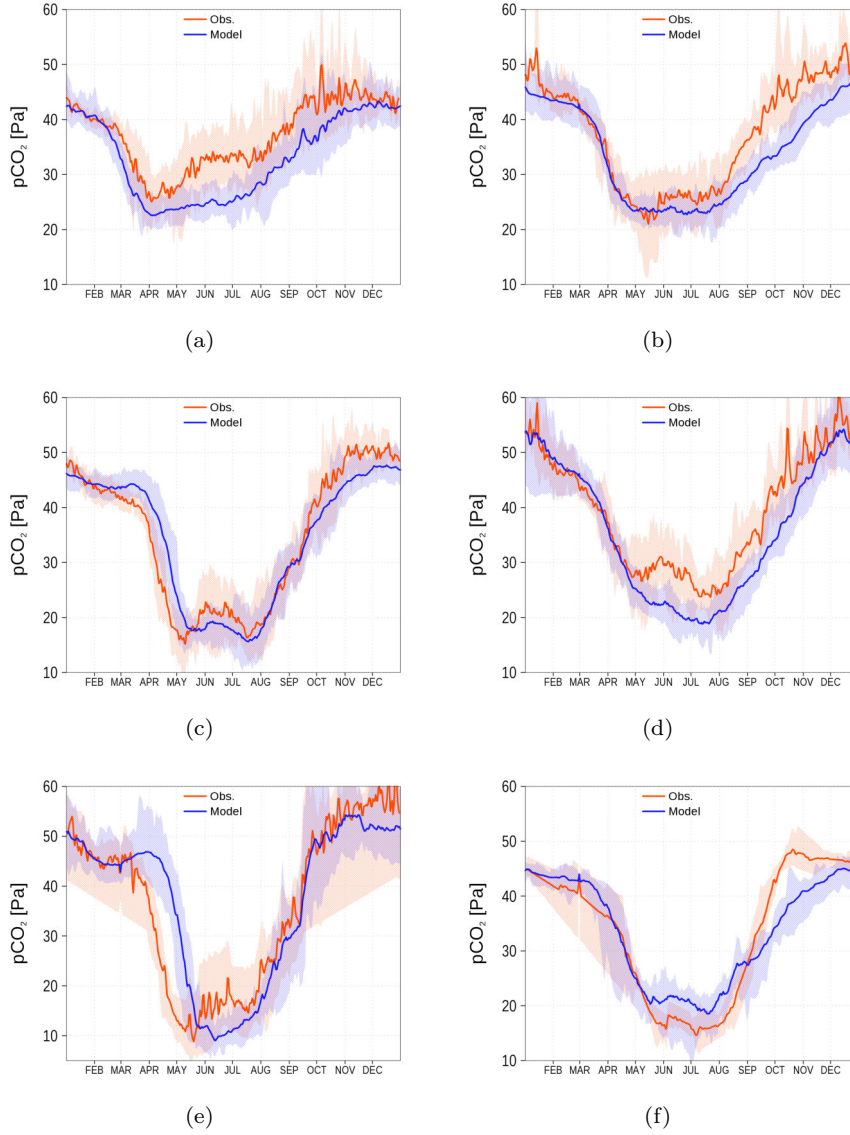


Figure 14. $spCO_2$ climatology (2003-2018) from observations (red) and from model simulation (blue). Shaded areas show the range between 10th and 90th percentile. The sub-figures a–f refer to the corresponding regions shown in Fig. 13 by green rectangles a–f. Observations are available from SOCAT (see *code and data availability*).

315 3.3.2 Alkalinity

Alkalinity in the model is estimated after the equation for τ_{alk} in appendix B4. Figure 15 shows the alkalinity climatology from observations (red diamonds) and from the model simulation (blue). We show the climatology for

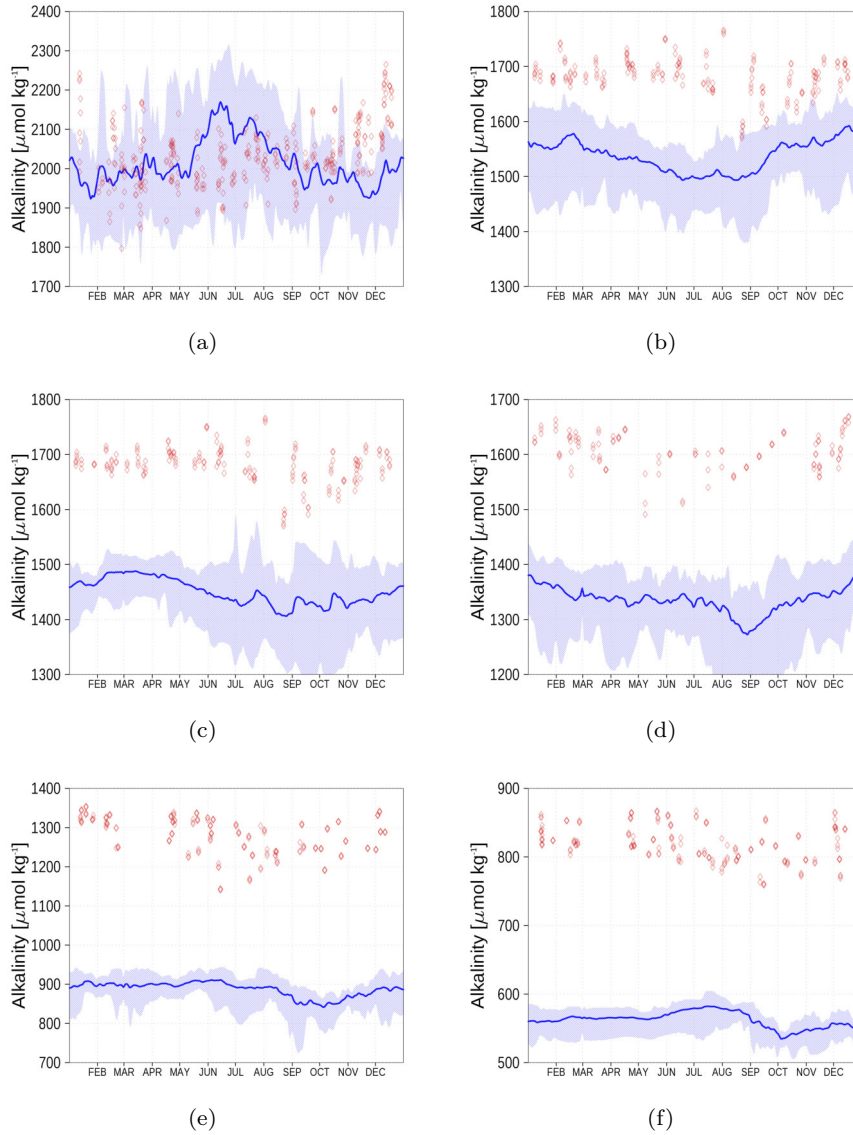


Figure 15. Surface alkalinity climatology (2013-2018) from Observations (red) and from model simulation (blue). Shaded areas show the range between 10th and 90th percentile. The subfigures represent stations AH (a), BY1 (b), BY15 (c), BY31 (d), C3 (e), and F9 (f) (Fig. 6). Observed alkalinity data are available from SHARK database (see *code and data availability*).

six stations from the Kattegat (a) to the Bothnian Bay (f). While in the Kattegat, the simulated alkalinity reflects observations reasonably well, the model's underestimation amounts to roughly 20% in the central Baltic Sea and increases further towards the northern Baltic Sea. This will also have an effect on the total inorganic carbon (DIC)

content. However, once in a quasi equilibrium with the atmosphere, the air-sea fluxes will be affected **marginally only** **only marginally**.

3.3.3 Nutrients

Nutrient surface concentrations are shown in App. A1. We have chosen 6 stations and regions to cover the whole
325 Baltic Sea. Figures A1–A6 show **the** climatology and time series of simulated nitrate and phosphate together with
observations. We find a good model performance for the western Baltic Sea, the central Baltic Sea, and the Gulf of
Finland. In the northern Baltic Sea, the Gulf of Bothnia, the model overestimates slightly the nutrient concentrations.
Nevertheless, the strong phosphate limitation in this region is well covered.

3.3.4 Oxygen

330 Oxygen concentrations of the near bottom water are shown in App. A2. Especially in the northern Baltic Sea,
simulated concentrations are lower compared to observations.

3.4 Budgets

In this section, we show selected budgets as estimated from the model simulation and demonstrate that the model
closes the budget.

345 3.4.1 Carbon budget

The carbon budget is shown in Fig. 16. The budget considers the inventory change of all carbon containing state
variables in the water column and in the sediment. Changes are the result of the boundary fluxes riverine load, air-sea
fluxes, transport from and to the North Sea, and burial of carbon in the sediment. The closed budget, which we show
with the yellow line, should be zero, a deviation reflects cumulated numerical inaccuracies that are obviously small
340 compared to the simulated signals. In Fig. 16a, annual fluxes and inventory changes are shown. Highest fluxes are the
carbon export towards the North Sea and riverine carbon loads followed by air-sea flux and burial. Figures 16b and c
show cumulated fluxes and inventory changes. Inventory changes are very small compared to the boundary fluxes.
Therefore, we show in Fig. 16c the inventory changes separately. The sediment inventory stays relatively constant.
In the water column, carbon inventory increases in response to higher nutrient loads in the 1960s and 70s .
345 **(loads shown in Figs. 18 and 19).**

3.4.2 Alkalinity budget

The alkalinity budget is shown in Fig. 17. The budget considers the inventory change of the alkalinity state variable
in the water column. Changes are the result of the boundary fluxes riverine load, and transport from and to the
North Sea. In contrast to the carbon budget, the alkalinity budget is not closed (yellow line **and Fig. 17c**). The
350 increasing sum of **fluxes, including the boundary fluxes and** inventory change, **which should cancel out each other in a**
closed budget, suggests an internal alkalinity source. According to the implemented processes affecting alkalinity

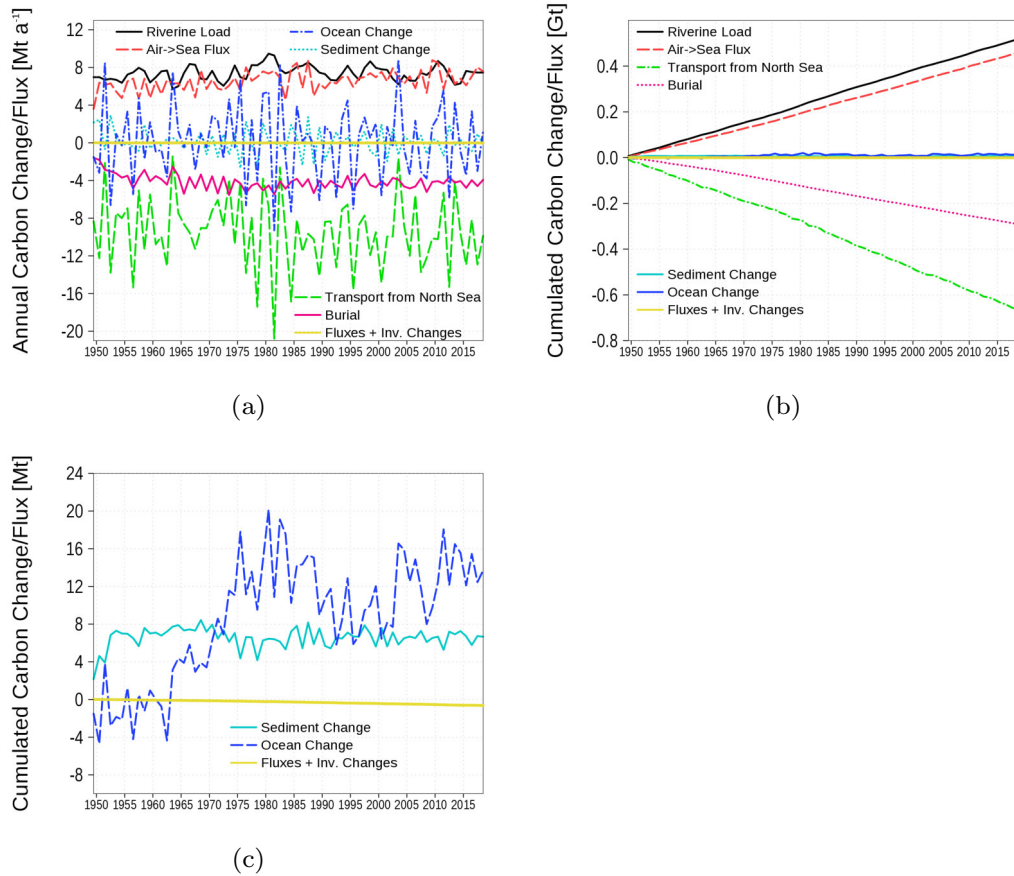


Figure 16. Model-domain integrated carbon budget. Shown are riverine loads, air-sea flux, burial, transport from the North Sea, and changes in the inventory of the ocean (water column) and the sediment. a) Fluxes and inventory change, b) cumulated fluxes, and c) detailed view on the cumulated inventory changes in the ocean and sediment. The yellow line is the sum of all fluxes and inventory changes, and should be zero in a closed budget. Note: We use negative sign for sinks (burial and export towards North Sea).

(Eq. for τ_{alk} in ??B4), we attribute the alkalinity generation mainly to denitrification. The alkalinity generation estimates roughly to 7% of the loads.

3.4.3 Nitrogen budget

355 The nitrogen budget is shown in Fig. 18 with inventory changes, boundary fluxes, loads, transport from and to the North Sea, burial in the sediment, and the internal sinks and sources denitrification and (denitrification) and sources (nitrogen fixation by cyanobacteria). The nitrogen load involves riverine, atmospheric, and point source loads. Strongest fluxes are due to loads as nitrogen source and sediment denitrification as sink. A detailed view on cumulated fluxes in

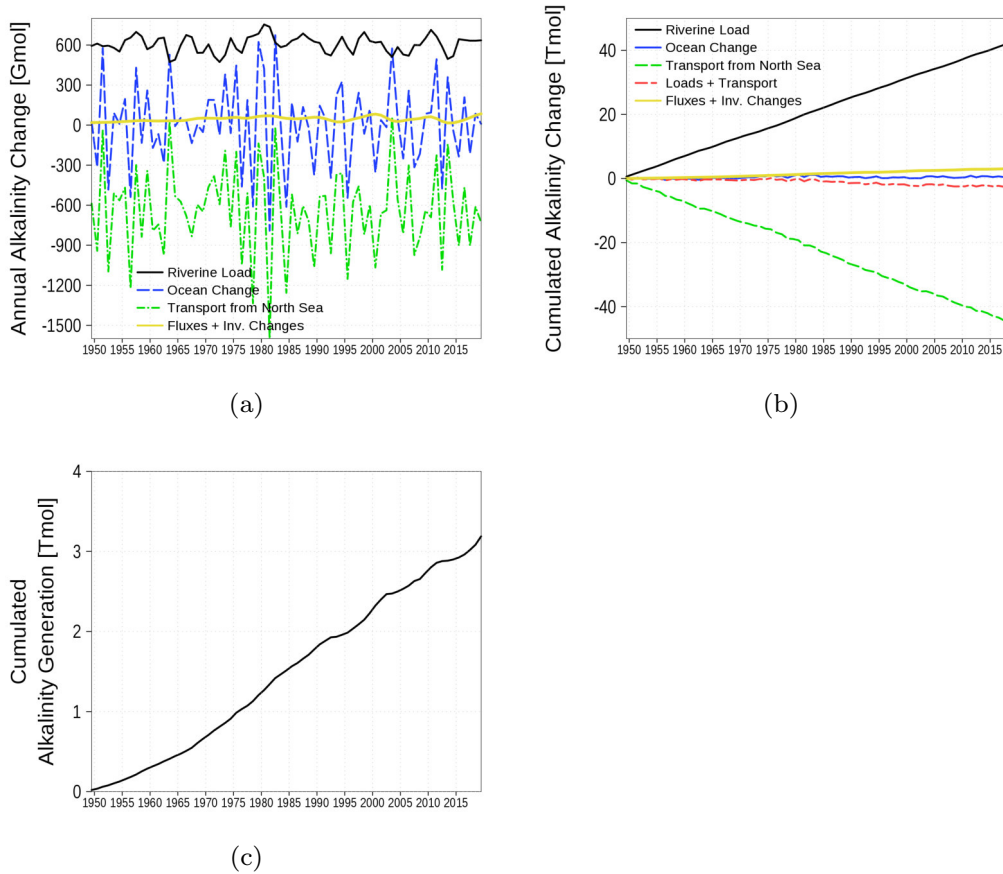


Figure 17. Model-domain integrated alkalinity budget. Shown are riverine loads, transport from the North Sea, and changes in the inventory of the ocean. a) Fluxes and inventory change, b) cumulated fluxes and inventory change, and c) residual of the budget which can be attributed to alkalinity generation. The yellow line is the sum of all fluxes and inventory change and should be zero in a closed budget. Note: We use a negative sign for sinks (export towards North Sea).

Fig. 18c demonstrates that nitrogen fixation is nearly balanced by denitrification in the water column and only a small amount nitrogen is exported towards the North Sea.

3.4.4 Phosphorus budget

The phosphorus budget in Fig. 19 shows inventory changes, boundary fluxes, loads, transport from and to the North Sea, and burial. The phosphorus load involves riverine, atmospheric, and point source loads. In contrast to nitrogen, no internal sinks and sources exist. The most important sink for phosphorus loads is the burial in the sediment. Similar to nitrogen, a small amount of phosphorus is exported towards the North Sea.

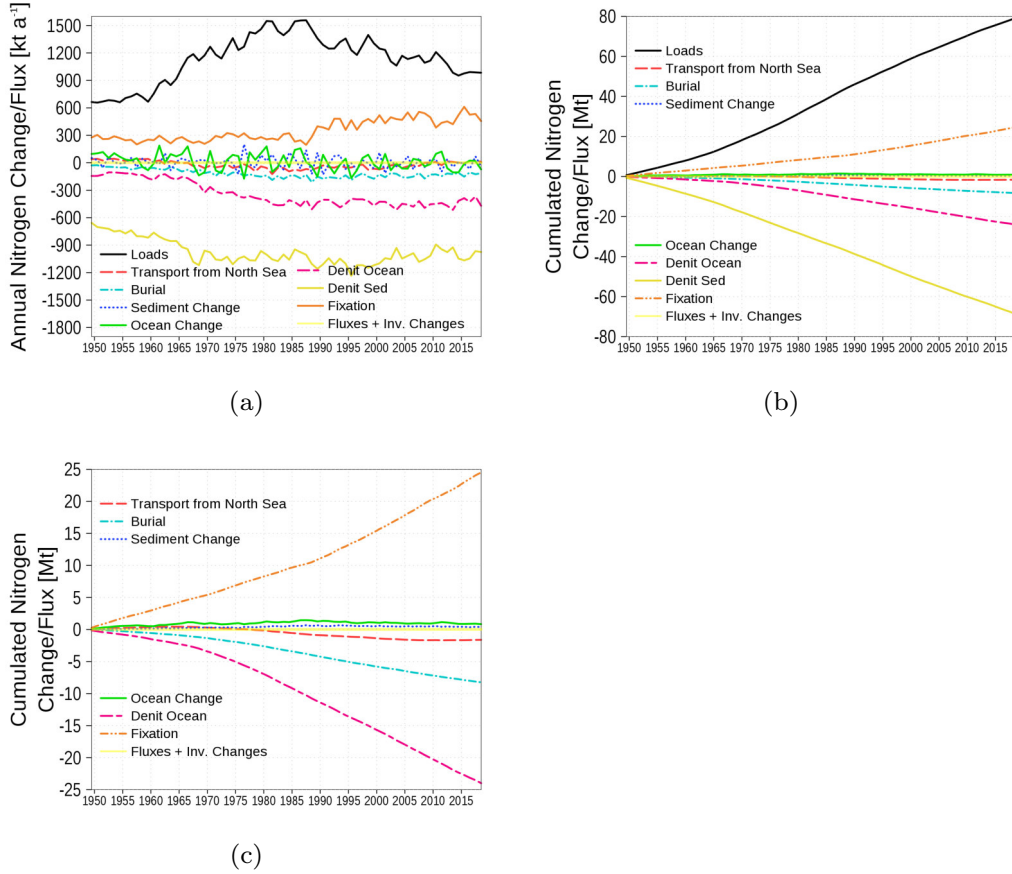


Figure 18. Model-domain integrated nitrogen budget. Shown are loads (riverine, atmospheric, point sources), transport from the North Sea, burial, changes in the inventory of ocean and sediment, denitrification in sediment and ocean, and nitrogen fixation. a) Fluxes and inventory change, b) cumulated fluxes and inventory changes, and c) detailed view without loads and sediment denitrification. The light yellow line is the sum of all fluxes and inventory changes and should be zero in a closed budget. Note: We use negative sign for sinks (burial, denitrification, and export towards North Sea).

4 Discussion and conclusion

We present a biogeochemical model for the Baltic Sea which is able to reproduce observed $spCO_2$ data. This could be achieved solely by implementing a non-Redfieldian stoichiometry in carbon fixation. We realize this by introducing ER due to primary production. ER results in DOM with a flexible elemental ratio and eventually flocculates into POM which sinks down. This approach reproduces observed $spCO_2$, nutrients, and oxygen concentrations reasonably well for the whole Baltic Sea. A different approach is used by Fransner et al. (2018). In their model, in addition to a release of DOC, phytoplankton is formulated as a quota model, that is, within the phytoplankton cells,

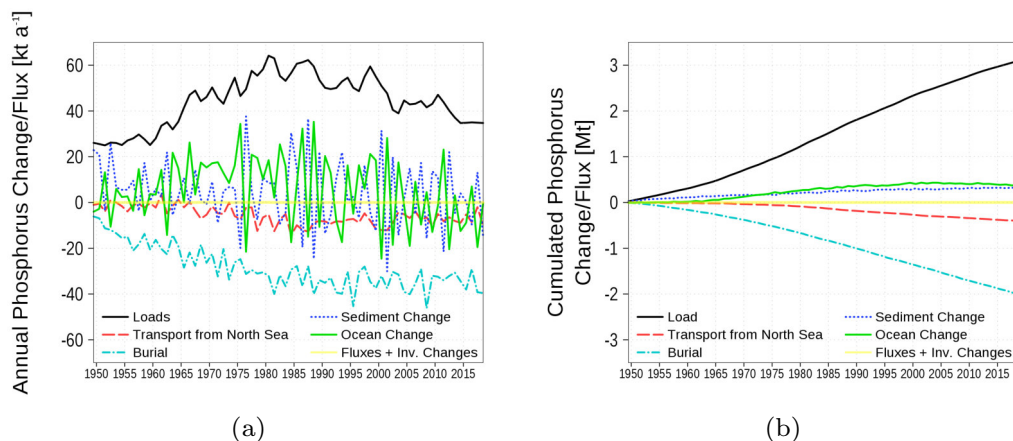


Figure 19. Model-domain integrated phosphorus budget. Shown are loads (riverine, atmospheric, point sources), transport from the North Sea, burial in the sediment, and changes in the inventory of ocean and sediment. a) Fluxes and inventory change, and b) cumulated fluxes and inventory changes. The light yellow line is the sum of all fluxes and should be zero in a closed budget. Note: We use negative sign for sinks (burial and export towards North Sea).

a certain flexibility of the elemental ratio is allowed. This model is applied for the northern part of the Baltic Sea and reproduces well $sp\text{CO}_2$ and surface nutrient concentrations. The main difference besides the quota approach is that DOM in our model shows a flexible elemental ratio. This might correspond to the quota flexibility in phytoplankton cells. between the models is the quota approach in Fransner et al. (2018) while in our model C/N/P uptake variations are directly transferred into ER. However, we have chosen the fixed ratio (Redfield ratio) in healthy phytoplankton cells because of some evidence from literature (Sec: 1) and less computational effort. We are also convinced that our approach is simpler to handle with respect to higher trophic levels which can rely on a fixed stoichiometry.

A similar model was introduced by Gustafsson et al. (2014a) also using the ER process to increase carbon fixation beyond the Redfield ratio. However, the authors do not show the model's performance with respect to $sp\text{CO}_2$ which might be due to missing or rare observations during this time. Macias et al. (2019) implemented a non-Redfieldian nutrient uptake in an ecosystem model for the Mediterranean Sea which results in a fairly flexible elemental ratio in phytoplankton. This model gives good results for nutrients N and P but does not consider carbon. A cell quota model for global Earth system models is proposed by Pahlow et al. (2020); Chien et al. (2020). Also this model This model also shows an advantage over fixed elemental ratio models with respect to nutrient concentration. However, a proof against variables of the carbon cycle is unfortunately missing.

First evaluations of the simulation show an alkalinity generation of about 50 Gmol a^{-1} (Fig. 17). Gustafsson et al. (2014b, 2019) estimated an alkalinity generation of 84 Gmol a^{-1} and 120 Gmol a^{-1} , respectively. Alkalinity river loads in our model are 600 Gmol a^{-1} and higher compared to loads in Gustafsson et al. (2014b, 2019) (470 Gmol a^{-1} , Tab. 2). Altogether, both models underestimate the alkalinity concentration (Fig. 15) and consequently, sources of

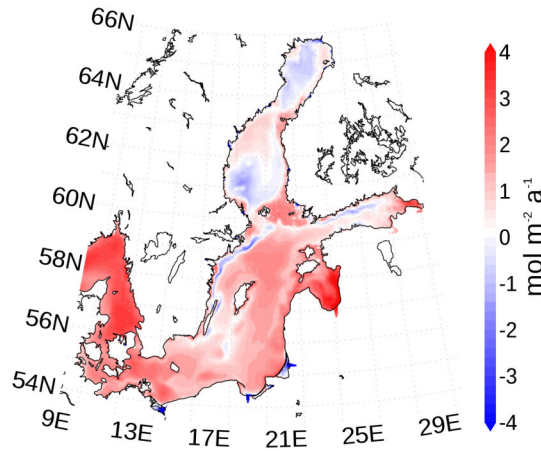


Figure 20. Mean atmosphere-ocean carbon dioxide flux. A positive flux is into the Baltic Sea. The map was created using the software package GrADS 2.1.1.b0 (<http://cola.gmu.edu/grads/>, last access: 14 December 2021).

alkalinity are missing or underrepresented. Gustafsson et al. (2014b) investigate investigated the contribution of a final pyrite burial in sediments to the missing alkalinity source with an advanced sediment model. However, pyrite burial can explain the missing source only partly. It remains still an open question whether riverine alkalinity loads are underestimated or an unknown source exists, e.g. groundwater discharge.

The Baltic Sea acts as a sink for carbon due to uptake of atmospheric carbon dioxide. The additional carbon is partly buried and the remaining fraction is exported towards the North Sea (Fig. 16). However, the northern Baltic Sea emits carbon dioxide into the atmosphere. Figure 20 shows the horizontal pattern of the mean atmosphere-ocean flux. Sources of carbon dioxide for the atmosphere are the northern Baltic Sea and upwelling regions. The latter are caused by prevailing westerly winds with upwelling near the Swedish coast and in the Gulf of Finland. The upwelled, carbon dioxide rich deep water eventually comes in contact with the atmosphere and equilibrates by outgassing of carbon dioxide. For the northern Baltic Sea, we hypothesize that low primary production due to low phosphate concentrations (Fig. A5) favors outgassing of carbon dioxide, which may be imported in subsurface waters from the south.

We compare our carbon budget with estimates from Gustafsson et al. (2017) in Table 3. The most pronounced difference is the 4-fold burial of carbon in our estimates. It corresponds to a rate of $9 \text{ g m}^{-2} \text{ a}^{-1}$. Leipe et al. (2010, Fig. 7) estimate an observation based carbon burial rate which is similar to our rate. However, uncertainties in such rates are large, specifically due to a strong spatial heterogeneity of the carbon burial.

Observations of the marine carbon cycle and especially the $sp\text{CO}_2$ provide an additional, independent state variable constraining ecosystem models. Therefore, models able to reproduce the carbon cycle in addition to e.g. nitrogen

Table 3. Total carbon budget for the whole model domain (NM) compared with estimates from Gustafsson et al. (2017, Tab. 6) (GS).

	GS	NM
Riverine loads	10646	7391
Air-sea flux	3878	6525
Export	13416	9614
Burial	909	4077

All carbon fluxes in kt a^{-1}

and phosphorus cycle should be more robust against changes in the forcing conditions (higher predictive capacity). This is especially important if the models will be used for projections or scenario simulations with changing forcing.

As a lot of observational effort in the past focused on N- and P-cycling, proper implementation of the carbon system requires additional observational and experimental data addressing the carbon cycle. For instance, the reason for the mismatch between observational and experimental alkalinity inventories needs to be addressed by re-addressing the alkalinity flux from the riverine input. Clear evidence has been provided for trends of increasing alkalinity in the major basins of the Baltic Sea (Müller et al., 2016) particularly pronounced in the Northern Basins, but a concerted effort to better constrain the alkalinity fluxes from the major riverine sources is currently lacking. Additional contributions from groundwater seepage can contribute to the alkalinity flux from land and have been shown to locally enhance alkalinity, but the importance on a basin-wide scale is unclear (e.g. Szymczycha et al., 2014).

The initial observational finding that the carbon loss during the spring bloom continues after nitrogen depletion had originally led to the hypothesis of N-fixation already in late-April (Schneider et al., 2009)(Schneider et al., 2009; Kuznetsov et al., 2011), an interpretation which has been revoked by the authors due to a lack of evidence of any known N-fixing organisms during that time of the year (Schneider and Müller, 2018). However, statistical analysis of observational data clearly revealed an increase in total N in the surface waters of the central Baltic Sea during this period (Eggert and Schneider, 2015), which would could not be reproduced by our model. The authors speculated on a potential vertical shuttling of nitrate by the mixotroph *mesodinium rubrum*, a theory later supported by observations in the Gulf of Finland (Lips and Lips, 2017). Recently, anomalous high carbon fixation in the surface layer under extreme sunny and calm spring conditions in 2018 have been also linked to potential vertical nutrient shuttling (Rehder et al., 2020). However, studies on a process level are needed to explore the mechanism and quantity of a potential nutrient shuttle.

Finally, we present a biogeochemical model for the Baltic Sea reproducing parts of the nutrients and carbon cycle reasonable reasonably well. This progress allows now for numerical quantitative studies especially with focus on carbon dynamics in the Baltic Sea under different forcing conditions.

Code and data availability. $spCO_2$ data used are available from <https://www.socat.info> (last access: 14 January 2022). Oceanographic data nutrients and oxygen used for model validation are available from <https://www.ices.dk/data/data-portals/Pages/default.aspx> (last access: 14 January 2022). DOC data used are available from IOW database ODIN <https://odin2.io-warnemuende.de/> (last access: 18 February 2022). Alkalinity data used are available from SHARK database <https://sharkweb.smhi.se/hamta-data/> (last access: 28 February 2022). The meteorological forcing is archived at https://doi.org/10.1594/WDCC/coastDat-2_COSMO-CLM (last access: 14 January 2022, Geyer and Rockel (2013)).

The code of the biogeochemical model is available at <https://ergom.net/> (last access: 14 January 2022). The ocean model "Modular Ocean Model MOM 5-1", used in this study, is available from the developers repository <https://github.com/mom-ocean/MOM5> (last access: 14 January 2022).

Model data can be accessed via https://thredds-iow.io-warnemuende.de/thredds/catalogs/projects/integral/catalog_pocNP_V04R25_3nm_agg_time.html (last access: 14 January 2022, Neumann (2021)). All data used in this study for analysis and figures are archived on Zenodo at <https://doi.org/10.5281/zenodo.6560174> (last access: 10 March 2022, Neumann (2022)).

The version of the model code used to produce the results in this study is archived on Zenodo at <https://doi.org/10.5281/zenodo.6560174> (last access: 10 March 2022, Neumann (2022)). In addition to the source code, the archive includes initial fields and boundary conditions except the meteorological forcing.

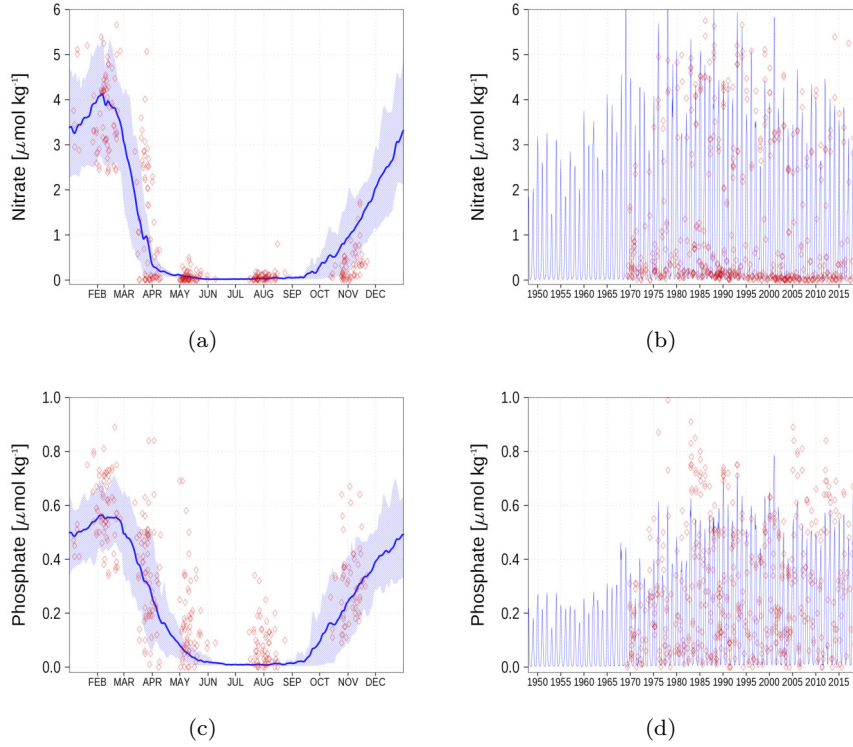


Figure A1. Surface nutrients concentrations at station BY1 (Fig. 6). Blue color are model simulations and observations are shown as red diamonds. The blue shaded area is the range between 10th and 90th percentile. Opacity of the red diamonds reflects the frequency of observations. a: Nitrate climatology, b: Nitrate time series, c: Phosphate climatology, d: Phosphate time series.

Appendix A: Model performance

In this section, we compare model results with observations in order to verify the model performance for biogeochemical variables.

A1 Surface nutrients concentrations

455 We demonstrate the model performance for surface nutrients at 6 stations and regions, respectively in Figs. A1–A6. For the climatology, we have chosen the time range 1990 until 2018 since observations for some stations are sparse for the period before 1990. Data for nutrients and oxygen have been extracted from the ICES database (see *code and data availability*).

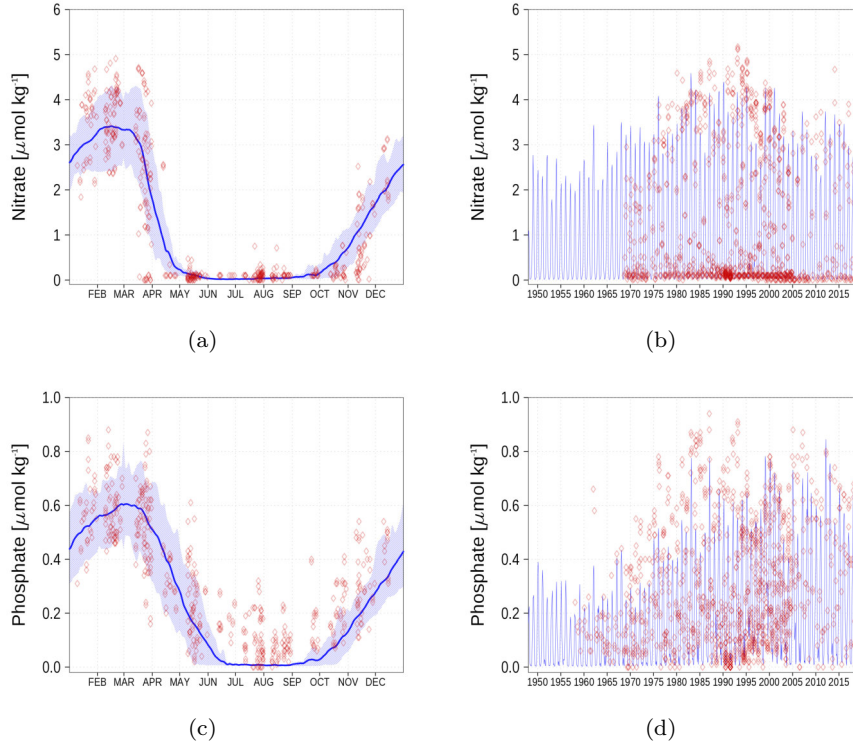


Figure A2. Surface nutrients concentrations at station BY5 (Fig. 6). Blue color are model simulations and observations are shown as red diamonds. The blue shaded area is the range between 10th and 90th percentile. Opacity of the red diamonds reflects the frequency of observations. a: Nitrate climatology, b: Nitrate time series, c: Phosphate climatology, d: Phosphate time series.

A2 Oxygen

460 In Fig. A7, we show oxygen concentration close to the sea floor at six different stations together with observations. Hydrogen sulfide is represented as negative oxygen equivalents. The simulated oxygen concentration follows reasonable the observations. An exception is the underestimation in the Gulf of Bothnia (Fig. A7d and e). Beginning in 1970, the simulated values start to deviate from the field data.

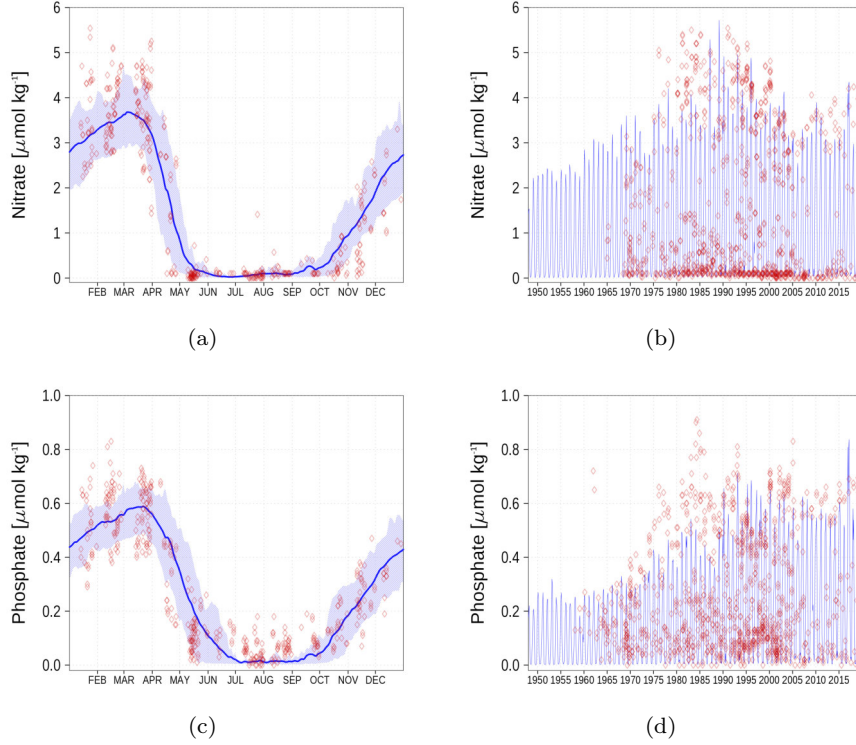


Figure A3. Surface nutrients concentrations at station BY15 (Fig. 6). Blue color are model simulations and observations are shown as red diamonds. The blue shaded area is the range between 10th and 90th percentile. Opacity of the red diamonds reflects the frequency of observations. a: Nitrate climatology, b: Nitrate time series, c: Phosphate climatology, d: Phosphate time series.

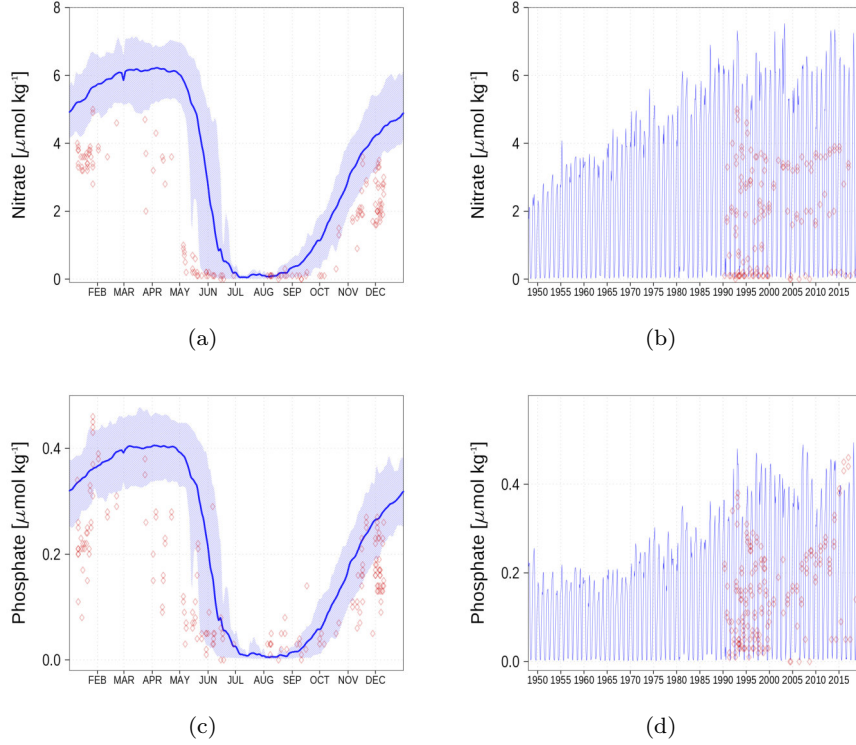


Figure A4. Surface nutrients concentrations at station F26 (Fig. 6). Blue color are model simulations and observations are shown as red diamonds. The blue shaded area is the range between 10th and 90th percentile. Opacity of the red diamonds reflects the frequency of observations. a: Nitrate climatology, b: Nitrate time series, c: Phosphate climatology, d: Phosphate time series.

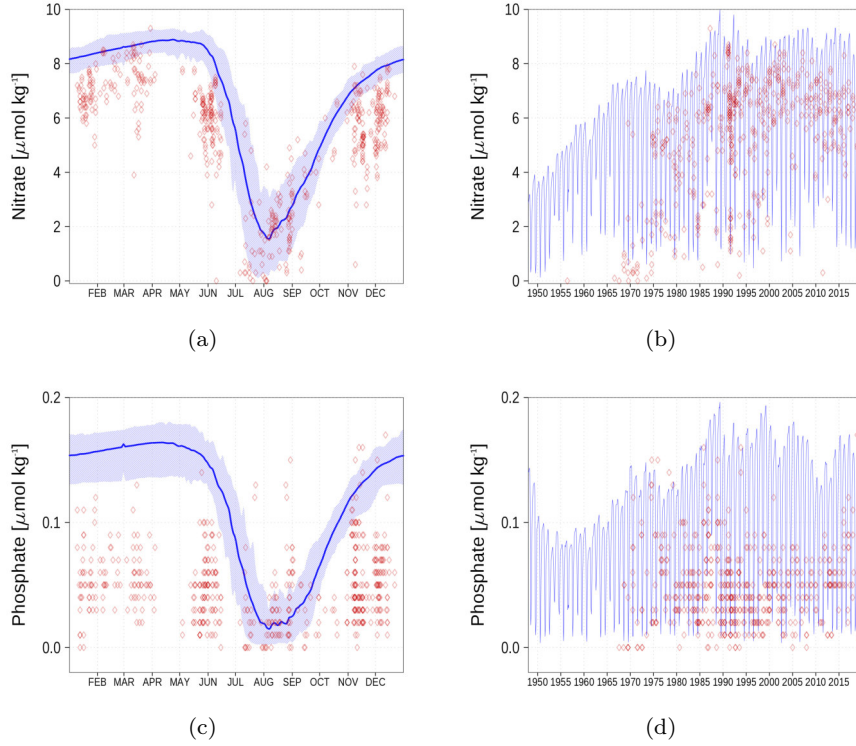


Figure A5. Surface nutrients concentrations in the Bothnian Bay (BoB, Fig. 6). Blue color are model simulations and observations are shown as red diamonds. The blue shaded area is the range between 10th and 90th percentile. Opacity of the red diamonds reflects the frequency of observations. a: Nitrate climatology, b: Nitrate time series, c: Phosphate climatology, d: Phosphate time series.

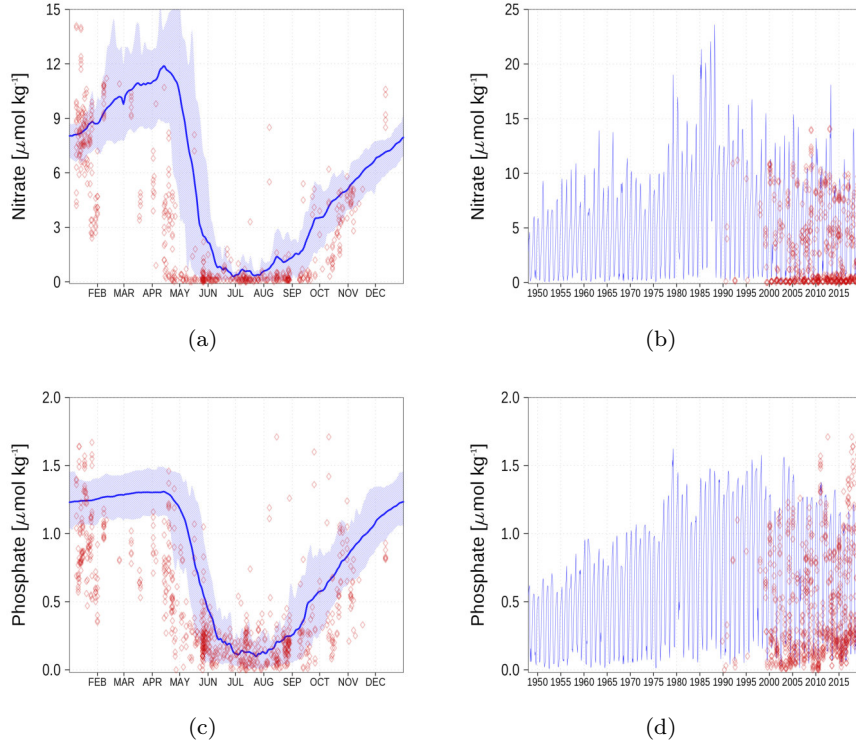


Figure A6. Surface nutrients concentrations at station Gulf of Finland (GoF, Fig. 6). Blue color are model simulations and observations are shown as red diamonds. The blue shaded area is the range between 10th and 90th percentile. Opacity of the red diamonds reflects the frequency of observations. a: Nitrate climatology, b: Nitrate time series, c: Phosphate climatology, d: Phosphate time series.

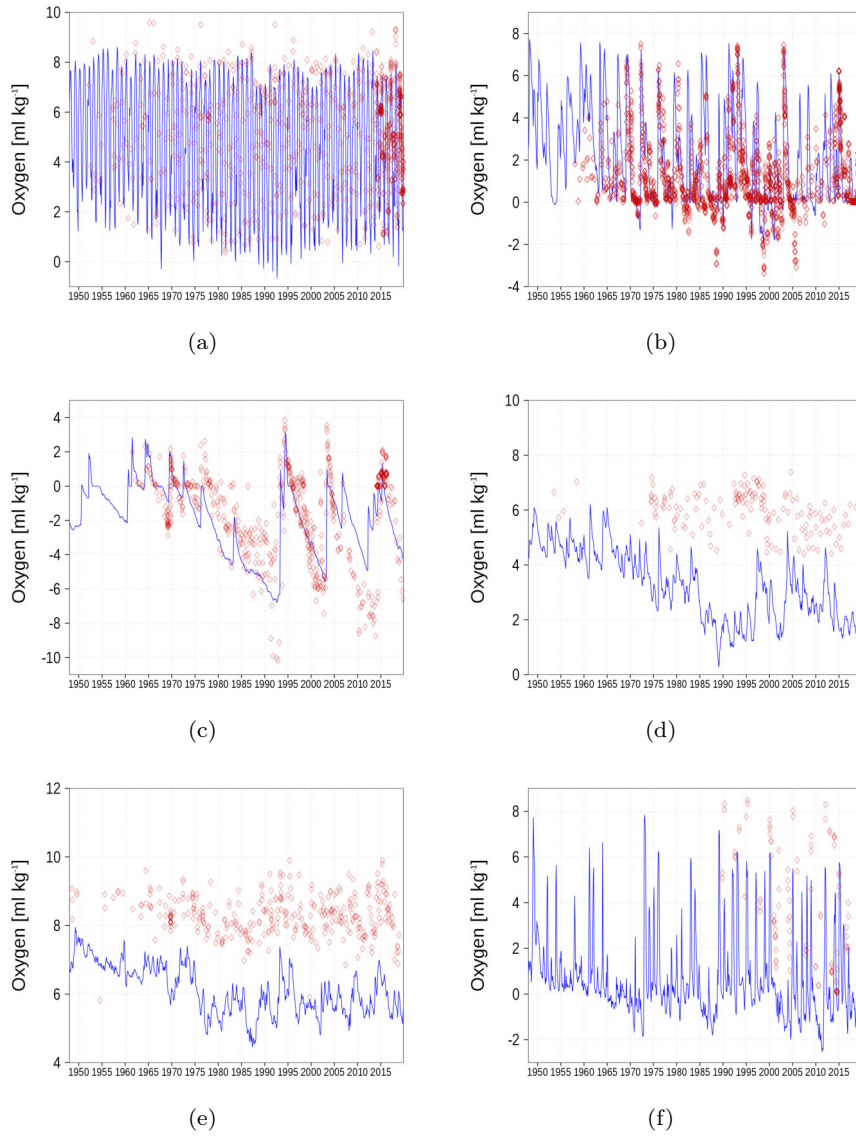


Figure A7. Bottom oxygen concentration at six stations in the Baltic Sea. Negative values denote the presence of hydrogen sulfide. Blue color are model simulations and observations are shown as red diamonds. Opacity of the red diamonds reflects the frequency of observations. a: BY1, b: BY5, c: BY15, d: F26, e: BoB, f: GoF (Fig. 6).

465

Contents

	Appendix B1: Introduction	37
	Appendix B2: Description of model state variables (tracers)	37
	Appendix B3: Description of model processes, ordered by process type	40
470	Appendix B3.1: Process type BGC/benthic/bioresuspension	40
	Appendix B3.1: Process type BGC/benthic/bioresuspension	40
	Appendix B3.1: Process type BGC/benthic/bioresuspension	40
	Appendix B3.2: Process type BGC/benthic/mineralisation	43
	Appendix B3.2: Process type BGC/benthic/mineralisation	43
475	Appendix B3.2: Process type BGC/benthic/mineralisation	43
	Appendix B3.3: Process type BGC/benthic/P_retention	49
	Appendix B3.3: Process type BGC/benthic/P_retention	49
	Appendix B3.3: Process type BGC/benthic/P_retention	49
	Appendix B3.4: Process type BGC/pelagic/mineralisation	50
480	Appendix B3.4: Process type BGC/pelagic/mineralisation	50
	Appendix B3.4: Process type BGC/pelagic/mineralisation	50
	Appendix B3.5: Process type BGC/pelagic/phytoplankton	57
	Appendix B3.5: Process type BGC/pelagic/phytoplankton	57
	Appendix B3.5: Process type BGC/pelagic/phytoplankton	57
485	Appendix B3.6: Process type BGC/pelagic/reoxidation	72
	Appendix B3.6: Process type BGC/pelagic/reoxidation	72
	Appendix B3.6: Process type BGC/pelagic/reoxidation	72
	Appendix B3.7: Process type BGC/pelagic/zooplankton	74
	Appendix B3.7: Process type BGC/pelagic/zooplankton	74
490	Appendix B3.7: Process type BGC/pelagic/zooplankton	74
	Appendix B3.8: Process type gas_exchange	77
	Appendix B3.8: Process type gas_exchange	77
	Appendix B3.8: Process type gas_exchange	77
	Appendix B3.9: Process type physics/erosion	82
495	Appendix B3.9: Process type physics/erosion	82
	Appendix B3.9: Process type physics/erosion	82
	Appendix B3.10: Process type physics/parametrization_deep_burial	85

	Appendix B3.10: Process type physics/parametrization_deep_burial	85
	Appendix B3.10: Process type physics/parametrization_deep_burial	85
500	Appendix B3.11: Process type physics/sedimentation	87
	Appendix B3.11: Process type physics/sedimentation	87
	Appendix B3.11: Process type physics/sedimentation	87
	Appendix B3.12: Process type standard	90
	Appendix B3.12: Process type standard	90
505	Appendix B3.12: Process type standard	90
	Appendix B4: Tracer equations	91

510

B1 Introduction

This is an automatically generated description of the ecosystem model ERGOM version CDOM 1.2 . Model formulation is provided by text files in compliance with the rules of the Code Generation Tool (CGT) by Hagen Radtke (see www.ergom.net).

515

The ecosystem state variables are concentrations of several substances and are called tracers. In the host ocean model they undergo physical advection, turbulent diffusion or vertical motion as sinking or rising. The ecosystem model component defines their sources or sinks from element turnover through the ecosystem. They are defined and described in Sec. B2.

The following Sec. B3 is the main part of this model description document. It describes the processes changing the tracer concentrations over time. Analogously to chemical processes, two components describe a process:

- 520
- A process equation which describes the transformation from precursors (on the left-hand side) to products (on the right-hand side), and
 - a turnover rate, describing how fast the process runs.

The time tendency of a tracer can then easily be determined by multiplying the process turnover rate with the stoichiometric ratio in which it consumes or produces the tracer according to the reaction equation.

525

The document structure reflects the different process types. All processes of one type (e.g. phytoplankton assimilation) are listed together with all their constants and auxiliary variables they depend on. For readability, some constants, such as stoichiometric ratios, will occur repeatedly. We take this compromise for the sake of readability, keeping all information required to understand a specific process in its own section.

530

For completeness, the tracer equations are given in Sec B4. However, we consider this as a supplementary chapter and suggest to study the model details from Sec. B3 instead.

B2 Description of model state variables (tracers)

Tracers in the water column only	
t_n2	dissolved molecular nitrogen (mol/kg)
t_o2	dissolved oxygen (mol/kg)
t_dic	dissolved inorganic carbon, treated as carbon dioxide (mol/kg)
t_nh4	ammonium (mol/kg)
t_no3	nitrate (mol/kg)
t_po4	phosphate (mol/kg)
t_spp	small-cell phytoplankton (mol/kg)
opacity =	58.0 m ² /mol
t_zoo	zooplankton (mol/kg)
t_h2s	hydrogen sulfide (mol/kg)
t_sul	sulfur (mol/kg)
t_alk	total alkalinity (mol/kg)
t_lip	limnic phytoplankton (mol/kg)
opacity =	58.0 m ² /mol
t_doc	dissolved organic carbon (mol/kg)
t_dop	phosphorus in dissolved organic carbon in Redfield ratio (mol/kg)
t_don	nitrogen in dissolved organic carbon in Redfield ratio (mol/kg)
opacity =	12.6 m ² /mol
continued on next page...	

t_cdom	colored dissolved organic carbon (mol/kg)
t_lpp	large-cell phytoplankton (mol/kg)
vertical speed =	-0.5 m/day
opacity =	58.0 m ² /mol
t_ipw	suspended iron phosphate (mol/kg)
vertical speed =	-1.0 m/day
t_cya	diazotroph cyanobacteria (mol/kg)
vertical speed =	1.0 m/day
opacity =	58.0 m ² /mol
t_det	detritus (mol/kg)
vertical speed =	-4.5 m/day
opacity =	53.2 m ² /mol
t_poc	particulate organic carbon (mol/kg)
vertical speed =	w_poc_var m/day
t_pocp	phosphorus in particulate organic carbon in Redfield ratio (mol/kg)
vertical speed =	-0.1 m/day
t_pocn	nitrogen in particulate organic carbon in Redfield ratio (mol/kg)
vertical speed =	-0.1 m/day

end of table **Tracers in the water column only**

Tracers in water and pore water

end of table **Tracers in water and pore water**

Tracers in fluff and sediment	
t_sed	sediment detritus (mol/m ²)
t_ips	iron phosphate in sediment (mol/m ²)
t_sed_poc	sediment particular carbon (mol/m ²)
t_sed_pocn	sediment particular organic N+C (mol/m ²)
t_sed_pocp	sediment particular organic P+C (mol/m ²)
end of table Tracers in fluff and sediment	

B3 Description of model processes, ordered by process type

5

B3.1 Process type BGC/benthic/bioresuspension

Processes
<p>bio resuspension of sedimentary detritus (sediment only) [mol/m²/day]</p> <p>t_sed -> t_det</p> <p>p_sed_biores_det = (r_biores*exp(-0.02*cgt_bottomdepth)*sed_active)*lim_t_o2_6*lim_t_sed_21</p>
<p>bio resuspension of iron PO4 (sediment only) [mol/m²/day]</p> <p>t_ips -> t_ipw</p> <p>p_ips_biores_ipw = (r_biores*exp(-0.02*cgt_bottomdepth)*t_ips)*lim_t_o2_6*lim_t_ips_23</p>
<p>bio resuspension of sedimentary poc (sediment only) [mol/m²/day]</p> <p>t_sed_poc -> t_poc</p>
continued on next page...

Processes, continued from previous page

p_sed_biores_poc = (r_biores*exp(-0.02*cgt_bottomdepth)*poc_active)*lim_t_o2_6*
lim_t_sed_poc_22

bio resuspension of sedimentary pocn (sediment only) [mol/m²/day]

t_sed_pocn -> t_pocn

p_sed_biores_pocn = (r_biores*exp(-0.02*cgt_bottomdepth)*pocn_active)*lim_t_o2_6*
lim_t_sed_pocn_27

bio resuspension of sedimentary pocp (sediment only) [mol/m²/day]

t_sed_pocp -> t_pocp

p_sed_biores_pocp = (r_biores*exp(-0.02*cgt_bottomdepth)*pocp_active)*lim_t_o2_6*
lim_t_sed_pocp_28

end of table **Processes**

Auxiliary variables

total carbon in sediment layer [mol/m²]

sed_tot = t_sed*rfr_c + t_sed_poc + t_sed_pocn*rfr_c + t_sed_pocp*rfr_cp

total carbon in active sediment layer [mol/m²]

sed_tot_active = max(0.0,min(sed_tot,sed_max*rfr_c))

detritus in active sediment layer [mol/m²]

sed_active = sed_tot_active * t_sed/sed_tot

poc in active sediment layer [mol/m²]

poc_active = sed_tot_active * t_sed_poc/sed_tot

pocn in active sediment layer [mol/m²]

pocn_active = sed_tot_active * t_sed_pocn/sed_tot

continued on next page...

Auxiliary variables, continued from previous page	
pocp in active sediment layer [mol/m**2]	
pocp_active =	sed_tot_active * t_sed_pocp/sed_tot
end of table Auxiliary variables	
Constants	
oxygen half-saturation constant for recycling of sediment detritus using oxygen [mol/kg]	
o2_min_sed_resp =	0.000064952
bio-resuspension rate [1/day]	
r_biores =	0.015
redfield ratio C/N	
rfr_c =	6.625
redfield ratio C/P	
rfr_cp =	106.0
maximum sediment detritus concentration that feels erosion [mol/m**2]	
sed_max =	1.0
end of table Constants	
Process limitation factors	
lim_t_o2_6 =	t_o2*t_o2/(t_o2*t_o2+o2_min_sed_resp*o2_min_sed_resp)
lim_t_sed_21 =	theta(t_sed-0.0)
lim_t_ips_23 =	theta(t_ips-0.0)
continued on next page...	

Process limitation factors, continued from previous page	
lim_t_sed_poc_22 =	theta(t_sed_poc-0.0)
lim_t_sed_pocn_27 =	theta(t_sed_pocn-0.0)
lim_t_sed_pocp_28 =	theta(t_sed_pocp-0.0)
end of table Process limitation factors	

535 5

B3.2 Process type BGC/benthic/mineralisation

Processes	
recycling of sedimentary detritus to ammonium using oxygen (respiration) (sediment only) [mol/m ² /day]	
t_sed + 6.625*t_o2 + 0.8125*h3oplus -> t_nh4 + rfr_p*t_po4 + rfr_c*t_dic + 7.4375*h2o	
p_sed_resp_nh4 =	(lr_sed_rec*sed_active)*lim_t_sed_21*lim_t_o2_2
coupled nitrification and denitrification after mineralization of detritus in oxic sediments (sediment only) [mol/m ² /day]	
t_nh4 + 0.75*t_o2 -> 0.5*h2o + h3oplus + 0.5*t_n2	
p_nh4_nitdenit_n2 =	(frac_denit_sed*(p_sed_resp_nh4+p_sed_pocn_resp)*theta(t_o2-5.0e-6))*lim_t_nh4_11*lim_t_o2_2
recycling of sedimentary detritus to ammonium using nitrate (denitrification) (sediment only) [mol/m ² /day]	
t_sed + 6.1125*h3oplus + 5.3*t_no3 -> rfr_c*t_dic + rfr_p*t_po4 + t_nh4 + 2.65*t_n2 + 15.3875*h2o	
p_sed_denit_nh4 =	(lr_sed_rec*sed_active)*(1.0-lim_t_o2_2)*lim_t_no3_3*lim_t_sed_21
recycling of sedimentary detritus to ammonium using sulfate (sulfate reduction) (sediment only) [mol/m ² /day]	
continued on next page...	

$t_{sed} + 3.3125 \cdot so_4 + 7.4375 \cdot h_3oplus \rightarrow t_{nh_4} + rfr_p \cdot t_{po_4} + rfr_c \cdot t_{dic} + 3.3125 \cdot t_{h_2s} + 14.0625 \cdot h_2o$
 $p_{sed_sulf_nh_4} = (lr_{sed_rec} \cdot sed_active) \cdot (1.0 - lim_t_{o_2_2}) \cdot (1.0 - lim_t_{no_3_3}) \cdot lim_t_{sed_21}$

recycling of sedimentary poc to dic using oxygen (respiration) (sediment only)

[mol/m²/day]

$t_{sed_poc} + t_{o_2} \rightarrow t_{dic} + h_2o$
 $p_{sed_poc_resp} = (lr_{sed_poc_rec} \cdot poc_active) \cdot lim_t_{sed_poc_22} \cdot lim_t_{o_2_2}$

recycling of sedimentary poc to dic using nitrate (denitrification) (sediment only)

[mol/m²/day]

$0.8 \cdot t_{no_3} + 0.8 \cdot h_3oplus + t_{sed_poc} \rightarrow 2.2 \cdot h_2o + 0.4 \cdot t_{n_2} + t_{dic}$
 $p_{sed_poc_denit} = (lr_{sed_poc_rec} \cdot poc_active) \cdot (1.0 - lim_t_{o_2_2}) \cdot lim_t_{no_3_3} \cdot lim_t_{sed_poc_22}$

recycling of sedimentary poc to dic using sulfate (sulfate reduction) (sediment only)

[mol/m²/day]

$h_3oplus + 0.5 \cdot so_4 + t_{sed_poc} \rightarrow 2.0 \cdot h_2o + 0.5 \cdot t_{h_2s} + t_{dic}$
 $p_{sed_poc_sulf} = (lr_{sed_poc_rec} \cdot poc_active) \cdot (1.0 - lim_t_{o_2_2}) \cdot (1.0 - lim_t_{no_3_3}) \cdot lim_t_{sed_poc_22}$

recycling of sedimentary pocn to dic and NH₄ using oxygen (respiration) (sediment only)

[mol/m²/day]

$6.625 \cdot t_{o_2} + t_{sed_pocn} + 0.5 \cdot h_3oplus \rightarrow 6.625 \cdot h_2o + 6.625 \cdot t_{dic} + t_{nh_4} + 0.5 \cdot ohminus$
 $p_{sed_pocn_resp} = (lr_{sed_rec} \cdot pocn_active) \cdot lim_t_{o_2_2} \cdot lim_t_{sed_pocn_27}$

recycling of sedimentary pocp to dic and PO₄ using oxygen (respiration) (sediment only)

[mol/m²/day]

$3 \cdot h_2o + t_{sed_pocp} + 106 \cdot t_{o_2} \rightarrow 106 \cdot h_2o + t_{po_4} + 106 \cdot t_{dic} + 3 \cdot h_3oplus$
 $p_{sed_pocp_resp} = (lr_{sed_rec} \cdot pocp_active) \cdot lim_t_{sed_pocp_28} \cdot lim_t_{o_2_2}$

continued on next page...

recycling of sedimentary pocn to dic and NH4 using nitrate (denitrification) (sediment only) [mol/m²/day]

$t_{\text{sed_pocn}} + 5.3*t_{\text{no3}} + 5.8*h3\text{oplus} \rightarrow 6.625*t_{\text{dic}} + t_{\text{nh4}} + 2.65*t_{\text{n2}} + 14.575*h2\text{o} + 0.5*oh\text{minus}$

$p_{\text{sed_pocn_denit}} = (lr_{\text{sed_rec}}*pocn_{\text{active}})*(1.0-lim_{t_o2_2})*lim_{t_no3_3}*lim_{t_sed_pocn_27}$

recycling of sedimentary pocp to dic and PO4 using nitrate (denitrification) (sediment only) [mol/m²/day]

$t_{\text{sed_pocp}} + 3*oh\text{minus} + 84.8*h3\text{oplus} + 84.8*t_{\text{no3}} \rightarrow 106*t_{\text{dic}} + t_{\text{po4}} + 42.4*t_{\text{n2}} + 236.2*h2\text{o}$

$p_{\text{sed_pocp_denit}} = (lr_{\text{sed_rec}}*pocp_{\text{active}})*(1.0-lim_{t_o2_2})*lim_{t_no3_3}*lim_{t_sed_pocp_28}$

recycling of sedimentary pocn to dic and NH4 using sulfate (sulfate reduction) (sediment only) [mol/m²/day]

$7.125*h3\text{oplus} + 3.3125*S04 + t_{\text{pocn}} \rightarrow 0.5*oh\text{minus} + 13.25*H2O + 3.3125*t_{\text{h2s}} + t_{\text{nh4}} + 6.625*t_{\text{dic}}$

$p_{\text{sed_pocn_sulf}} = (lr_{\text{sed_rec}}*pocn_{\text{active}})*(1.0-lim_{t_o2_2})*(1.0-lim_{t_no3_3})*lim_{t_pocn_14}$

recycling of sedimentary pocp to dic and PO4 using sulfate (sulfate reduction) (sediment only) [mol/m²/day]

$t_{\text{pocp}} + 53*so4 + 106*h3\text{oplus} + 3*oh\text{minus} \rightarrow 106*t_{\text{dic}} + 215*h2\text{o} + 53*t_{\text{h2s}} + t_{\text{po4}}$

$p_{\text{sed_pocp_sulf}} = (lr_{\text{sed_rec}}*pocp_{\text{active}})*(1.0-lim_{t_o2_2})*(1.0-lim_{t_no3_3})*lim_{t_pocp_13}$

coupled nitrification and denitrification after mineralization of pocn-detritus in oxic sediments (sediment only) [mol/m²/day]

$t_{\text{nh4}} + 0.75*t_{\text{o2}} \rightarrow 0.5*h2\text{o} + h3\text{oplus} + 0.5*t_{\text{n2}}$

continued on next page...

Processes, continued from previous page	
$\frac{(\text{frac_denit_sed} * \text{p_sed_pocn_resp} * \theta(t_{o2} - 5.0e-6)) * \text{lim_t_nh4_11} * \text{p_nh4_nitdenit_pocn_n2lim_t_o2_2}}{=}$	
end of table Processes	
Auxiliary variables	
fraction of ammonium that is immediately nitrified and denitrified after remineralization in oxic sediments	
frac_denit_sed =	frac_denit_scal*(0.5+0.5*exp(-0.01*cgt_bottomdepth))
total carbon in sediment layer [mol/m**2]	
sed_tot =	t_sed*rfr_c + t_sed_poc + t_sed_pocn*rfr_c + t_sed_pocp*rfr_cp
total carbon in active sediment layer [mol/m**2]	
sed_tot_active =	max(0.0,min(sed_tot,sed_max*rfr_c))
detritus in active sediment layer [mol/m**2]	
sed_active =	sed_tot_active * t_sed/sed_tot
recycling rate of sediment detritus, limited by oxygen [1/d]	
lr_sed_rec =	r_sed_rec*exp(q10_sed_rec*cgt_temp)*(1.0-reduced_rec*theta(2*t_h2s-t_o2))
recycling rate of sediment POC, limited by oxygen [1/d]	
lr_sed_poc_rec =	r_sed_poc_rec*exp(q10_sed_rec*cgt_temp)*(1.0-reduced_rec*theta(2*t_h2s-t_o2))
poc in active sediment layer [mol/m**2]	
poc_active =	sed_tot_active * t_sed_poc/sed_tot
continued on next page...	

Auxiliary variables, continued from previous page	
pocn in active sediment layer [mol/m**2]	
pocn_active =	sed_tot_active * t_sed_pocn/sed_tot
pocp in active sediment layer [mol/m**2]	
pocp_active =	sed_tot_active * t_sed_pocp/sed_tot
end of table Auxiliary variables	
Constants	
nitrate half-saturation concentration for denitrification in the water column [mol/kg]	
no3_min_sed_denit =	1.423E-7
q10 rule factor for detritus recycling in the sediment [1/K]	
q10_sed_rec =	0.175
maximum recycling rate for sedimentary detritus [1/d]	
r_sed_rec =	0.003
maximum recycling rate for sedimentary POC [1/d]	
r_sed_poc_rec =	0.0005
redfield ratio C/N	
rfr_c =	6.625
redfield ratio P/N	
rfr_p =	0.0625
redfield ratio C/P	
rfr_cp =	106.0
maximum sediment detritus concentration that feels erosion [mol/m**2]	
continued on next page...	

Constants, continued from previous page	
sed_max =	1.0
scaling frac_denit_sed	
frac_denit_scal =	1.0
decrease recycling in sed under anoxia by reduce_rec	
reduced_rec =	0.8
end of table Constants	
Process limitation factors	
lim_t_o2_2 =	theta(t_o2-0.0)
lim_t_nh4_11 =	theta(t_nh4-0.0)
lim_t_no3_3 =	t_no3*t_no3/(t_no3*t_no3+no3_min_sed_denit*no3_min_sed_denit)
lim_t_sed_21 =	theta(t_sed-0.0)
lim_t_sed_poc_22 =	theta(t_sed_poc-0.0)
lim_t_sed_pocn_27 =	theta(t_sed_pocn-0.0)
lim_t_sed_pocp_28 =	theta(t_sed_pocp-0.0)
lim_t_pocp_13 =	theta(t_pocp-0.0)
lim_t_pocn_14 =	theta(t_pocn-0.0)
end of table Process limitation factors	

B3.3 Process type BGC/benthic/P_retention

Processes
<p>retention of phosphate in the sediment under oxic conditions (sediment only)</p> <p>[mol/m²/day]</p> <p>rfr_p*t_po4 + rfr_p*fe3plus -> rfr_p*t_ips</p> <p>p_po4_retent_ips = (p_sed_resp_nh4*frac_po4retent)*lim_t_o2_4*lim_t_po4_10</p>
<p>liberation of phosphate from the sediment under anoxic conditions (sediment only)</p> <p>[mol/m²/day]</p> <p>t_ips -> fe3plus + t_po4</p> <p>p_ips_liber_po4 = (t_ips*r_ips_liber)*lim_t_h2s_5*lim_t_ips_23</p>
end of table Processes
Auxiliary variables
<p>fraction of phosphate which is retained as iron-bound phosphate instead of being released after mineralization in the sediment [1]</p> <p>frac_po4retent = ret_po4_1 + ret_po4_2*theta(cgt_latitude-60.75) + ret_po4_3*theta(cgt_latitude-63.75)</p>
end of table Auxiliary variables
Constants
<p>minimum h2s concentration for liberation of iron phosphate from the sediment [mol/kg]</p> <p>h2s_min_po4_liber = 1.0E-6</p>
<p>oxygen half-saturation concentration for retension of phosphate during sediment denitrification [mol/kg]</p> <p>o2_min_po4_retent = 0.0000375</p>
continued on next page...

Constants, continued from previous page	
PO4 liberation rate under anoxic conditions [1/day]	
r_ips_liber =	0.1
redfield ratio P/N	
rfr_p =	0.0625
PO4 retention in oxic sediments	
ret_po4_1 =	0.1
additional PO4 retention in oxic sediments of the Bothnian Sea	
ret_po4_2 =	0.5
additional PO4 retention in oxic sediments of the Bothnian Sea	
ret_po4_3 =	0.13
end of table Constants	
Process limitation factors	
lim_t_o2_4 =	$t_{o2} * t_{o2} / (t_{o2} * t_{o2} + o2_min_po4_retent * o2_min_po4_retent)$
lim_t_po4_10 =	$\theta(t_{po4} - 0.0)$
lim_t_h2s_5 =	$\theta(t_{h2s} - h2s_min_po4_liber)$
lim_t_ips_23 =	$\theta(t_{ips} - 0.0)$
end of table Process limitation factors	

Processes

recycling of POC using nitrate (denitrification) [mol/kg/day]

$t_poc + 0.8*t_no3 + 0.8*h3oplus \rightarrow t_dic + 2.2*h2o + 0.4*t_n2$

$p_poc_denit = (t_poc*r_poc_rec*exp(q10_det_rec*cgt_temp))*(1.0-lim_t_o2_0)*lim_t_no3_1*lim_t_poc_12$

Mineralization of POC, e-acceptor sulfate (sulfate reduction) [mol/kg/day]

$t_poc + 0.5*so4 + h3oplus \rightarrow t_dic + 0.5*t_h2s + 2*h2o$

$p_poc_sulf = (t_poc*r_poc_rec*exp(q10_det_rec*cgt_temp))*(1.0-lim_t_o2_0)*(1.0-lim_t_no3_1)*lim_t_poc_12$

respiration of POCP [mol/kg/day]

$106*t_o2 + t_pocp + 3*H2O \rightarrow 106*t_dic + t_po4 + 106*H2O + 3*h3oplus$

$p_pocp_resp = (t_pocp * lr_pocp * exp(q10_det_rec * cgt_temp))*lim_t_o2_0*lim_t_pocp_13$

recycling of POC using nitrate (denitrification) [mol/kg/day]

$3*ohminus + 84.8*h3oplus + 84.8*t_no3 + t_pocp \rightarrow t_po4 + 42.4*t_n2 + 236.2*H2O + 106*t_dic$

$p_pocp_denit = (t_pocp*r_pocp_rec*exp(q10_det_rec*cgt_temp))*(1.0-lim_t_o2_0)*lim_t_no3_1*lim_t_pocp_13$

Mineralization of POC, e-acceptor sulfate (sulfate reduction) [mol/kg/day]

$t_pocp + 53*so4 + 106*h3oplus + 3*ohminus \rightarrow 106*t_dic + 215*h2o + 53*t_h2s + t_po4$

$p_pocp_sulf = (t_pocp*r_pocp_rec*exp(q10_det_rec*cgt_temp))*(1.0-lim_t_o2_0)*(1.0-lim_t_no3_1)*lim_t_pocp_13$

respiration of POCN [mol/kg/day]

$0.5*h3oplus + 6.625*t_o2 + t_pocn \rightarrow 0.5*ohminus + 6.625*H2O + t_nh4 + 6.625*t_dic$

$p_pocn_resp = (t_pocn * lr_pocn * exp(q10_det_rec * cgt_temp))*lim_t_o2_0*lim_t_pocn_14$

recycling of POCN using nitrate (denitrification) [mol/kg/day]

continued on next page...

5.8*h3oplus + 5.3*t_no3 + t_pocn -> 0.5*ohminus + 14.575*H2O + 2.65*t_n2 + t_nh4 +
6.625*t_dic
p_pocn_denit = (t_pocn*r_pocn_rec*exp(q10_det_rec*cgt_temp))*(1.0-lim_t_o2_0)*
lim_t_no3_1*lim_t_pocn_14

Mineralization of POCN, e-acceptor sulfate (sulfate reduction) [mol/kg/day]

t_pocn + 3.3125*S04 + 7.125*h3oplus -> 6.625*t_dic + t_nh4 + 3.3125*t_h2s + 13.25*H2O
+ 0.5*ohminus
p_pocn_sulf = (t_pocn*r_pocn_rec*exp(q10_det_rec*cgt_temp))*(1.0-lim_t_o2_0)*
(1.0-lim_t_no3_1)*lim_t_pocn_14

recycling of detritus using oxygen (respiration) [mol/kg/day]

t_det + 6.625*t_o2 + 0.8125*h3oplus -> t_nh4 + rfr_p*t_po4 + rfr_c*t_dic + 7.4375*h2o
p_det_resp_nh4 = (t_det*r_det_rec*exp(q10_det_rec*cgt_temp))*lim_t_o2_0*
lim_t_det_20

recycling of detritus using nitrate (denitrification) [mol/kg/day]

t_det + 5.3*t_no3 + 6.1125*h3oplus -> 2.65*t_n2 + 15.3875*h2o + t_nh4 + rfr_p*t_po4 +
rfr_c*t_dic
p_det_denit_nh4 = (t_det*r_det_rec*exp(q10_det_rec*cgt_temp))*(1.0-lim_t_o2_0)*
lim_t_no3_1*lim_t_det_20

recycling of detritus using sulfate (sulfate reduction) [mol/kg/day]

7.4375*h3oplus + 3.3125*so4 + t_det -> 14.0625*h2o + 3.3125*t_h2s + rfr_c*t_dic +
rfr_p*t_po4 + t_nh4
p_det_sulf_nh4 = (t_det*r_det_rec*exp(q10_det_rec*cgt_temp))*(1.0-lim_t_o2_0)*
(1.0-lim_t_no3_1)*lim_t_det_20

recycling of DOC using nitrate (denitrification) [mol/kg/day]

t_doc + 0.8*t_no3 + 0.8*h3oplus -> t_dic + 2.2*h2o + 0.4*t_n2
p_doc_denit = (t_doc*r_doc_rec*exp(q10_det_rec*cgt_temp))*(1.0-lim_t_o2_0)*
lim_t_no3_1*lim_t_doc_29

continued on next page...

Mineralization of DOC, e-acceptor sulfate (sulfate reduction) [mol/kg/day]

$t_{doc} + 0.5 \cdot so_4 + h_3o_{plus} \rightarrow t_{dic} + 0.5 \cdot t_{h_2s} + 2 \cdot h_2o$

$$p_{doc_sulf} = (t_{doc} \cdot r_{doc_rec} \cdot \exp(q_{10_det_rec} \cdot cgt_temp)) \cdot (1.0 - lim_t_{o_2_0}) \cdot (1.0 - lim_t_{no_3_1}) \cdot lim_t_{doc_29}$$

respiration of DOP [mol/kg/day]

$3 \cdot H_2O + t_{dop} + 106 \cdot t_{o_2} \rightarrow 3 \cdot h_3o_{plus} + 106 \cdot H_2O + t_{po_4} + 106 \cdot t_{dic}$

$$p_{dop_resp} = (t_{dop} \cdot lr_{dop} \cdot \exp(q_{10_det_rec} \cdot cgt_temp)) \cdot lim_t_{o_2_0} \cdot lim_t_{dop_30}$$

recycling of DOP using nitrate (denitrification) [mol/kg/day]

$t_{dop} + 84.8 \cdot t_{no_3} + 84.8 \cdot h_3o_{plus} + 3 \cdot oh_{minus} \rightarrow 106 \cdot t_{dic} + 236.2 \cdot H_2O + 42.4 \cdot t_{n_2} + t_{po_4}$

$$p_{dop_denit} = (t_{dop} \cdot r_{dop_rec} \cdot \exp(q_{10_det_rec} \cdot cgt_temp)) \cdot (1.0 - lim_t_{o_2_0}) \cdot lim_t_{no_3_1} \cdot lim_t_{dop_30}$$

Mineralization of DOP, e-acceptor sulfate (sulfate reduction) [mol/kg/day]

$3 \cdot oh_{minus} + 106 \cdot h_3o_{plus} + 53 \cdot so_4 + t_{dop} \rightarrow t_{po_4} + 53 \cdot t_{h_2s} + 215 \cdot h_2o + 106 \cdot t_{dic}$

$$p_{dop_sulf} = (t_{dop} \cdot r_{dop_rec} \cdot \exp(q_{10_det_rec} \cdot cgt_temp)) \cdot (1.0 - lim_t_{o_2_0}) \cdot (1.0 - lim_t_{no_3_1}) \cdot lim_t_{dop_30}$$

respiration of DON [mol/kg/day]

$0.5 \cdot h_3o_{plus} + 6.625 \cdot t_{o_2} + t_{don} \rightarrow 0.5 \cdot oh_{minus} + 6.625 \cdot H_2O + t_{nh_4} + 6.625 \cdot t_{dic}$

$$p_{don_resp} = (t_{don} \cdot lr_{don} \cdot \exp(q_{10_det_rec} \cdot cgt_temp)) \cdot lim_t_{o_2_0} \cdot lim_t_{don_31}$$

recycling of DON using nitrate (denitrification) [mol/kg/day]

$5.8 \cdot h_3o_{plus} + 5.3 \cdot t_{no_3} + t_{don} \rightarrow 0.5 \cdot oh_{minus} + 14.575 \cdot H_2O + 2.65 \cdot t_{n_2} + t_{nh_4} + 6.625 \cdot t_{dic}$

$$p_{don_denit} = (t_{don} \cdot r_{don_rec} \cdot \exp(q_{10_det_rec} \cdot cgt_temp)) \cdot (1.0 - lim_t_{o_2_0}) \cdot lim_t_{no_3_1} \cdot lim_t_{don_31}$$

continued on next page...

Mineralization of DON, e-acceptor sulfate (sulfate reduction) [mol/kg/day]

$7.125 \cdot h3o_{plus} + 3.3125 \cdot S04 + t_{don} \rightarrow 0.5 \cdot oh_{minus} + 13.25 \cdot H2O + 3.3125 \cdot t_{h2s} + t_{nh4} + 6.625 \cdot t_{dic}$

$p_{don_sulf} = (t_{don} \cdot r_{don_rec} \cdot \exp(q10_det_rec \cdot cgt_temp)) \cdot (1.0 - lim_t_{o2_0}) \cdot (1.0 - lim_t_{no3_1}) \cdot lim_t_{don_31}$

decay of cdom due to light [mol/kg/day]

$t_{cdom} \rightarrow$

$p_{cdom_decay} = (t_{cdom} \cdot r_{cdom_decay} \cdot cgt_light / r_{cdom_light}) \cdot lim_t_{cdom_32}$

end of table **Processes**

Auxiliary variables

dissolved inorganic nitrogen [mol/kg]

$din = t_{no3} + t_{nh4}$

squared DIN [mol²/kg²]

$din_sq = din \cdot din$

squared phosphate [mol²/kg²]

$po4_sq = t_{po4} \cdot t_{po4}$

modifies pocp recycling towards Redfield ratio if PO4 is depleted

$ref_p_sw = (1 - (po4_sq / (rfr_p \cdot din_min_lpp \cdot rfr_p \cdot din_min_lpp + po4_sq))) / (1 + \exp(6.0 \cdot (1 - din / (t_{po4} / rfr_p + \epsilon))))$

modifies pocn recycling towards Redfield ratio if DIN is depleted

$ref_n_sw = (1 - (din_sq / (din_min_lpp \cdot din_min_lpp + din_sq))) / (1 + \exp(6.0 \cdot (1 - t_{po4} / rfr_p / (din + \epsilon))))$

continued on next page...

add an additional POCP recycling if PO4 below Redfield but sufficient DIN

lr_pocp = r_pocp_rec*(1 + fac_enh_rec*ref_p_sw)

add an additional DOP recycling if PO4 is below Redfield but sufficient DIN

lr_dop = r_dop_rec*(1 + fac_enh_rec*ref_p_sw)

add an additional POCN recycling if DIN below Redfield but sufficient PO4

lr_pocn = r_pocn_rec*(1 + fac_enh_rec*ref_n_sw)

add an additional DON recycling if DIN below Redfield but sufficient PO4

lr_don = r_don_rec*(1 + fac_enh_rec*ref_n_sw)

end of table **Auxiliary variables**

Constants

DIN half saturation constant for large-cell phytoplankton growth [mol/kg]

din_min_lpp = 1.0E-6

no division by 0

epsilon = 4.5E-17

minimum no3 concentration for recycling of detritus using nitrate (denitrification)

no3_min_det_denit = 1.0E-9

oxygen half-saturation constant for detritus recycling [mol/kg]

o2_min_det_resp = 1.0E-6

q10 rule factor for recycling [1/K]

q10_det_rec = 0.15

recycling rate (detritus to ammonium) at 0°C [1/day]

continued on next page...

Constants, continued from previous page	
r_det_rec =	0.003
redfield ratio C/N	
rfr_c =	6.625
redfield ratio P/N	
rfr_p =	0.0625
recycling rate (poc to dic) at 0°C [1/day]	
r_poc_rec =	0.003
recycling rate (pocp to dic and po4) at 0°C [1/day]	
r_pocp_rec =	0.002
recycling rate (pocn to dic and nh4) at 0°C [1/day]	
r_pocn_rec =	0.002
enhance recyclig of DON,POCN/DOP,POCP in case of limiting DIN/DIP	
fac_enh_rec =	10.0
recycling rate (doc to dic) at 0°C [1/day]	
r_doc_rec =	0.001
recycling rate (don to dic and NH4) at 0°C [1/day]	
r_don_rec =	0.001
recycling rate (dop to dic and PO4) at 0°C [1/day]	
r_dop_rec =	0.001
decay rate of cdom	
r_cdom_decay =	0.0035

| continued on next page... | |

Constants, continued from previous page	
PAR intensity controlling CDOM decay	
r_cdom_light =	40.0
end of table Constants	
Process limitation factors	
lim_t_o2_0 =	1.0-exp(-t_o2/o2_min_det_resp)
lim_t_no3_1 =	1.0-exp(-t_no3/no3_min_det_denit)
lim_t_doc_29 =	theta(t_doc-0.0)
lim_t_dop_30 =	theta(t_dop-0.0)
lim_t_don_31 =	theta(t_don-0.0)
lim_t_cdom_32 =	theta(t_cdom-0.0)
lim_t_det_20 =	theta(t_det-0.0)
lim_t_poc_12 =	theta(t_poc-0.0)
lim_t_pocp_13 =	theta(t_pocp-0.0)
lim_t_pocn_14 =	theta(t_pocn-0.0)
end of table Process limitation factors	

B3.5 Process type BGC/pelagic/phytoplankton

assimilation of nitrate by large-cell phytoplankton [mol/kg/day]

```
t_no3 + rfr_p*t_po4 + rfr_c*t_dic + 6.4375*h2o + 1.1875*h3oplus -> t_lpp + 8.625*t_o2
p_no3_assim_lpp =      (lpp_plus_lpp0*lr_assim_lpp*t_no3/(din+epsilon))*lim_t_no3_9*
                        lim_t_po4_10*lim_t_dic_8
```

assimilation of ammonium by large-cell phytoplankton [mol/kg/day]

```
7.4375*h2o + rfr_c*t_dic + rfr_p*t_po4 + t_nh4 -> 0.8125*h3oplus + 6.625*t_o2 + t_lpp
p_nh4_assim_lpp =      (lpp_plus_lpp0*lr_assim_lpp*t_nh4/(din+epsilon))*lim_t_dic_8*
                        lim_t_po4_10*lim_t_nh4_11
```

assimilation of nitrate by small-cell phytoplankton [mol/kg/day]

```
t_no3 + rfr_p*t_po4 + rfr_c*t_dic + 6.4375*h2o + 1.1875*h3oplus -> t_spp + 8.625*t_o2
p_no3_assim_spp =      (spp_plus_spp0*lr_assim_spp*t_no3/(din+epsilon))*lim_t_no3_9*
                        lim_t_po4_10*lim_t_dic_8
```

assimilation of ammonium by small-cell phytoplankton [mol/kg/day]

```
7.4375*h2o + rfr_c*t_dic + rfr_p*t_po4 + t_nh4 -> 0.8125*h3oplus + 6.625*t_o2 + t_spp
p_nh4_assim_spp =      (spp_plus_spp0*lr_assim_spp*t_nh4/(din+epsilon))*lim_t_dic_8*
                        lim_t_po4_10*lim_t_nh4_11
```

assimilation of ammonium by limnic phytoplankton [mol/kg/day]

```
t_nh4 + rfr_p*t_po4 + rfr_c*t_dic + 7.4375*h2o -> t_lip + 6.625*t_o2 + 0.8125*h3oplus
p_nh4_assim_lip =      (lip_plus_lip0*lr_assim_lip*t_nh4/(din+epsilon))*lim_t_nh4_11*
                        lim_t_po4_10*lim_t_dic_8
```

assimilation of nitrate by limnic phytoplankton [mol/kg/day]

```
1.1875*h3oplus + 6.4375*h2o + rfr_c*t_dic + rfr_p*t_po4 + t_no3 -> 8.625*t_o2 + t_lip
p_no3_assim_lip =      (lip_plus_lip0*lr_assim_lip*t_no3/(din+epsilon))*lim_t_dic_8*
                        lim_t_po4_10*lim_t_no3_9
```

fixation of dinitrogen by diazotroph cyanobacteria [mol/kg/day]

continued on next page...

$7.9375 \cdot h2o + rfr_c \cdot t_dic + rfr_p \cdot t_po4 + 0.5 \cdot t_n2 + 0.1875 \cdot h3oplus \rightarrow 7.375 \cdot t_o2 + t_cya$
 $p_n2_assim_cya = (cya_plus_cya0 \cdot lr_assim_cya) \cdot lim_t_dic_8 \cdot lim_t_po4_10 \cdot lim_t_n2_7$

Production of DOC by LPP [mol/kg/day]

$h2o + t_dic \rightarrow t_o2 + t_doc$
 $p_assim_lpp_doc = (rfr_c \cdot t_lpp \cdot lr_assim_lpp_doc) \cdot lim_t_dic_8$

Production of DOC by SPP [mol/kg/day]

$h2o + t_dic \rightarrow t_o2 + t_doc$
 $p_assim_spp_doc = (rfr_c \cdot t_spp \cdot lr_assim_spp_doc) \cdot lim_t_dic_8$

Production of DOC by LPP [mol/kg/day]

$t_dic + h2o \rightarrow t_doc + t_o2$
 $p_assim_lip_doc = (rfr_c \cdot t_lip \cdot lr_assim_lip_doc) \cdot lim_t_dic_8$

Production of DOC by CYA [mol/kg/day]

$t_dic + h2o \rightarrow t_doc + t_o2$
 $p_assim_cya_doc = (rfr_c \cdot t_cya \cdot lr_assim_cya_doc) \cdot lim_t_dic_8$

Production of DOP by LPP [mol/kg/day]

$3 \cdot h3oplus + 106 \cdot h2o + t_po4 + 106 \cdot t_dic \rightarrow 3 \cdot h2o + 106 \cdot t_o2 + t_dop$
 $p_assim_lpp_dop = (rfr_p \cdot t_lpp \cdot lr_assim_lpp_dop) \cdot lim_t_po4_10 \cdot lim_t_dic_8$

Production of DOP by SPP [mol/kg/day]

$106 \cdot t_dic + t_po4 + 106 \cdot h2o + 3 \cdot h3oplus \rightarrow t_dop + 106 \cdot t_o2 + 3 \cdot h2o$
 $p_assim_spp_dop = (rfr_p \cdot t_spp \cdot lr_assim_spp_dop) \cdot lim_t_dic_8 \cdot lim_t_po4_10$

Production of DOP by LIP [mol/kg/day]

$3 \cdot h3oplus + 106 \cdot h2o + t_po4 + 106 \cdot t_dic \rightarrow 3 \cdot h2o + 106 \cdot t_o2 + t_dop$
 $p_assim_lip_dop = (rfr_p \cdot t_lip \cdot lr_assim_lip_dop) \cdot lim_t_po4_10 \cdot lim_t_dic_8$

continued on next page...

Production of DON by LPP [mol/kg/day]

```
rfr_c*t_dic + t_nh4 + 6.625*H2O + ohminus -> t_don + 6.625*t_o2 + H2O
p_nh4_assim_lpp_don = (t_lpp * lr_assim_lpp_don*t_nh4/(din+epsilon))*lim_t_dic_8*
lim_t_nh4_11
```

Production of DON by LPP [mol/kg/day]

```
h3oplus + 6.625*H2O + t_no3 + rfr_c*t_dic -> 8.625*t_o2 + t_don
p_no3_assim_lpp_don = (t_lpp * lr_assim_lpp_don*t_no3/(din+epsilon))*lim_t_no3_9*
lim_t_dic_8
```

Production of DON by SPP [mol/kg/day]

```
ohminus + 6.625*H2O + t_nh4 + rfr_c*t_dic -> H2O + 6.625*t_o2 + t_don
p_nh4_assim_spp_don = (t_spp * lr_assim_spp_don*t_nh4/(din+epsilon))*lim_t_nh4_11*
lim_t_dic_8
```

Production of DON by SPP [mol/kg/day]

```
rfr_c*t_dic + t_no3 + 6.625*H2O + h3oplus -> t_don + 8.625*t_o2
p_no3_assim_spp_don = (t_spp * lr_assim_spp_don*t_no3/(din+epsilon))*lim_t_dic_8*
lim_t_no3_9
```

Production of DON by LIP [mol/kg/day]

```
ohminus + 6.625*H2O + t_nh4 + rfr_c*t_dic -> H2O + 6.625*t_o2 + t_don
p_nh4_assim_lip_don = (t_lip * lr_assim_lip_don*t_nh4/(din+epsilon))*lim_t_nh4_11*
lim_t_dic_8
```

Production of DON by LIP [mol/kg/day]

```
rfr_c*t_dic + t_no3 + 6.625*H2O + h3oplus -> t_don + 8.625*t_o2
p_no3_assim_lip_don = (t_lip * lr_assim_lip_don*t_no3/(din+epsilon))*lim_t_dic_8*
lim_t_no3_9
```

respiration of POC [mol/kg/day]

```
t_poc + t_o2 -> t_dic + h2o
```

continued on next page...

p_poc_resp = (t_poc * r_poc_rec * exp(q10_det_rec * cgt_temp))*lim_t_o2_0*
lim_t_poc_12

respiration of large-cell phytoplankton [mol/kg/day]

t_lpp + 6.625*t_o2 + 0.8125*h3oplus -> don_fraction*t_don + (1-don_fraction)*t_nh4 +
rfr_p*t_po4 + rfr_c*t_dic + 7.4375*h2o
p_lpp_resp_nh4 = (t_lpp*r_lpp_resp)*lim_t_lpp_15*lim_t_o2_2

respiration of small-cell phytoplankton [mol/kg/day]

0.8125*h3oplus + 6.625*t_o2 + t_spp -> 7.4375*h2o + rfr_c*t_dic + rfr_p*t_po4 + (1-
don_fraction)*t_nh4 + don_fraction*t_don
p_spp_resp_nh4 = (t_spp*r_spp_resp)*lim_t_o2_2*lim_t_spp_16

respiration of limnic phytoplankton [mol/kg/day]

0.8125*h3oplus + 6.625*t_o2 + t_lip -> 7.4375*h2o + rfr_c*t_dic + rfr_p*t_po4 + (1-
don_fraction)*t_nh4 + don_fraction*t_don
p_lip_resp_nh4 = (t_lip*r_lip_resp)*lim_t_o2_2*lim_t_lip_18

respiration of diazotroph cyanobacteria [mol/kg/day]

0.8125*h3oplus + 6.625*t_o2 + t_cya -> 7.4375*h2o + rfr_c*t_dic + rfr_p*t_po4 +
don_fraction*t_don + (1-don_fraction)*t_nh4
p_cya_resp_nh4 = (t_cya*r_cya_resp)*lim_t_o2_2*lim_t_cya_17

mortality of large-cell phytoplankton [mol/kg/day]

t_lpp -> t_det
p_lpp_mort_det = (t_lpp*r_pp_mort*(1+9*theta(5.0e-6-t_o2)))*lim_t_lpp_15

mortality of small-scale phytoplankton [mol/kg/day]

t_spp -> t_det
p_spp_mort_det = (t_spp*r_pp_mort*(1+9*theta(5.0e-6-t_o2)))*lim_t_spp_16

mortality of limnic phytoplankton [mol/kg/day]

continued on next page...

t_lip -> t_det

p_lip_mort_det = (t_lip*r_pp_mort*(1+9*theta(5.0e-6-t_o2)))*lim_t_lip_18

mortality of diazotroph cyanobacteria [mol/kg/day]

t_cya -> t_det

p_cya_mort_det = (t_cya*r_pp_mort*(1+9*theta(5.0e-6-t_o2)))*lim_t_cya_17

mortality of diazotroph cyanobacteria due to strong turbulence [mol/kg/day]

t_cya -> t_det

p_cya_mort_det_diff = (t_cya*r_pp_mort*(r_cya_mort_diff*theta(cgt_diffusivity-
r_cya_mort_thresh)))*lim_t_cya_17

respiration of DOC [mol/kg/day]

t_o2 + t_doc -> h2o + t_dic

p_doc_resp = (t_doc * r_doc_rec * exp(q10_doc_rec * cgt_temp))*lim_t_o2_0*
lim_t_doc_29

end of table **Processes**

Auxiliary variables

square of positive temperature [°C * °C]

temp_sq = max(0.0,cgt_temp)*max(0.0,cgt_temp)

dissolved inorganic nitrogen [mol/kg]

din = t_no3+t_nh4

squared DIN [mol²/kg²]

din_sq = din*din

squared phosphate [mol²/kg²]

po4_sq = t_po4*t_po4

continued on next page...

large-cell phytoplankton plus seed concentration [mol/kg]

lpp_plus_lpp0 = t_lpp+lpp0

small-cell phytoplankton plus seed concentration [mol/kg]

spp_plus_spp0 = t_spp+spp0

limnic phytoplankton plus seed concentration [mol/kg]

lip_plus_lip0 = t_lip+lip0

diazotroph cyanobacteria plus seed concentration [mol/kg]

cya_plus_cya0 = t_cya+cya0

light limitation factor for large-cell phytoplankton growth [1]

temp1 = max(cgt_light/2.0,light_opt_lpp)

lim_light_lpp = cgt_light/temp1*exp(1-cgt_light/temp1)

light limitation factor for small-cell phytoplankton growth [1]

temp1 = max(cgt_light/2.0,light_opt_spp)

lim_light_spp = cgt_light/temp1*exp(1-cgt_light/temp1)

light limitation factor for limnic phytoplankton growth [1]

temp1 = max(cgt_light/2.0,light_opt_lip)

lim_light_lip = cgt_light/temp1*exp(1-cgt_light/temp1)

light limitation factor for diazotroph cyanobacteria growth [1]

temp1 = max(cgt_light/2.0,light_opt_cya)

lim_light_cya = cgt_light/temp1*exp(1-cgt_light/temp1)

growth rate of large-cell phytoplankton, limited by DIN, DIP, light and oxygen [1/day]

continued on next page...

```
lr_assim_lpp =      r_lpp_assim*theta(t_o2-2*t_h2s)*min(din_sq/(din_sq+din_min_lpp*  
                  din_min_lpp),min(po4_sq/(po4_sq+din_min_lpp*din_min_lpp*rfr_p*  
                  rfr_p),lim_light_lpp))
```

growth rate of small-cell phytoplankton, limited by DIN, DIP, light, oxygen and temperature [1/day]

```
lr_assim_spp =      r_spp_assim*theta(t_o2-2*t_h2s)*min(din_sq/(din_sq+din_min_spp*  
                  din_min_spp),min(po4_sq/(po4_sq+din_min_spp*din_min_spp*rfr_p*  
                  rfr_p),lim_light_spp))*(1+temp_sq/(temp_sq+temp_min_spp*  
                  temp_min_spp))
```

growth rate of limnic phytoplankton, limited by DIN, DIP, light, salt and oxygen [1/day]

```
lr_assim_lip =      r_lip_assim*theta(t_o2-2*t_h2s)*min(din_sq/(din_sq+din_min_lip*  
                  din_min_lip),min(po4_sq/(po4_sq+din_min_lip*din_min_lip*rfr_p*  
                  rfr_p),lim_light_lip))*(1/(1+exp(cgt_sali*cgt_sali-sali_max_lip*  
                  sali_max_lip)))
```

growth rate of diazotroph cyanobacteria, limited by DIP, light, oxygen, temperature and salinity [1/day]

```
lr_assim_cya =      r_cya_assim*theta(t_o2-2*t_h2s)*min(po4_sq/(po4_sq+dip_min_cya*  
                  dip_min_cya),lim_light_cya)*(1/(1+exp(temp_switch_cya*  
                  (temp_min_cya-cgt_temp))))*(1/(1+exp(cgt_sali-sali_max_cya)))*  
                  (1/(1+exp(sali_min_cya-cgt_sali)))*(1/(1+exp(nit_switch_cya*(din-  
                  nit_max_cya))))
```

production rate of DOC by LPP

```
lr_assim_lpp_doc =  fac_doc_assim_lpp * r_lpp_assim * theta(t_o2-2*t_h2s) * min(max(1  
                  - din_sq/(din_sq+din_min_lpp*din_min_lpp),1 -  
                  po4_sq/(din_min_lpp*din_min_lpp*rfr_p*rfr_p + po4_sq)),  
                  lim_light_lpp)
```

production rate of DOC by SPP

continued on next page...

```
lr_assim_spp_doc = fac_doc_assim_spp * r_spp_assim * theta(t_o2-2*t_h2s) * min(max(1
- din_sq/(din_sq+din_min_spp*din_min_spp),1 -
po4_sq/(din_min_spp*din_min_spp*rfr_p*rfr_p + po4_sq)),
lim_light_spp)*(1+temp_sq/(temp_sq+temp_min_spp*temp_min_spp))
```

production rate of DOC by CYA

```
lr_assim_cya_doc = fac_doc_assim_cya * r_cya_assim*theta(t_o2-2*t_h2s)*min(1 -
po4_sq/(po4_sq+dip_min_cya*dip_min_cya),lim_light_cya)*(1/(1+
exp(temp_switch_cya*(temp_min_cya-cgt_temp))))*(1/(1+
exp(cgt_sali-sali_max_cya)))*(1/(1+exp(sali_min_cya-cgt_sali)))
```

production rate of DOC by LPP

```
lr_assim_lip_doc = fac_doc_assim_lip * r_lip_assim * theta(t_o2-2*t_h2s) * min(max(1
- din_sq/(din_sq+din_min_lip*din_min_lip),1 -
po4_sq/(din_min_lip*din_min_lip*rfr_p*rfr_p + po4_sq)),
lim_light_lip)*(1/(1+exp(cgt_sali-sali_max_lip))))
```

production rate of DOP by LPP

```
lr_assim_lpp_dop = fac_dop_assim * r_lpp_assim * theta(t_o2-2*t_h2s) * min(min(1 -
din_sq/(din_sq+din_min_lpp*din_min_lpp),po4_sq/(din_min_lpp*
din_min_lpp*rfr_p*rfr_p + po4_sq)), lim_light_lpp)
```

production rate of DOP by SPP

```
lr_assim_spp_dop = fac_dop_assim * r_spp_assim * theta(t_o2-2*t_h2s) * min(min(1 -
din_sq/(din_sq+din_min_spp*din_min_spp),po4_sq/(din_min_spp*
din_min_spp*rfr_p*rfr_p + po4_sq)), lim_light_spp)*(1+
temp_sq/(temp_sq+temp_min_spp*temp_min_spp))
```

production rate of DOP by LPP

continued on next page...

Auxiliary variables, continued from previous page	
lr_assim_lip_dop =	$\text{fac_dop_assim} * \text{r_lip_assim} * \text{theta}(\text{t_o2}-2*\text{t_h2s}) * \min(\min(1 - \text{din_sq}/(\text{din_sq}+\text{din_min_lip}*\text{din_min_lip}), \text{po4_sq}/(\text{din_min_lip}*\text{din_min_lip}*\text{rfr_p}*\text{rfr_p} + \text{po4_sq})), \text{lim_light_lip})*(1/(1+\exp(\text{cgt_sali}-\text{sali_max_lip})))$
production rate of DON by LPP	
lr_assim_lpp_don =	$\text{fac_don_assim} * \text{r_lpp_assim} * \text{theta}(\text{t_o2}-2*\text{t_h2s}) * \min(\min(\text{din_sq}/(\text{din_sq}+\text{din_min_lpp}*\text{din_min_lpp}), 1 - \text{po4_sq}/(\text{din_min_lpp}*\text{din_min_lpp}*\text{rfr_p}*\text{rfr_p} + \text{po4_sq})), \text{lim_light_lpp})$
production rate of DON by SPP	
lr_assim_spp_don =	$\text{fac_don_assim} * \text{r_spp_assim} * \text{theta}(\text{t_o2}-2*\text{t_h2s}) * \min(\min(\text{din_sq}/(\text{din_sq}+\text{din_min_spp}*\text{din_min_spp}), 1 - \text{po4_sq}/(\text{din_min_spp}*\text{din_min_spp}*\text{rfr_p}*\text{rfr_p} + \text{po4_sq})), \text{lim_light_spp})*(1+\text{temp_sq}/(\text{temp_sq}+\text{temp_min_spp}*\text{temp_min_spp}))$
production rate of DON by limnic phytoplankton	
lr_assim_lip_don =	$\text{fac_don_assim} * \text{r_lip_assim} * \text{theta}(\text{t_o2}-2*\text{t_h2s}) * \min(\min(\text{din_sq}/(\text{din_sq}+\text{din_min_lip}*\text{din_min_lip}), 1 - \text{po4_sq}/(\text{din_min_lip}*\text{din_min_lip}*\text{rfr_p}*\text{rfr_p} + \text{po4_sq})), \text{lim_light_lip})*(1/(1+\exp(\text{cgt_sali}-\text{sali_max_lip})))$
end of table Auxiliary variables	
Constants	
seed concentration for diazotroph cyanobacteria [mol/kg]	
cya0 =	9.0E-8
DIN half saturation constant for large-cell phytoplankton growth [mol/kg]	
din_min_lpp =	1.0E-6
continued on next page...	

DIN half saturation constant for small-cell phytoplankton growth [mol/kg]

din_min_spp = 1.6E-7

DIP half saturation constant for diazotroph cyanobacteria growth [mol/kg]

dip_min_cya = 1.0E-8

DIN half saturation constant for limnic phytoplankton growth [mol/kg]

din_min_lip = 1.0E-6

no division by 0

epsilon = 4.5E-17

optimal light for diazotroph cyanobacteria growth [W/m**2]

light_opt_cya = 50.0

optimal light for large-cell phytoplankton growth [W/m**2]

light_opt_lpp = 35.0

optimal light for small-cell phytoplankton growth [W/m**2]

light_opt_spp = 50.0

optimal light for limnic phytoplankton growth [W/m**2]

light_opt_lip = 30.0

seed concentration for limnic phytoplankton [mol/kg]

lip0 = 4.5E-9

seed concentration for large-cell phytoplankton [mol/kg]

lpp0 = 4.5E-9

oxygen half-saturation constant for detritus recycling [mol/kg]

continued on next page...

o2_min_det_resp = 1.0E-6

q10 rule factor for recycling [1/K]

q10_det_rec = 0.15

q10 rule factor for DOC recycling [1/K]

q10_doc_rec = 0.069

maximum rate for nutrient uptake of diazotroph cyanobacteria [1/day]

r_cya_assim = 0.75

respiration rate of cyanobacteria to ammonium [1/day]

r_cya_resp = 0.01

maximum rate for nutrient uptake of large-cell phytoplankton [1/day]

r_lpp_assim = 1.38

respiration rate of large phytoplankton to ammonium [1/day]

r_lpp_resp = 0.075

maximum rate for nutrient uptake of limnic phytoplankton [1/day]

r_lip_assim = 1.38

respiration rate of limnic phytoplankton to ammonium [1/day]

r_lip_resp = 0.075

mortality rate of phytoplankton [1/day]

r_pp_mort = 0.03

enhanced cya mortality due to strong turbulence

r_cya_mort_diff = 40.0

continued on next page...

diffusivity threshold for enhanced cyano mortality

r_cya_mort_thresh = 0.02

maximum rate for nutrient uptake of small-cell phytoplankton [1/day]

r_spp_assim = 0.4

respiration rate of small phytoplankton to ammonium [1/day]

r_spp_resp = 0.0175

redfield ratio C/N

rfr_c = 6.625

redfield ratio P/N

rfr_p = 0.0625

upper salinity limit - diazotroph cyanobacteria [psu]

sali_max_cya = 8.0

lower salinity limit - diazotroph cyanobacteria [psu]

sali_min_cya = 4.0

limits cyano growth in DIN reach environment

nit_max_cya = 5.0E-7

strengs of DIN control for cyano growth

nit_switch_cya = 8.0

lower salinity limit - limnic phytoplankton [psu]

sali_max_lip = 2.0

seed concentration for small-cell phytoplankton [mol/kg]

spp0 = 4.5E-9

continued on next page...

lower temperature limit - diazotroph cyanobacteria [°C]

temp_min_cya = 13.5

strengs of temperature control for cyano growth

temp_switch_cya = 4.0

lower temperature limit - small-cell phytoplankton [°C]

temp_min_spp = 10.0

fraction of DON in respiration products

don_fraction = 0.0

recycling rate (poc to dic) at 0°C [1/day]

r_poc_rec = 0.003

factor modifying DOC assimilation rate of large phytoplankton LPP

fac_doc_assim_lpp = 1.0

factor modifying DOC assimilation rate of cyanobacteria

fac_doc_assim_cya = 1.0

factor modifying DOC assimilation rate of small phytoplankton SPP

fac_doc_assim_spp = 1.0

factor modifying DOC assimilation rate of limnic phytoplankton LIP

fac_doc_assim_lip = 1.0

factor modifying assimilation rate for POCP production

fac_dop_assim = 0.5

factor modifying assimilation rate for POCN production

continued on next page...

Constants, continued from previous page	
fac_don_assim =	1.0
recycling rate (doc to dic) at 0°C [1/day]	
r_doc_rec =	0.001
end of table Constants	
Process limitation factors	
lim_t_n2_7 =	theta(t_n2-0.0)
lim_t_o2_0 =	1.0-exp(-t_o2/o2_min_det_resp)
lim_t_o2_2 =	theta(t_o2-0.0)
lim_t_dic_8 =	theta(t_dic-0.0)
lim_t_nh4_11 =	theta(t_nh4-0.0)
lim_t_no3_9 =	theta(t_no3-0.0)
lim_t_po4_10 =	theta(t_po4-0.0)
lim_t_spp_16 =	theta(t_spp-0.0)
lim_t_lip_18 =	theta(t_lip-0.0)
lim_t_doc_29 =	theta(t_doc-0.0)
lim_t_lpp_15 =	theta(t_lpp-0.0)
lim_t_cya_17 =	theta(t_cya-0.0)
continued on next page...	

B3.6 Process type BGC/pelagic/reoxidation

72

Processes, continued from previous page	
p_sul_oxno3_so4 =	(t_sul*t_no3*k_sul_no3*exp(q10_h2s*cgt_temp))*lim_t_sul_25* lim_t_no3_9
end of table Processes	
Auxiliary variables	
end of table Auxiliary variables	
Constants	
reaction constant h2s oxidation with no3 [kg/mol/day]	
k_h2s_no3 =	800000.0
reaction constant h2s oxidation with o2 [kg/mol/day]	
k_h2s_o2 =	800000.0
reaction constant sul oxidation with no3 [kg/mol/day]	
k_sul_no3 =	20000.0
reaction constant sul oxidation with o2 [kg/mol/day]	
k_sul_o2 =	20000.0
q10 rule factor for oxidation of h2s and sul [1/K]	
q10_h2s =	0.0693
q10 rule factor for nitrification [1/K]	
q10_nit =	0.11
nitrification rate at 0°C [1/day]	
r_nh4_nitrif =	0.05
end of table Constants	

Process limitation factors	
lim_t_o2_2 =	theta(t_o2-0.0)
lim_t_nh4_11 =	theta(t_nh4-0.0)
lim_t_no3_9 =	theta(t_no3-0.0)
lim_t_h2s_24 =	theta(t_h2s-0.0)
lim_t_sul_25 =	theta(t_sul-0.0)
end of table Process limitation factors	

545 5

B3.7 Process type BGC/pelagic/zooplankton

Processes	
grazing of zooplankton eating large-cell phytoplankton [mol/kg/day]	
t_lpp -> t_zoo	
p_lpp_graz_zoo =	((t_zoo+zoo0)*lr_graz_zoo*t_lpp/max(food_zoo,epsilon))* lim_t_lpp_15
grazing of zooplankton eating small-cell phytoplankton [mol/kg/day]	
t_spp -> t_zoo	
p_spp_graz_zoo =	((t_zoo+zoo0)*lr_graz_zoo*t_spp/max(food_zoo,epsilon))* lim_t_spp_16
grazing of zooplankton eating diazotroph cyanobacteria [mol/kg/day]	
t_cya -> t_zoo	
p_cya_graz_zoo =	((t_zoo+zoo0)*lr_graz_zoo*(0.5*t_cya)/max(food_zoo,epsilon))* lim_t_cya_17
continued on next page...	

grazing of zooplankton eating limnic phytoplankton [mol/kg/day]

t_lip -> t_zoo

p_lip_graz_zoo = ((t_zoo+zoo0)*lr_graz_zoo*t_lip/max(food_zoo,epsilon))*
lim_t_lip_18

respiration of zooplankton [mol/kg/day]

0.8125*h3oplus + 6.625*t_o2 + t_zoo -> 7.4375*h2o + rfr_c*t_dic + rfr_p*t_po4 + (1-
don_fraction)*t_nh4 + don_fraction*t_don

p_zoo_resp_nh4 = (zoo_eff*r_zoo_resp)*lim_t_o2_2*lim_t_zoo_19

mortality of zooplankton [mol/kg/day]

t_zoo -> t_det

p_zoo_mort_det = (zoo_eff*r_zoo_mort*(1+9*theta(5.0e-6-t_o2)))*lim_t_zoo_19

end of table **Processes**

Auxiliary variables

square of positive temperature [°C * °C]

temp_sq = max(0.0,cgt_temp)*max(0.0,cgt_temp)

effectice zooplankton concentration assumed for mortality and respiration process [mol/kg]

zoo_eff = t_zoo*t_zoo/zoo_cl

suitable food for zooplankton (weighted with food preferences) [mol/kg]

food_zoo = t_lpp+t_spp+t_lip+0.5*t_cya

growth rate of zooplankton, limited by food, oxygen and temperature [1/day]

lr_graz_zoo = r_zoo_graz*(1-exp(-food_zoo*food_zoo/(food_min_zoo*food_min_zoo))
)*theta(t_o2-2*t_h2s)*(1.0+temp_sq/(temp_opt_zoo*temp_opt_zoo))*
exp(2.0-cgt_temp*2.0/temp_opt_zoo))

end of table **Auxiliary variables**

Constants	
no division by 0	
epsilon =	4.5E-17
Ivlev phytoplankton concentration for zooplankton grazing [mol/kg]	
food_min_zoo =	4.108E-6
maximum zooplankton grazing rate [1/day]	
r_zoo_graz =	0.5
mortality rate of zooplankton [1/day]	
r_zoo_mort =	0.03
respiration rate of zooplankton [1/day]	
r_zoo_resp =	0.01
redfield ratio C/N	
rfr_c =	6.625
redfield ratio P/N	
rfr_p =	0.0625
optimal temperature for zooplankton grazing [°C]	
temp_opt_zoo =	20.0
seed concentration for zooplankton [mol/kg]	
zoo0 =	4.5E-9
zooplankton closure parameter [mol/kg]	
zoo_cl =	9.0E-8
fraction of DON in respiration products	
don_fraction =	0.0
continued on next page...	

Constants, continued from previous page	
end of table Constants	
Process limitation factors	
lim_t_o2_2 =	theta(t_o2-0.0)
lim_t_spp_16 =	theta(t_spp-0.0)
lim_t_zoo_19 =	theta(t_zoo-0.0)
lim_t_lip_18 =	theta(t_lip-0.0)
lim_t_lpp_15 =	theta(t_lpp-0.0)
lim_t_cya_17 =	theta(t_cya-0.0)
end of table Process limitation factors	

5

B3.8 Process type gas_exchange

Processes	
end of table Processes	
Auxiliary variables	
absolute temperature [K]	
temp_k =	cgt_temp + 273.15
temporary value assumed for pH [1]	
continued on next page...	

ph_temp = 0.0-log(h3o)/log(10.0)
calculated iteratively, 10 iterations, initial value = 0.0

self-ionization constant of Water [mol²/kg²]

k_water = exp(-13847.26 / temp_k + 148.96502 - 23.6521 * log(temp_k) +
(118.67/temp_k - 5.977 + 1.0495 * log(temp_k)) * sqrt(cgt_sali) -
0.01615 * cgt_sali)

Solubility of CO2 [mol/kg/Pa]

k0_co2 = exp(9345.17 / temp_k - 60.2409 + 23.3585 * (log(temp_k) -
4.605170186) + cgt_sali*(0.023517 - 0.00023656 * temp_k +
0.00000047036 *temp_k*temp_k))/101325.0

Acid dissociation constant CO2 + 2 H2O <-> HCO3- + H3O+ [mol/kg]

k1_co2 = power(10.0,(-3633.86 / temp_k + 61.2172 - 9.6777 * log(temp_k) +
0.011555 * cgt_sali - 0.0001152 * cgt_sali * cgt_sali))

Acid dissociation constant HCO3- + H2O <-> [CO3 2-] + H3O+ [mol/kg]

k2_co2 = power(10.0,(-471.78 / temp_k - 25.929 + 3.16967 * log(temp_k) +
0.01781 * cgt_sali - 0.0001122 * cgt_sali * cgt_sali))

Acid dissociation constant of boric acid [mol/kg]

k_boron = exp((-8966.9 - 2890.53*sqrt(cgt_sali) - 77.942*cgt_sali + 1.728*
cgt_sali*sqrt(cgt_sali) - 0.0996*cgt_sali*cgt_sali) / temp_k +
148.0248 + 137.1942*sqrt(cgt_sali) + 1.62142*cgt_sali + (-24.4344
- 25.085*sqrt(cgt_sali) - 0.2474*cgt_sali)*log(temp_k) +
0.053105*sqrt(cgt_sali)*temp_k)

Acid dissociation constant H3PO4 + H2O <-> [H2PO4 -] + H3O+ [mol/kg]

k1_po4 = exp(-4576.752/temp_k + 115.525 - 18.453*log(temp_k) + (0.69171 -
106.736/temp_k)*sqrt(cgt_sali) - (0.01844 + 0.65643/temp_k)*
cgt_sali)

continued on next page...

Acid dissociation constant [H₂PO₄⁻] + H₂O <-> [HPO₄²⁻] + H₃O⁺ [mol/kg]

$$k2_po4 = \exp(-8814.715/\text{temp_k} + 172.0883 - 27.927 \cdot \log(\text{temp_k}) + (1.35660 - 160.340/\text{temp_k}) \cdot \sqrt{\text{cgt_sali}} - (0.05778 - 0.37335/\text{temp_k}) \cdot \text{cgt_sali})$$

Acid dissociation constant [HPO₄²⁻] + H₂O <-> [PO₄³⁻] + H₃O⁺ [mol/kg]

$$k3_po4 = \exp(-3070.75/\text{temp_k} - 18.141 + (2.81197 + 17.27039/\text{temp_k}) \cdot \sqrt{\text{cgt_sali}} - (0.09984 + 44.99486/\text{temp_k}) \cdot \text{cgt_sali})$$

Acid dissociation constant H₂S + H₂O <-> HS⁻ + H₃O⁺ [mol/kg]

$$k1_h2s = \exp(-3131.42/\text{temp_k} + 5.818 + 0.368 \cdot (\text{power}(\max(0.0, \text{cgt_sali}), (1.0/3.0))))$$

total concentration of boron [mol/kg]

$$\text{boron_total} = 0.000416 \cdot \text{cgt_sali}/35.0$$

boron alkalinity [mol/kg]

$$\text{alk_boron} = \text{boron_total} \cdot k_boron / (k_boron + h3o)$$

calculated iteratively, 10 iterations, initial value = 0.0

hydrogen sulfide alkalinity [mol/kg]

$$\text{alk_h2s} = t_h2s \cdot k1_h2s / (k1_h2s + h3o)$$

calculated iteratively, 10 iterations, initial value = 0.0

water alkalinity [mol/kg]

$$\text{alk_water} = k_water / h3o - h3o$$

calculated iteratively, 10 iterations, initial value = 0.0

denominator in phosphate alkalinity formula [mol³/kg³]

$$\text{alk_po4_denominator} = (h3o \cdot h3o \cdot h3o + k1_po4 \cdot h3o \cdot h3o + k1_po4 \cdot k2_po4 \cdot h3o + k1_po4 \cdot k2_po4 \cdot k3_po4)$$

continued on next page...

calculated iteratively, 10 iterations, initial value = 0.0

phosphate alkalinity [mol/kg]

$$\text{alk_po4} = \frac{t_po4 * (k1_po4 * k2_po4 * h3o + 2.0 * k1_po4 * k2_po4 * k3_po4 - h3o * h3o * h3o)}{\text{alk_po4_denominator}}$$

calculated iteratively, 10 iterations, initial value = 0.0

denominator in carbonate alkalinity formula [mol2/kg2]

$$\text{alk_co2_denominator} = (h3o * h3o + k1_co2 * h3o + k1_co2 * k2_co2)$$

calculated iteratively, 10 iterations, initial value = 0.0

carbonate alkalinity [mol/kg]

$$\text{alk_co2} = \frac{t_dic * k1_co2 * (h3o + 2 * k2_co2)}{\text{alk_co2_denominator}}$$

calculated iteratively, 10 iterations, initial value = 0.0

error in total alkalinity calculation at the assumed pH [mol/kg]

$$\text{alk_residual} = t_alk - \text{alk_co2} - \text{alk_po4} - \text{alk_boron} - \text{alk_h2s} - \text{alk_water}$$

calculated iteratively, 10 iterations, initial value = 0.0

derivative of phosphate alkalinity with respect to h3o [1]

$$\begin{aligned} \text{dalkp_dh3o} = & \frac{t_po4 * (0.0 - k1_po4 * h3o * h3o * h3o * h3o - 4 * k1_po4 * k2_po4 * h3o * h3o * h3o - \\ & (k1_po4 * k1_po4 * k2_po4 + 9 * k1_po4 * k2_po4 * k3_po4) * h3o * h3o - 4 * k1_po4 * \\ & k1_po4 * k2_po4 * k3_po4 * h3o - k1_po4 * k1_po4 * k2_po4 * k2_po4 * k3_po4)}{(\text{alk_po4_denominator} * \text{alk_po4_denominator})} \end{aligned}$$

calculated iteratively, 10 iterations, initial value = 0.0

derivative of carbonate alkalinity with respect to h3o [1]

$$\text{dalkc_dh3o} = \frac{t_dic * (0.0 - k1_co2 * h3o * h3o - k1_co2 * k1_co2 * k2_co2 - 4 * k1_co2 * k2_co2 * h3o)}{(\text{alk_co2_denominator} * \text{alk_co2_denominator})}$$

calculated iteratively, 10 iterations, initial value = 0.0

derivative of residual_alk with respect to pH [mol/kg]

continued on next page...

Auxiliary variables, continued from previous page	
dalkresidual_d pH =	0.0-log(10.0)*h3o*(alk_boron/(k_boron+h3o)+alk_h2s/(k1_h2s+h3o)+ k_water/(h3o*h3o)+1-dalkp_dh3o-dalkc_dh3o)
calculated iteratively, 10 iterations, initial value = 0.0	
newly determined pH value [1]	
temp1 =	alk_residual/dalkresidual_d pH
ph =	ph_temp - temp1 + theta(abs(temp1) - 1)*0.5*temp1
calculated iteratively, 10 iterations, initial value = 0.0	
h3o ion concentration [mol/kg]	
h3o =	power(10.0,0.0-max(1.0,min(13.0,ph)))
calculated iteratively, 10 iterations, initial value = 1.0e-8	
co2 partial pressure [Pa]	
pco2 =	t_dic / k0_co2 / (1 + k1_co2/h3o + k1_co2*k2_co2/h3o/h3o)
oxygen saturation concentration [mol/kg]	
o2_sat =	(10.18e0+((5.306e-3-4.8725e-5*cgt_temp)*cgt_temp-0.2785e0)* cgt_temp+cgt_sali*((2.2258e-3+(4.39e-7*cgt_temp-4.645e-5)* cgt_temp)*cgt_temp-6.33e-2))*44.66e0*1e-6
dissolved molecular nitrogen saturation concentration [mol/kg]	
temp1 =	log((298.15-cgt_temp)/(273.15+cgt_temp))
temp2 =	temp1*temp1
temp3 =	temp2*temp1
n2_sat =	1e-6*exp(6.42931 + 2.92704*temp1 + 4.32531*temp2 + 4.69149*temp3 + cgt_sali*(0.0 -7.44129e-3 - 8.02566e-3*temp1 - 1.46775e-2* temp2))
end of table Auxiliary variables	

Constants	
atmospheric partial pressure of CO2 [Pa]	
patm_co2 =	38.0
piston velocity for co2 surface flux [m/d]	
w_co2_stf =	4.0
piston velocity for n2 surface flux [m/d]	
w_n2_stf =	5.0
piston velocity for oxygen surface flux [m/d]	
w_o2_stf =	5.0
end of table Constants	
Process limitation factors	
lim_t_n2_7 =	theta(t_n2-0.0)
lim_t_o2_2 =	theta(t_o2-0.0)
lim_t_dic_8 =	theta(t_dic-0.0)
end of table Process limitation factors	

5

550 **B3.9** **Process type physics/erosion**

Processes	
sedimentary detritus erosion (sediment only) [mol/m ² /day]	
t_sed -> t_det	
p_sed_ero_det =	(erosion_is_active*r_sed_ero*sed_active)*lim_t_sed_21
continued on next page...	

erosion of iron PO4 (sediment only) [mol/m²/day]

t_ips -> t_ipw

p_ips_ero_ipw = (erosion_is_active*r_ips_ero*t_ips)*lim_t_ips_23

sedimentary poc erosion (sediment only) [mol/m²/day]

t_sed_poc -> t_poc

p_sed_ero_poc = (erosion_is_active*r_sed_ero*poc_active)*lim_t_sed_poc_22

sedimentary pocn erosion (sediment only) [mol/m²/day]

t_sed_pocn -> t_pocn

p_sed_ero_pocn = (erosion_is_active*r_sed_ero*pocn_active)*lim_t_sed_pocn_27

sedimentary pocp erosion (sediment only) [mol/m²/day]

t_sed_pocp -> t_pocp

p_sed_ero_pocp = (erosion_is_active*r_sed_ero*pocp_active)*lim_t_sed_pocp_28

end of table **Processes**

Auxiliary variables

total carbon in sediment layer [mol/m²]

sed_tot = t_sed*rfr_c + t_sed_poc + t_sed_pocn*rfr_c + t_sed_pocp*rfr_cp

total carbon in active sediment layer [mol/m²]

sed_tot_active = max(0.0,min(sed_tot,sed_max*rfr_c))

detritus in active sediment layer [mol/m²]

sed_active = sed_tot_active * t_sed/sed_tot

switch (1=erosion, 0=no erosion) which depends on the combined bottom stress of currents and waves

continued on next page...

Auxiliary variables, continued from previous page	
erosion_is_active =	theta(cgt_current_wave_stress - critical_stress)
poc in active sediment layer [mol/m**2]	
poc_active =	sed_tot_active * t_sed_poc/sed_tot
pocn in active sediment layer [mol/m**2]	
pocn_active =	sed_tot_active * t_sed_pocn/sed_tot
pocp in active sediment layer [mol/m**2]	
pocp_active =	sed_tot_active * t_sed_pocp/sed_tot
end of table Auxiliary variables	
Constants	
critical shear stress for sediment erosion [N/m2]	
critical_stress =	0.016
erosion rate for iron PO4 [1/day]	
r_ips_ero =	6.0
maximum sediment detritus erosion rate [1/day]	
r_sed_ero =	6.0
redfield ratio C/N	
rfr_c =	6.625
redfield ratio C/P	
rfr_cp =	106.0
maximum sediment detritus concentration that feels erosion [mol/m**2]	
sed_max =	1.0
continued on next page...	

Constants, continued from previous page	
end of table Constants	
Process limitation factors	
lim_t_sed_21 =	theta(t_sed-0.0)
lim_t_ips_23 =	theta(t_ips-0.0)
lim_t_sed_poc_22 =	theta(t_sed_poc-0.0)
lim_t_sed_pocn_27 =	theta(t_sed_pocn-0.0)
lim_t_sed_pocp_28 =	theta(t_sed_pocp-0.0)
end of table Process limitation factors	

5

B3.10 Process type physics/parametrization_deep_burial

Processes	
burial of detritus deeper than max_sed (sediment only) [mol/m ² /day]	
t_sed ->	
p_sed_burial =	((sed_tot-sed_tot_burial)/cgt_timestep*t_sed/sed_tot)* lim_t_sed_21
burial of iron PO4 (sediment only) [mol/m ² /day]	
t_ips ->	
p_ips_burial =	(fac_ips_burial*(sed_tot-sed_tot_burial)/cgt_timestep* t_ips/sed_tot)*lim_t_ips_23
continued on next page...	

burial of poc deeper than max_sed (sediment only) [mol/m²/day]

t_sed_poc ->

p_poc_burial = ((sed_tot-sed_tot_burial)/cgt_timestep*t_sed_poc/sed_tot)*
lim_t_sed_poc_22

burial of pocn deeper than max_sed (sediment only) [mol/m²/day]

t_sed_pocn ->

p_pocn_burial = ((sed_tot-sed_tot_burial)/cgt_timestep*t_sed_pocn/sed_tot)*
lim_t_sed_pocn_27

burial of pocp deeper than max_sed (sediment only) [mol/m²/day]

t_sed_pocp ->

p_pocp_burial = ((sed_tot-sed_tot_burial)/cgt_timestep*t_sed_pocp/sed_tot)*
lim_t_sed_pocp_28

end of table **Processes**

Auxiliary variables

total carbon in sediment layer [mol/m²]

sed_tot = t_sed*rfr_c + t_sed_poc + t_sed_pocn*rfr_c + t_sed_pocp*rfr_cp

total carbon in sediment layer before burial [mol/m²]

sed_tot_burial = max(0.0,min(sed_tot,sed_burial*rfr_c))

end of table **Auxiliary variables**

Constants

redfield ratio C/N

rfr_c = 6.625

continued on next page...

Constants, continued from previous page	
redfield ratio C/P	
rfr_cp =	106.0
maximum sediment load before burial	
sed_burial =	1.0
reduced burial of t_ips, mimicing resolving iron-P complexes in deeper sediment and subsequent upward PO4 flux	
fac_ips_burial =	0.5
end of table Constants	
Process limitation factors	
lim_t_sed_21 =	theta(t_sed-0.0)
lim_t_ips_23 =	theta(t_ips-0.0)
lim_t_sed_poc_22 =	theta(t_sed_poc-0.0)
lim_t_sed_pocn_27 =	theta(t_sed_pocn-0.0)
lim_t_sed_pocp_28 =	theta(t_sed_pocp-0.0)
end of table Process limitation factors	

5

B3.11 Process type physics/sedimentation

Processes
detritus sedimentation (sediment only) [mol/m²/day]
continued on next page...

t_det -> t_sed

p_det_sedi_sed = ((1.0-erosion_is_active)*(0.0-w_det_sedi)*t_det*cgt_density)*
lim_t_det_20

sedimentation of iron PO4 (sediment only) [mol/m²/day]

t_ipw -> t_ips

p_ipw_sedi_ips = ((1.0-erosion_is_active)*(0.0-w_ipw_sedi)*t_ipw*cgt_density)*
lim_t_ipw_26

poc sedimentation (sediment only) [mol/m²/day]

t_poc -> t_sed_poc

p_poc_sedi_sed = ((1.0-erosion_is_active)*(0.0-w_poc_var)*t_poc*cgt_density)*
lim_t_poc_12

pocn sedimentation (sediment only) [mol/m²/day]

t_pocn -> t_sed_pocn

p_pocn_sedi_sed = ((1.0-erosion_is_active)*(0.0-w_pocn_sedi)*t_pocn*cgt_density)*
lim_t_pocn_14

pocp sedimentation (sediment only) [mol/m²/day]

t_pocp -> t_sed_pocp

p_pocp_sedi_sed = ((1.0-erosion_is_active)*(0.0-w_pocp_sedi)*t_pocp*cgt_density)*
lim_t_pocp_13

end of table **Processes**

Auxiliary variables

**switch (1=erosion, 0=no erosion) which depends on the combined bottom stress of
currents and waves**

erosion_is_active = theta(cgt_current_wave_stress - critical_stress)

continued on next page...

Auxiliary variables, continued from previous page	
depth dependent POC sinking speed	
w_poc_var =	martin_fac_poc * cgt_bottomdepth * (-1.0)
end of table Auxiliary variables	
Constants	
critical shear stress for sediment erosion [N/m2]	
critical_stress =	0.016
sedimentation velocity (negative for downward) [m/day]	
w_det_sedi =	-2.25
sedimentation velocity for iron PO4 [m/day]	
w_ipw_sedi =	-0.5
sedimentation velocity (negative for downward) [m/day]	
w_pocp_sedi =	-0.05
sedimentation velocity (negative for downward) [m/day]	
w_pocn_sedi =	-0.05
[1/d], depth dependence of POC sinking speed	
martin_fac_poc =	0.01
end of table Constants	
Process limitation factors	
lim_t_ipw_26 =	theta(t_ipw-0.0)
lim_t_det_20 =	theta(t_det-0.0)
continued on next page...	

Process limitation factors, continued from previous page	
lim_t_poc_12 =	theta(t_poc-0.0)
lim_t_pocp_13 =	theta(t_pocp-0.0)
lim_t_pocn_14 =	theta(t_pocn-0.0)
end of table Process limitation factors	

555 5

B3.12 Process type standard

Processes	
particle formation from DOC [mol/kg/day]	
t_doc -> t_poc	
p_doc2pco =	(t_doc * r_doc2poc)*lim_t_doc_29
particle formation from DOP [mol/kg/day]	
t_dop -> t_pocp	
p_dop2pocp =	(t_dop * r_dop2pocp)*lim_t_dop_30
particle formation from DON [mol/kg/day]	
t_don -> t_pocn	
p_don2pocn =	(t_don * r_don2pocn)*lim_t_don_31
end of table Processes	
Auxiliary variables	
end of table Auxiliary variables	

Constants	
POC formation rate	
r_doc2poc =	0.01
POCN formation rate	
r_don2pocn =	0.01
POCP formation rate	
r_dop2pocp =	0.01
end of table Constants	
Process limitation factors	
lim_t_doc_29 =	theta(t_doc-0.0)
lim_t_dop_30 =	theta(t_dop-0.0)
lim_t_don_31 =	theta(t_don-0.0)
end of table Process limitation factors	

B4 Tracer equations

Tracer equations	
Change of: dissolved molecular nitrogen	
$\frac{d}{dt} \text{ t_n2} =$	
+ (p_poc_denit)*(0.4)	recycling of POC using nitrate (denitrification)
+ (p_pocp_denit)*(42.4)	recycling of POC using nitrate (denitrification)
+ (p_pocn_denit)*(2.65)	recycling of POCN using nitrate (denitrification)
continued on next page...	

+ (p_det_denit_nh4)*(2.65)	recycling of detritus using nitrate (denitrification)
+ (p_nh4_nitdenit_n2)*(0.5)	coupled nitrification and denitrification after
/(cgt_cellheight*cgt_density)	mineralization of detritus in oxic sediments
+ (p_sed_denit_nh4)*(2.65)	recycling of sedimentary detritus to ammonium
/(cgt_cellheight*cgt_density)	using nitrate (denitrification)
+ (p_sed_poc_denit)*(0.4)	recycling of sedimentary poc to dic using nitrate
/(cgt_cellheight*cgt_density)	(denitrification)
+ (p_h2s_oxno3_sul)*(0.2)	oxidation of hydrogen sulfide with nitrate
+ (p_sul_oxno3_so4)*(0.6)	oxidation of elemental sulfur with nitrate
+ (p_sed_pocn_denit)*(2.65)	recycling of sedimentary pocn to dic and NH4 using
/(cgt_cellheight*cgt_density)	nitrate (denitrification)
+ (p_sed_pocp_denit)*(42.4)	recycling of sedimentary pocp to dic and PO4 using
/(cgt_cellheight*cgt_density)	nitrate (denitrification)
+ (p_nh4_nitdenit_pocn_n2)*(0.5)	coupled nitrification and denitrification after
/(cgt_cellheight*cgt_density)	mineralization of pocn-detritus in oxic sediments
+ (p_doc_denit)*(0.4)	recycling of DOC using nitrate (denitrification)
+ (p_dop_denit)*(42.4)	recycling of DOP using nitrate (denitrification)
+ (p_don_denit)*(2.65)	recycling of DON using nitrate (denitrification)
- (p_n2_assim_cya)*(0.5)	fixation of dinitrogen by diazotroph cyanobacteria

continued on next page...

Change of: dissolved oxygen

$\frac{d}{dt} \text{t_o2} =$	
+ (p_no3_assim_lpp)*(8.625)	assimilation of nitrate by large-cell phytoplankton
+ (p_nh4_assim_lpp)*(6.625)	assimilation of ammonium by large-cell phytoplankton
+ (p_no3_assim_spp)*(8.625)	assimilation of nitrate by small-cell phytoplankton
+ (p_nh4_assim_spp)*(6.625)	assimilation of ammonium by small-cell phytoplankton
+ (p_nh4_assim_lip)*(6.625)	assimilation of ammonium by limnic phytoplankton
+ (p_no3_assim_lip)*(8.625)	assimilation of nitrate by limnic phytoplankton
+ (p_n2_assim_cya)*(7.375)	fixation of dinitrogen by diazotroph cyanobacteria
+ p_assim_lpp_doc	Production of DOC by LPP
+ p_assim_spp_doc	Production of DOC by SPP
+ p_assim_lip_doc	Production of DOC by LPP
+ p_assim_cya_doc	Production of DOC by CYA
+ (p_assim_lpp_dop)*(106)	Production of DOP by LPP
+ (p_assim_spp_dop)*(106)	Production of DOP by SPP

continued on next page...

+ (p_assim_lip_dop)*(106)	Production of DOP by LIP
+ (p_nh4_assim_lpp_don)*(6.625)	Production of DON by LPP
+ (p_no3_assim_lpp_don)*(8.625)	Production of DON by LPP
+ (p_nh4_assim_spp_don)*(6.625)	Production of DON by SPP
+ (p_no3_assim_spp_don)*(8.625)	Production of DON by SPP
+ (p_nh4_assim_lip_don)*(6.625)	Production of DON by LIP
+ (p_no3_assim_lip_don)*(8.625)	Production of DON by LIP
- p_poc_resp	respiration of POC
- (p_pocp_resp)*(106)	respiration of POCP
- (p_pocn_resp)*(6.625)	respiration of POCN
- (p_lpp_resp_nh4)*(6.625)	respiration of large-cell phytoplankton
- (p_spp_resp_nh4)*(6.625)	respiration of small-cell phytoplankton
- (p_lip_resp_nh4)*(6.625)	respiration of limnic phytoplankton
- (p_cya_resp_nh4)*(6.625)	respiration of diazotroph cyanobacteria
- (p_zoo_resp_nh4)*(6.625)	respiration of zooplankton
- (p_nh4_nit_no3)*(2)	nitrification

continued on next page...

- (p_det_resp_nh4)*(6.625)	recycling of detritus using oxygen (respiration)
- (p_sed_resp_nh4)*(6.625) /(cgt_cellheight*cgt_density)	recycling of sedimentary detritus to ammonium using oxygen (respiration)
- (p_nh4_nitdenit_n2)*(0.75) /(cgt_cellheight*cgt_density)	coupled nitrification and denitrification after mineralization of detritus in oxic sediments
- p_sed_poc_resp/(cgt_cellheight* cgt_density)	recycling of sedimentary poc to dic using oxygen (respiration)
- (p_h2s_oxo2_sul)*(0.5)	oxidation of hydrogen sulfide with oxygen
- (p_sul_oxo2_so4)*(1.5)	oxidation of elemental sulfur with oxygen
- (p_sed_pocn_resp)*(6.625) /(cgt_cellheight*cgt_density)	recycling of sedimentary pocn to dic and NH4 using oxygen (respiration)
- (p_sed_pocp_resp)*(106) /(cgt_cellheight*cgt_density)	recycling of sedimentary pocp to dic and PO4 using oxygen (respiration)
- (p_nh4_nitdenit_pocn_n2)* (0.75)/(cgt_cellheight* cgt_density)	coupled nitrification and denitrification after mineralization of pocn-detritus in oxic sediments
- p_doc_resp	respiration of DOC
- (p_dop_resp)*(106)	respiration of DOP
- (p_don_resp)*(6.625)	respiration of DON

continued on next page...

Change of: dissolved inorganic carbon, treated as carbon dioxide

$\frac{d}{dt} \text{ t_dic} =$	
+ p_poc_resp	respiration of POC
+ p_poc_denit	recycling of POC using nitrate (denitrification)
+ p_poc_sulf	Mineralization of POC, e-acceptor sulfate (sulfate reduction)
+ (p_pocp_resp)*(106)	respiration of POCP
+ (p_pocp_denit)*(106)	recycling of POC using nitrate (denitrification)
+ (p_pocp_sulf)*(106)	Mineralization of POC, e-acceptor sulfate (sulfate reduction)
+ (p_pocn_resp)*(6.625)	respiration of POCN
+ (p_pocn_denit)*(6.625)	recycling of POCN using nitrate (denitrification)
+ (p_pocn_sulf)*(6.625)	Mineralization of POCN, e-acceptor sulfate (sulfate reduction)
+ (p_lpp_resp_nh4)*(rfr_c)	respiration of large-cell phytoplankton
+ (p_spp_resp_nh4)*(rfr_c)	respiration of small-cell phytoplankton
+ (p_lip_resp_nh4)*(rfr_c)	respiration of limnic phytoplankton
+ (p_cya_resp_nh4)*(rfr_c)	respiration of diazotroph cyanobacteria

continued on next page...

+ (p_zoo_resp_nh4)*(rfr_c)	respiration of zooplankton
+ (p_det_resp_nh4)*(rfr_c)	recycling of detritus using oxygen (respiration)
+ (p_det_denit_nh4)*(rfr_c)	recycling of detritus using nitrate (denitrification)
+ (p_det_sulf_nh4)*(rfr_c)	recycling of detritus using sulfate (sulfate reduction)
+ (p_sed_resp_nh4)*(rfr_c) /(cgt_cellheight*cgt_density)	recycling of sedimentary detritus to ammonium using oxygen (respiration)
+ (p_sed_denit_nh4)*(rfr_c) /(cgt_cellheight*cgt_density)	recycling of sedimentary detritus to ammonium using nitrate (denitrification)
+ (p_sed_sulf_nh4)*(rfr_c) /(cgt_cellheight*cgt_density)	recycling of sedimentary detritus to ammonium using sulfate (sulfate reduction)
+ p_sed_poc_resp/(cgt_cellheight* cgt_density)	recycling of sedimentary poc to dic using oxygen (respiration)
+ p_sed_poc_denit/(cgt_cellheight* cgt_density)	recycling of sedimentary poc to dic using nitrate (denitrification)
+ p_sed_poc_sulf/(cgt_cellheight* cgt_density)	recycling of sedimentary poc to dic using sulfate (sulfate reduction)
+ (p_sed_pocn_resp)*(6.625) /(cgt_cellheight*cgt_density)	recycling of sedimentary pocn to dic and NH4 using oxygen (respiration)

continued on next page...

+ (p_sed_pocp_resp)*(106) /(cgt_cellheight*cgt_density)	recycling of sedimentary pocp to dic and PO4 using oxygen (respiration)
+ (p_sed_pocn_denit)*(6.625) /(cgt_cellheight*cgt_density)	recycling of sedimentary pocn to dic and NH4 using nitrate (denitrification)
+ (p_sed_pocp_denit)*(106) /(cgt_cellheight*cgt_density)	recycling of sedimentary pocp to dic and PO4 using nitrate (denitrification)
+ (p_sed_pocn_sulf)*(6.625) /(cgt_cellheight*cgt_density)	recycling of sedimentary pocn to dic and NH4 using sulfate (sulfate reduction)
+ (p_sed_pocp_sulf)*(106) /(cgt_cellheight*cgt_density)	recycling of sedimentary pocp to dic and PO4 using sulfate (sulfate reduction)
+ p_doc_resp	respiration of DOC
+ p_doc_denit	recycling of DOC using nitrate (denitrification)
+ p_doc_sulf	Mineralization of DOC, e-acceptor sulfate (sulfate reduction)
+ (p_dop_resp)*(106)	respiration of DOP
+ (p_dop_denit)*(106)	recycling of DOP using nitrate (denitrification)
+ (p_dop_sulf)*(106)	Mineralization of DOP, e-acceptor sulfate (sulfate reduction)
+ (p_don_resp)*(6.625)	respiration of DON
+ (p_don_denit)*(6.625)	recycling of DON using nitrate (denitrification)

continued on next page...

+ (p_don_sulf)*(6.625)	Mineralization of DON, e-acceptor sulfate (sulfate reduction)
- (p_no3_assim_lpp)*(rfr_c)	assimilation of nitrate by large-cell phytoplankton
- (p_nh4_assim_lpp)*(rfr_c)	assimilation of ammonium by large-cell phytoplankton
- (p_no3_assim_spp)*(rfr_c)	assimilation of nitrate by small-cell phytoplankton
- (p_nh4_assim_spp)*(rfr_c)	assimilation of ammonium by small-cell phytoplankton
- (p_nh4_assim_lip)*(rfr_c)	assimilation of ammonium by limnic phytoplankton
- (p_no3_assim_lip)*(rfr_c)	assimilation of nitrate by limnic phytoplankton
- (p_n2_assim_cya)*(rfr_c)	fixation of dinitrogen by diazotroph cyanobacteria
- p_assim_lpp_doc	Production of DOC by LPP
- p_assim_spp_doc	Production of DOC by SPP
- p_assim_lip_doc	Production of DOC by LPP
- p_assim_cya_doc	Production of DOC by CYA
- (p_assim_lpp_dop)*(106)	Production of DOP by LPP
- (p_assim_spp_dop)*(106)	Production of DOP by SPP

continued on next page...

- (p_assim_lip_dop)*(106) Production of DOP by LIP

- (p_nh4_assim_lpp_don)*(rfr_c) Production of DON by LPP

- (p_no3_assim_lpp_don)*(rfr_c) Production of DON by LPP

- (p_nh4_assim_spp_don)*(rfr_c) Production of DON by SPP

- (p_no3_assim_spp_don)*(rfr_c) Production of DON by SPP

- (p_nh4_assim_lip_don)*(rfr_c) Production of DON by LIP

- (p_no3_assim_lip_don)*(rfr_c) Production of DON by LIP

Change of: ammonium

$$\frac{d}{dt} t_{nh4} =$$

- + p_pocn_resp respiration of POCN

- + p_pocn_denit recycling of POCN using nitrate (denitrification)

- + p_pocn_sulf Mineralization of POCN, e-acceptor sulfate (sulfate reduction)

- + (p_lpp_resp_nh4)*((1-don_fraction)) respiration of large-cell phytoplankton

- + (p_spp_resp_nh4)*((1-don_fraction)) respiration of small-cell phytoplankton

- + (p_lip_resp_nh4)*((1-don_fraction)) respiration of limnic phytoplankton

continued on next page...

+ (p_cya_resp_nh4)*((1- don_fraction))	respiration of diazotroph cyanobacteria
+ (p_zoo_resp_nh4)*((1- don_fraction))	respiration of zooplankton
+ p_det_resp_nh4	recycling of detritus using oxygen (respiration)
+ p_det_denit_nh4	recycling of detritus using nitrate (denitrification)
+ p_det_sulf_nh4	recycling of detritus using sulfate (sulfate reduction)
+ p_sed_resp_nh4/(cgt_cellheight* cgt_density)	recycling of sedimentary detritus to ammonium using oxygen (respiration)
+ p_sed_denit_nh4/(cgt_cellheight* cgt_density)	recycling of sedimentary detritus to ammonium using nitrate (denitrification)
+ p_sed_sulf_nh4/(cgt_cellheight* cgt_density)	recycling of sedimentary detritus to ammonium using sulfate (sulfate reduction)
+ p_sed_pocn_resp/(cgt_cellheight* cgt_density)	recycling of sedimentary pocn to dic and NH4 using oxygen (respiration)
+ p_sed_pocn_denit/(cgt_cellheight* cgt_density)	recycling of sedimentary pocn to dic and NH4 using nitrate (denitrification)

continued on next page...

+	recycling of sedimentary pocn to dic and NH4 using p_sed_pocn_sulf/(cgt_cellheight*sulfate (sulfate reduction) cgt_density)
+ p_don_resp	respiration of DON
+ p_don_denit	recycling of DON using nitrate (denitrification)
+ p_don_sulf	Mineralization of DON, e-acceptor sulfate (sulfate reduction)
- p_nh4_assim_lpp	assimilation of ammonium by large-cell phytoplankton
- p_nh4_assim_spp	assimilation of ammonium by small-cell phytoplankton
- p_nh4_assim_lip	assimilation of ammonium by limnic phytoplankton
- p_nh4_assim_lpp_don	Production of DON by LPP
- p_nh4_assim_spp_don	Production of DON by SPP
- p_nh4_assim_lip_don	Production of DON by LIP
- p_nh4_nit_no3	nitrification
-	coupled nitrification and denitrification after p_nh4_nitdenit_n2/(cgt_cellheightmineralization of detritus in oxic sediments cgt_density)

continued on next page...

- coupled nitrification and denitrification after
p_nh4_nitdenit_pocn_n2/(cgt_cellmineralization of pocn-detritus in oxic sediments
cgt_density)

Change of: nitrate

$\frac{d}{dt} \text{t_no3} =$	
+ p_nh4_nit_no3	nitrification
- p_no3_assim_lpp	assimilation of nitrate by large-cell phytoplankton
- p_no3_assim_spp	assimilation of nitrate by small-cell phytoplankton
- p_no3_assim_lip	assimilation of nitrate by limnic phytoplankton
- p_no3_assim_lpp_don	Production of DON by LPP
- p_no3_assim_spp_don	Production of DON by SPP
- p_no3_assim_lip_don	Production of DON by LIP
- (p_poc_denit)*(0.8)	recycling of POC using nitrate (denitrification)
- (p_pocp_denit)*(84.8)	recycling of POC using nitrate (denitrification)
- (p_pocn_denit)*(5.3)	recycling of POCN using nitrate (denitrification)
- (p_det_denit_nh4)*(5.3)	recycling of detritus using nitrate (denitrification)
- (p_sed_denit_nh4)*(5.3)	recycling of sedimentary detritus to ammonium
/ (cgt_cellheight*cgt_density)	using nitrate (denitrification)

continued on next page...

- (p_sed_poc_denit)*(0.8) /(cgt_cellheight*cgt_density)	recycling of sedimentary poc to dic using nitrate (denitrification)
- (p_h2s_oxno3_sul)*(0.4)	oxidation of hydrogen sulfide with nitrate
- (p_sul_oxno3_so4)*(1.2)	oxidation of elemental sulfur with nitrate
- (p_sed_pocn_denit)*(5.3) /(cgt_cellheight*cgt_density)	recycling of sedimentary pocn to dic and NH4 using nitrate (denitrification)
- (p_sed_pocp_denit)*(84.8) /(cgt_cellheight*cgt_density)	recycling of sedimentary pocp to dic and PO4 using nitrate (denitrification)
- (p_doc_denit)*(0.8)	recycling of DOC using nitrate (denitrification)
- (p_dop_denit)*(84.8)	recycling of DOP using nitrate (denitrification)
- (p_don_denit)*(5.3)	recycling of DON using nitrate (denitrification)

Change of: phosphate

$$\frac{d}{dt} t_{po4} =$$

+ p_pocp_resp	respiration of POCP
+ p_pocp_denit	recycling of POC using nitrate (denitrification)
+ p_pocp_sulf	Mineralization of POC, e-acceptor sulfate (sulfate reduction)
+ (p_lpp_resp_nh4)*(rfr_p)	respiration of large-cell phytoplankton
+ (p_spp_resp_nh4)*(rfr_p)	respiration of small-cell phytoplankton

continued on next page...

+ (p_lip_resp_nh4)*(rfr_p)	respiration of limnic phytoplankton
+ (p_cya_resp_nh4)*(rfr_p)	respiration of diazotroph cyanobacteria
+ (p_zoo_resp_nh4)*(rfr_p)	respiration of zooplankton
+ (p_det_resp_nh4)*(rfr_p)	recycling of detritus using oxygen (respiration)
+ (p_det_denit_nh4)*(rfr_p)	recycling of detritus using nitrate (denitrification)
+ (p_det_sulf_nh4)*(rfr_p)	recycling of detritus using sulfate (sulfate reduction)
+ (p_sed_resp_nh4)*(rfr_p) /(cgt_cellheight*cgt_density)	recycling of sedimentary detritus to ammonium using oxygen (respiration)
+ (p_sed_denit_nh4)*(rfr_p) /(cgt_cellheight*cgt_density)	recycling of sedimentary detritus to ammonium using nitrate (denitrification)
+ (p_sed_sulf_nh4)*(rfr_p) /(cgt_cellheight*cgt_density)	recycling of sedimentary detritus to ammonium using sulfate (sulfate reduction)
+ p_ips_liber_po4/(cgt_cellheight*cgt_density)	liberation of phosphate from the sediment under anoxic conditions
+ p_sed_pocp_resp/(cgt_cellheight*cgt_density)	recycling of sedimentary pocp to dic and PO4 using oxygen (respiration)

continued on next page...

+	recycling of sedimentary pocp to dic and PO4 using $p_sed_pocp_denit / (cgt_cellheight * nitrate)$ (denitrification) $cgt_density$)
+	recycling of sedimentary pocp to dic and PO4 using $p_sed_pocp_sulf / (cgt_cellheight * sulfate)$ (sulfate reduction) $cgt_density$)
+ p_dop_resp	respiration of DOP
+ p_dop_denit	recycling of DOP using nitrate (denitrification)
+ p_dop_sulf	Mineralization of DOP, e-acceptor sulfate (sulfate reduction)
- $(p_no3_assim_lpp) * (rfr_p)$	assimilation of nitrate by large-cell phytoplankton
- $(p_nh4_assim_lpp) * (rfr_p)$	assimilation of ammonium by large-cell phytoplankton
- $(p_no3_assim_spp) * (rfr_p)$	assimilation of nitrate by small-cell phytoplankton
- $(p_nh4_assim_spp) * (rfr_p)$	assimilation of ammonium by small-cell phytoplankton
- $(p_nh4_assim_lip) * (rfr_p)$	assimilation of ammonium by limnic phytoplankton
- $(p_no3_assim_lip) * (rfr_p)$	assimilation of nitrate by limnic phytoplankton
- $(p_n2_assim_cya) * (rfr_p)$	fixation of dinitrogen by diazotroph cyanobacteria
- $p_assim_lpp_dop$	Production of DOP by LPP

continued on next page...

- p_assim_spp_dop	Production of DOP by SPP
- p_assim_lip_dop	Production of DOP by LIP
- (p_po4_retent_ips)*(rfr_p) /(cgt_cellheight*cgt_density)	retention of phosphate in the sediment under oxic conditions

Change of: small-cell phytoplankton

$$\frac{d}{dt} \mathbf{t}_{\text{spp}} =$$

+ p_no3_assim_spp	assimilation of nitrate by small-cell phytoplankton
+ p_nh4_assim_spp	assimilation of ammonium by small-cell phytoplankton
- p_spp_graz_zoo	grazing of zooplankton eating small-cell phytoplankton
- p_spp_resp_nh4	respiration of small-cell phytoplankton
- p_spp_mort_det	mortality of small-scale phytoplankton

Change of: zooplankton

$$\frac{d}{dt} \mathbf{t}_{\text{zoo}} =$$

+ p_lpp_graz_zoo	grazing of zooplankton eating large-cell phytoplankton
+ p_spp_graz_zoo	grazing of zooplankton eating small-cell phytoplankton

continued on next page...

+ p_cya_graz_zoo	grazing of zooplankton eating diazotroph cyanobacteria
+ p_lip_graz_zoo	grazing of zooplankton eating limnic phytoplankton
- p_zoo_resp_nh4	respiration of zooplankton
- p_zoo_mort_det	mortality of zooplankton

Change of: hydrogen sulfide

 $\frac{d}{dt} t_{h2s} =$

+ (p_poc_sulf)*(0.5)	Mineralization of POC, e-acceptor sulfate (sulfate reduction)
+ (p_pocp_sulf)*(53)	Mineralization of POC, e-acceptor sulfate (sulfate reduction)
+ (p_pocn_sulf)*(3.3125)	Mineralization of POCN, e-acceptor sulfate (sulfate reduction)
+ (p_det_sulf_nh4)*(3.3125)	recycling of detritus using sulfate (sulfate reduction)
+ (p_sed_sulf_nh4)*(3.3125) /(cgt_cellheight*cgt_density)	recycling of sedimentary detritus to ammonium using sulfate (sulfate reduction)
+ (p_sed_poc_sulf)*(0.5) /(cgt_cellheight*cgt_density)	recycling of sedimentary poc to dic using sulfate (sulfate reduction)
+ (p_sed_pocn_sulf)*(3.3125) /(cgt_cellheight*cgt_density)	recycling of sedimentary pocn to dic and NH4 using sulfate (sulfate reduction)

continued on next page...

+ (p_sed_pocp_sulf)*(53) /(cgt_cellheight*cgt_density)	recycling of sedimentary pocp to dic and PO4 using sulfate (sulfate reduction)
+ (p_doc_sulf)*(0.5)	Mineralization of DOC, e-acceptor sulfate (sulfate reduction)
+ (p_dop_sulf)*(53)	Mineralization of DOP, e-acceptor sulfate (sulfate reduction)
+ (p_don_sulf)*(3.3125)	Mineralization of DON, e-acceptor sulfate (sulfate reduction)
- p_h2s_oxo2_sul	oxidation of hydrogen sulfide with oxygen
- p_h2s_oxno3_sul	oxidation of hydrogen sulfide with nitrate

Change of: sulfur

$$\frac{d}{dt} \mathbf{t_sul} =$$

+ p_h2s_oxo2_sul	oxidation of hydrogen sulfide with oxygen
+ p_h2s_oxno3_sul	oxidation of hydrogen sulfide with nitrate
- p_sul_oxo2_so4	oxidation of elemental sulfur with oxygen
- p_sul_oxno3_so4	oxidation of elemental sulfur with nitrate

Change of: total alkalinity

$$\frac{d}{dt} \mathbf{t_alk} =$$

+ (1)*(p_pocn_resp)*(0.5)	respiration of POCN (produces ohminus)
---------------------------	--

continued on next page...

+ (1)*(p_pocn_denit)*(0.5)	recycling of POCN using nitrate (denitrification) (produces ohminus)
+ (1)*(p_pocn_sulf)*(0.5)	Mineralization of POCN, e-acceptor sulfate (sulfate reduction) (produces ohminus)
+ (1)*(p_sed_pocn_resp)*(0.5) /(cgt_cellheight*cgt_density)	recycling of sedimentary pocn to dic and NH4 using oxygen (respiration) (produces ohminus)
+ (1)*(p_sed_pocn_denit)*(0.5) /(cgt_cellheight*cgt_density)	recycling of sedimentary pocn to dic and NH4 using nitrate (denitrification) (produces ohminus)
+ (1)*(p_sed_pocn_sulf)*(0.5) /(cgt_cellheight*cgt_density)	recycling of sedimentary pocn to dic and NH4 using sulfate (sulfate reduction) (produces ohminus)
+ (1)*(p_don_resp)*(0.5)	respiration of DON (produces ohminus)
+ (1)*(p_don_denit)*(0.5)	recycling of DON using nitrate (denitrification) (produces ohminus)
+ (1)*(p_don_sulf)*(0.5)	Mineralization of DON, e-acceptor sulfate (sulfate reduction) (produces ohminus)
- (1)*(p_nh4_assim_lpp_don)	Production of DON by LPP (consumes ohminus)
- (1)*(p_nh4_assim_spp_don)	Production of DON by SPP (consumes ohminus)
- (1)*(p_nh4_assim_lip_don)	Production of DON by LIP (consumes ohminus)
- (1)*(p_pocp_denit)*(3)	recycling of POC using nitrate (denitrification) (consumes ohminus)

continued on next page...

- (1)*(p_pocp_sulf)*(3)	Mineralization of POC, e-acceptor sulfate (sulfate reduction) (consumes ohminus)
- (1)*(p_sed_pocp_denit)*(3) /(cgt_cellheight*cgt_density)	recycling of sedimentary pocp to dic and PO4 using nitrate (denitrification) (consumes ohminus)
- (1)*(p_sed_pocp_sulf)*(3) /(cgt_cellheight*cgt_density)	recycling of sedimentary pocp to dic and PO4 using sulfate (sulfate reduction) (consumes ohminus)
- (1)*(p_dop_denit)*(3)	recycling of DOP using nitrate (denitrification) (consumes ohminus)
- (1)*(p_dop_sulf)*(3)	Mineralization of DOP, e-acceptor sulfate (sulfate reduction) (consumes ohminus)
+ (-1)*(p_nh4_assim_lpp)*(0.8125)	assimilation of ammonium by large-cell phytoplankton (produces h3oplus)
+ (-1)*(p_nh4_assim_spp)*(0.8125)	assimilation of ammonium by small-cell phytoplankton (produces h3oplus)
+ (-1)*(p_nh4_assim_lip)*(0.8125)	assimilation of ammonium by limnic phytoplankton (produces h3oplus)
+ (-1)*(p_pocp_resp)*(3)	respiration of POCP (produces h3oplus)
+ (-1)*(p_nh4_nit_no3)*(2)	nitrification (produces h3oplus)
+ (-1)*(p_nh4_nitdenit_n2) /(cgt_cellheight*cgt_density)	coupled nitrification and denitrification after mineralization of detritus in oxic sediments (produces h3oplus)

continued on next page...

+ (-1)*(p_sul_oxo2_so4)*(2)	oxidation of elemental sulfur with oxygen (produces h3oplus)
+ (-1)*(p_sul_oxno3_so4)*(0.8)	oxidation of elemental sulfur with nitrate (produces h3oplus)
+ (-1)*(p_sed_pocp_resp)*(3) /(cgt_cellheight*cgt_density)	recycling of sedimentary pocp to dic and PO4 using oxygen (respiration) (produces h3oplus)
+ (-1)*(p_nh4_nitdenit_pocn_n2) /(cgt_cellheight*cgt_density)	coupled nitrification and denitrification after mineralization of pocn-detritus in oxic sediments (produces h3oplus)
+ (-1)*(p_dop_resp)*(3)	respiration of DOP (produces h3oplus)
- (-1)*(p_no3_assim_lpp)*(1.1875)	assimilation of nitrate by large-cell phytoplankton (consumes h3oplus)
- (-1)*(p_no3_assim_spp)*(1.1875)	assimilation of nitrate by small-cell phytoplankton (consumes h3oplus)
- (-1)*(p_no3_assim_lip)*(1.1875)	assimilation of nitrate by limnic phytoplankton (consumes h3oplus)
- (-1)*(p_n2_assim_cya)*(0.1875)	fixation of dinitrogen by diazotroph cyanobacteria (consumes h3oplus)
- (-1)*(p_assim_lpp_dop)*(3)	Production of DOP by LPP (consumes h3oplus)
- (-1)*(p_assim_spp_dop)*(3)	Production of DOP by SPP (consumes h3oplus)
- (-1)*(p_assim_lip_dop)*(3)	Production of DOP by LIP (consumes h3oplus)

continued on next page...

- $(-1) \cdot (p_no3_assim_lpp_don)$	Production of DON by LPP (consumes h3oplus)
- $(-1) \cdot (p_no3_assim_spp_don)$	Production of DON by SPP (consumes h3oplus)
- $(-1) \cdot (p_no3_assim_lip_don)$	Production of DON by LIP (consumes h3oplus)
- $(-1) \cdot (p_poc_denit) \cdot (0.8)$	recycling of POC using nitrate (denitrification) (consumes h3oplus)
- $(-1) \cdot (p_poc_sulf)$	Mineralization of POC, e-acceptor sulfate (sulfate reduction) (consumes h3oplus)
- $(-1) \cdot (p_pocp_denit) \cdot (84.8)$	recycling of POC using nitrate (denitrification) (consumes h3oplus)
- $(-1) \cdot (p_pocp_sulf) \cdot (106)$	Mineralization of POC, e-acceptor sulfate (sulfate reduction) (consumes h3oplus)
- $(-1) \cdot (p_pocn_resp) \cdot (0.5)$	respiration of POCN (consumes h3oplus)
- $(-1) \cdot (p_pocn_denit) \cdot (5.8)$	recycling of POCN using nitrate (denitrification) (consumes h3oplus)
- $(-1) \cdot (p_pocn_sulf) \cdot (7.125)$	Mineralization of POCN, e-acceptor sulfate (sulfate reduction) (consumes h3oplus)
- $(-1) \cdot (p_lpp_resp_nh4) \cdot (0.8125)$	respiration of large-cell phytoplankton (consumes h3oplus)
- $(-1) \cdot (p_spp_resp_nh4) \cdot (0.8125)$	respiration of small-cell phytoplankton (consumes h3oplus)

continued on next page...

- $(-1) \cdot (p_{lip_resp_nh4}) \cdot (0.8125)$ respiration of limnic phytoplankton (consumes
h3oplus)
- $(-1) \cdot (p_{cya_resp_nh4}) \cdot (0.8125)$ respiration of diazotroph cyanobacteria (consumes
h3oplus)
- $(-1) \cdot (p_{zoo_resp_nh4}) \cdot (0.8125)$ respiration of zooplankton (consumes h3oplus)
- $(-1) \cdot (p_{det_resp_nh4}) \cdot (0.8125)$ recycling of detritus using oxygen (respiration)
(consumes h3oplus)
- $(-1) \cdot (p_{det_denit_nh4}) \cdot (6.1125)$ recycling of detritus using nitrate (denitrification)
(consumes h3oplus)
- $(-1) \cdot (p_{det_sulf_nh4}) \cdot (7.4375)$ recycling of detritus using sulfate (sulfate
reduction) (consumes h3oplus)
- $(-1) \cdot (p_{sed_resp_nh4}) \cdot (0.8125)$ recycling of sedimentary detritus to ammonium
 $/(cgt_cellheight \cdot cgt_density)$ using oxygen (respiration) (consumes h3oplus)
- $(-1) \cdot (p_{sed_denit_nh4}) \cdot (6.1125)/(cgt_cellheight \cdot cgt_density)$ recycling of sedimentary detritus to ammonium
using nitrate (denitrification) (consumes h3oplus)
- $(-1) \cdot (p_{sed_sulf_nh4}) \cdot (7.4375)$ recycling of sedimentary detritus to ammonium
 $/(cgt_cellheight \cdot cgt_density)$ using sulfate (sulfate reduction) (consumes h3oplus)
- $(-1) \cdot (p_{sed_poc_denit}) \cdot (0.8)$ recycling of sedimentary poc to dic using nitrate
 $/(cgt_cellheight \cdot cgt_density)$ (denitrification) (consumes h3oplus)

continued on next page...

- $(-1) \cdot (p_sed_poc_sulf)$ $/(cgt_cellheight \cdot cgt_density)$	recycling of sedimentary poc to dic using sulfate (sulfate reduction) (consumes h3oplus)
- $(-1) \cdot (p_h2s_oxno3_sul) \cdot (0.4)$	oxidation of hydrogen sulfide with nitrate (consumes h3oplus)
- $(-1) \cdot (p_sed_pocn_resp) \cdot (0.5)$ $/(cgt_cellheight \cdot cgt_density)$	recycling of sedimentary pocn to dic and NH4 using oxygen (respiration) (consumes h3oplus)
- $(-1) \cdot (p_sed_pocn_denit) \cdot (5.8)$ $/(cgt_cellheight \cdot cgt_density)$	recycling of sedimentary pocn to dic and NH4 using nitrate (denitrification) (consumes h3oplus)
- $(-1) \cdot (p_sed_pocp_denit) \cdot (84.8)$ $/(cgt_cellheight \cdot cgt_density)$	recycling of sedimentary pocp to dic and PO4 using nitrate (denitrification) (consumes h3oplus)
- $(-1) \cdot (p_sed_pocn_sulf) \cdot (7.125)$ $/(cgt_cellheight \cdot cgt_density)$	recycling of sedimentary pocn to dic and NH4 using sulfate (sulfate reduction) (consumes h3oplus)
- $(-1) \cdot (p_sed_pocp_sulf) \cdot (106)$ $/(cgt_cellheight \cdot cgt_density)$	recycling of sedimentary pocp to dic and PO4 using sulfate (sulfate reduction) (consumes h3oplus)
- $(-1) \cdot (p_doc_denit) \cdot (0.8)$	recycling of DOC using nitrate (denitrification) (consumes h3oplus)
- $(-1) \cdot (p_doc_sulf)$	Mineralization of DOC, e-acceptor sulfate (sulfate reduction) (consumes h3oplus)
- $(-1) \cdot (p_dop_denit) \cdot (84.8)$	recycling of DOP using nitrate (denitrification) (consumes h3oplus)
- $(-1) \cdot (p_dop_sulf) \cdot (106)$	Mineralization of DOP, e-acceptor sulfate (sulfate reduction) (consumes h3oplus)

continued on next page...

- (-1)*(p_don_resp)*(0.5)	respiration of DON (consumes h3oplus)
- (-1)*(p_don_denit)*(5.8)	recycling of DON using nitrate (denitrification) (consumes h3oplus)
- (-1)*(p_don_sulf)*(7.125)	Mineralization of DON, e-acceptor sulfate (sulfate reduction) (consumes h3oplus)
+ (2)*(p_pocp_resp)	respiration of POCP (produces t_po4)
+ (2)*(p_pocp_denit)	recycling of POC using nitrate (denitrification) (produces t_po4)
+ (2)*(p_pocp_sulf)	Mineralization of POC, e-acceptor sulfate (sulfate reduction) (produces t_po4)
+ (2)*(p_lpp_resp_nh4)*(rfr_p)	respiration of large-cell phytoplankton (produces t_po4)
+ (2)*(p_spp_resp_nh4)*(rfr_p)	respiration of small-cell phytoplankton (produces t_po4)
+ (2)*(p_lip_resp_nh4)*(rfr_p)	respiration of limnic phytoplankton (produces t_po4)
+ (2)*(p_cya_resp_nh4)*(rfr_p)	respiration of diazotroph cyanobacteria (produces t_po4)
+ (2)*(p_zoo_resp_nh4)*(rfr_p)	respiration of zooplankton (produces t_po4)

continued on next page...

+ (2)*(p_det_resp_nh4)*(rfr_p)	recycling of detritus using oxygen (respiration) (produces t_po4)
+ (2)*(p_det_denit_nh4)*(rfr_p)	recycling of detritus using nitrate (denitrification) (produces t_po4)
+ (2)*(p_det_sulf_nh4)*(rfr_p)	recycling of detritus using sulfate (sulfate reduction) (produces t_po4)
+ (2)*(p_sed_resp_nh4)*(rfr_p) /(cgt_cellheight*cgt_density)	recycling of sedimentary detritus to ammonium using oxygen (respiration) (produces t_po4)
+ (2)*(p_sed_denit_nh4)*(rfr_p) /(cgt_cellheight*cgt_density)	recycling of sedimentary detritus to ammonium using nitrate (denitrification) (produces t_po4)
+ (2)*(p_sed_sulf_nh4)*(rfr_p) /(cgt_cellheight*cgt_density)	recycling of sedimentary detritus to ammonium using sulfate (sulfate reduction) (produces t_po4)
+ (2)*(p_ips_liber_po4) /(cgt_cellheight*cgt_density)	liberation of phosphate from the sediment under anoxic conditions (produces t_po4)
+ (2)*(p_sed_pocp_resp) /(cgt_cellheight*cgt_density)	recycling of sedimentary pocp to dic and PO4 using oxygen (respiration) (produces t_po4)
+ (2)*(p_sed_pocp_denit) /(cgt_cellheight*cgt_density)	recycling of sedimentary pocp to dic and PO4 using nitrate (denitrification) (produces t_po4)
+ (2)*(p_sed_pocp_sulf) /(cgt_cellheight*cgt_density)	recycling of sedimentary pocp to dic and PO4 using sulfate (sulfate reduction) (produces t_po4)
+ (2)*(p_dop_resp)	respiration of DOP (produces t_po4)

continued on next page...

+ (2)*(p_dop_denit)	recycling of DOP using nitrate (denitrification) (produces t_po4)
+ (2)*(p_dop_sulf)	Mineralization of DOP, e-acceptor sulfate (sulfate reduction) (produces t_po4)
- (2)*(p_no3_assim_lpp)*(rfr_p)	assimilation of nitrate by large-cell phytoplankton (consumes t_po4)
- (2)*(p_nh4_assim_lpp)*(rfr_p)	assimilation of ammonium by large-cell phytoplankton (consumes t_po4)
- (2)*(p_no3_assim_spp)*(rfr_p)	assimilation of nitrate by small-cell phytoplankton (consumes t_po4)
- (2)*(p_nh4_assim_spp)*(rfr_p)	assimilation of ammonium by small-cell phytoplankton (consumes t_po4)
- (2)*(p_nh4_assim_lip)*(rfr_p)	assimilation of ammonium by limnic phytoplankton (consumes t_po4)
- (2)*(p_no3_assim_lip)*(rfr_p)	assimilation of nitrate by limnic phytoplankton (consumes t_po4)
- (2)*(p_n2_assim_cya)*(rfr_p)	fixation of dinitrogen by diazotroph cyanobacteria (consumes t_po4)
- (2)*(p_assim_lpp_dop)	Production of DOP by LPP (consumes t_po4)
- (2)*(p_assim_spp_dop)	Production of DOP by SPP (consumes t_po4)
- (2)*(p_assim_lip_dop)	Production of DOP by LIP (consumes t_po4)

continued on next page...

- $(2) * (p_po4_retent_ips) * (rfr_p)$ retention of phosphate in the sediment under oxic
/ $(cgt_cellheight * cgt_density)$ conditions (consumes t_po4)

Change of: sediment detritus

$$\frac{d}{dt} t_sed =$$

- + $p_det_sedi_sed$ detritus sedimentation
- $p_sed_resp_nh4$ recycling of sedimentary detritus to ammonium
using oxygen (respiration)
- $p_sed_denit_nh4$ recycling of sedimentary detritus to ammonium
using nitrate (denitrification)
- $p_sed_sulf_nh4$ recycling of sedimentary detritus to ammonium
using sulfate (sulfate reduction)
- $p_sed_ero_det$ sedimentary detritus erosion
- $p_sed_biores_det$ bio resuspension of sedimentary detritus
- p_sed_burial burial of detritus deeper than max_sed

Change of: iron phosphate in sediment

$$\frac{d}{dt} t_ips =$$

- + $(p_po4_retent_ips) * (rfr_p)$ retention of phosphate in the sediment under oxic
conditions
- + $p_ipw_sedi_ips$ sedimentation of iron PO4

continued on next page...

- p_ips_liber_po4	liberation of phosphate from the sediment under anoxic conditions
- p_ips_ero_ipw	erosion of iron PO4
- p_ips_biores_ipw	bio resuspension of iron PO4
- p_ips_burial	burial of iron PO4

Change of: limnic phytoplankton

$$\frac{d}{dt} t_{lip} =$$

+ p_nh4_assim_lip	assimilation of ammonium by limnic phytoplankton
+ p_no3_assim_lip	assimilation of nitrate by limnic phytoplankton
- p_lip_graz_zoo	grazing of zooplankton eating limnic phytoplankton
- p_lip_resp_nh4	respiration of limnic phytoplankton
- p_lip_mort_det	mortality of limnic phytoplankton

Change of: dissolved organic carbon

$$\frac{d}{dt} t_{doc} =$$

+ p_assim_lpp_doc	Production of DOC by LPP
+ p_assim_spp_doc	Production of DOC by SPP
+ p_assim_lip_doc	Production of DOC by LPP
+ p_assim_cya_doc	Production of DOC by CYA

continued on next page...

- p_doc2pco	particle formation from DOC
- p_doc_resp	respiration of DOC
- p_doc_denit	recycling of DOC using nitrate (denitrification)
- p_doc_sulf	Mineralization of DOC, e-acceptor sulfate (sulfate reduction)

Change of: phosphorus in dissolved organic carbon in Redfield ratio

$\frac{d}{dt} \text{ t_dop} =$	
+ p_assim_lpp_dop	Production of DOP by LPP
+ p_assim_spp_dop	Production of DOP by SPP
+ p_assim_lip_dop	Production of DOP by LIP
- p_dop2pocp	particle formation from DOP
- p_dop_resp	respiration of DOP
- p_dop_denit	recycling of DOP using nitrate (denitrification)
- p_dop_sulf	Mineralization of DOP, e-acceptor sulfate (sulfate reduction)

Change of: nitrogen in dissolved organic carbon in Redfield ratio

$\frac{d}{dt} \text{ t_don} =$	
+ p_nh4_assim_lpp_don	Production of DON by LPP

continued on next page...

+ p_no3_assim_lpp_don	Production of DON by LPP
+ p_nh4_assim_spp_don	Production of DON by SPP
+ p_no3_assim_spp_don	Production of DON by SPP
+ p_nh4_assim_lip_don	Production of DON by LIP
+ p_no3_assim_lip_don	Production of DON by LIP
+ (p_lpp_resp_nh4)* (don_fraction)	respiration of large-cell phytoplankton
+ (p_spp_resp_nh4)* (don_fraction)	respiration of small-cell phytoplankton
+ (p_lip_resp_nh4)* (don_fraction)	respiration of limnic phytoplankton
+ (p_cya_resp_nh4)* (don_fraction)	respiration of diazotroph cyanobacteria
+ (p_zoo_resp_nh4)* (don_fraction)	respiration of zooplankton
- p_don2pocn	particle formation from DON
- p_don_resp	respiration of DON
- p_don_denit	recycling of DON using nitrate (denitrification)

continued on next page...

- p_don_sulf Mineralization of DON, e-acceptor sulfate (sulfate reduction)

Change of: sediment particular carbon

$$\frac{d}{dt} t_{sed_poc} =$$

- + p_poc_sedi_sed poc sedimentation
- p_sed_poc_resp recycling of sedimentary poc to dic using oxygen (respiration)
- p_sed_poc_denit recycling of sedimentary poc to dic using nitrate (denitrification)
- p_sed_poc_sulf recycling of sedimentary poc to dic using sulfate (sulfate reduction)
- p_sed_ero_poc sedimentary poc erosion
- p_sed_biores_poc bio resuspension of sedimentary poc
- p_poc_burial burial of poc deeper than max_sed

Change of: sediment particular organic N+C

$$\frac{d}{dt} t_{sed_pocn} =$$

- + p_pocn_sedi_sed pocn sedimentation
- p_sed_ero_pocn sedimentary pocn erosion
- p_sed_biores_pocn bio resuspension of sedimentary pocn

continued on next page...

- | | |
|--------------------|--|
| - p_pocn_burial | burial of pocn deeper than max_sed |
| - p_sed_pocn_resp | recycling of sedimentary pocn to dic and NH4 using oxygen (respiration) |
| - p_sed_pocn_denit | recycling of sedimentary pocn to dic and NH4 using nitrate (denitrification) |

Change of: sediment particular organic P+C

$$\frac{d}{dt} t_{\text{sed_pocp}} =$$

- | | |
|---------------------|--|
| + p_pocp_sedi_sed | pocp sedimentation |
| - p_sed_ero_pocp | sedimentary pocp erosion |
| - p_sed_biores_pocp | bio resuspension of sedimentary pocp |
| - p_pocp_burial | burial of pocp deeper than max_sed |
| - p_sed_pocp_resp | recycling of sedimentary pocp to dic and PO4 using oxygen (respiration) |
| - p_sed_pocp_denit | recycling of sedimentary pocp to dic and PO4 using nitrate (denitrification) |

Change of: colored dissolved organic carbon

$$\frac{d}{dt} t_{\text{cdom}} =$$

- | | |
|----------------|----------------------------|
| - p_cdom_decay | decay of cdom due to light |
|----------------|----------------------------|

Change of: large-cell phytoplankton

continued on next page...

$$\begin{aligned} \frac{d}{dt} \mathbf{t_lpp} = & \\ & + \mathbf{p_no3_assim_lpp} \quad \text{assimilation of nitrate by large-cell phytoplankton} \\ & + \mathbf{p_nh4_assim_lpp} \quad \text{assimilation of ammonium by large-cell} \\ & \quad \text{phytoplankton} \\ & - \mathbf{p_lpp_graz_zoo} \quad \text{grazing of zooplankton eating large-cell} \\ & \quad \text{phytoplankton} \\ & - \mathbf{p_lpp_resp_nh4} \quad \text{respiration of large-cell phytoplankton} \\ & - \mathbf{p_lpp_mort_det} \quad \text{mortality of large-cell phytoplankton} \end{aligned}$$

Change of: suspended iron phosphate

$$\begin{aligned} \frac{d}{dt} \mathbf{t_ipw} = & \\ & + \mathbf{p_ips_ero_ipw/(cgt_cellheight*erosion\ of\ iron\ PO4} \\ & \quad \mathbf{cgt_density)} \\ & + \quad \text{bio resuspension of iron PO4} \\ & \mathbf{p_ips_biores_ipw/(cgt_cellheight*} \\ & \quad \mathbf{cgt_density)} \\ & - \quad \text{sedimentation of iron PO4} \\ & \mathbf{p_ipw_sedi_ips/(cgt_cellheight*} \\ & \quad \mathbf{cgt_density)} \end{aligned}$$

Change of: diazotroph cyanobacteria

$$\begin{aligned} \frac{d}{dt} \mathbf{t_cya} = & \\ & + \mathbf{p_n2_assim_cya} \quad \text{fixation of dinitrogen by diazotroph cyanobacteria} \end{aligned}$$

continued on next page...

- p_cya_graz_zoo	grazing of zooplankton eating diazotroph cyanobacteria
- p_cya_resp_nh4	respiration of diazotroph cyanobacteria
- p_cya_mort_det	mortality of diazotroph cyanobacteria
- p_cya_mort_det_diff	mortality of diazotroph cyanobacteria due to strong turbulence

Change of: detritus

$$\frac{d}{dt} t_{det} =$$

+ p_lpp_mort_det	mortality of large-cell phytoplankton
+ p_spp_mort_det	mortality of small-scale phytoplankton
+ p_lip_mort_det	mortality of limnic phytoplankton
+ p_cya_mort_det	mortality of diazotroph cyanobacteria
+ p_cya_mort_det_diff	mortality of diazotroph cyanobacteria due to strong turbulence
+ p_zoo_mort_det	mortality of zooplankton
+ p_sed_ero_det/(cgt_cellheight* sedimentary detritus erosion cgt_density)	
+ p_sed_biores_det/(cgt_cellheight* cgt_density)	bio resuspension of sedimentary detritus

continued on next page...

- p_det_resp_nh4	recycling of detritus using oxygen (respiration)
- p_det_denit_nh4	recycling of detritus using nitrate (denitrification)
- p_det_sulf_nh4	recycling of detritus using sulfate (sulfate reduction)
-	detritus sedimentation
p_det_sedi_sed/(cgt_cellheight* cgt_density)	

Change of: particulate organic carbon

$$\frac{d}{dt} t_{poc} =$$

+ p_sed_ero_poc/(cgt_cellheight* cgt_density)	sedimentary poc erosion
+ p_sed_biores_poc/(cgt_cellheight* cgt_density)	bio resuspension of sedimentary poc
+ p_doc2pco	particle formation from DOC
- p_poc_resp	respiration of POC
- p_poc_denit	recycling of POC using nitrate (denitrification)
- p_poc_sulf	Mineralization of POC, e-acceptor sulfate (sulfate reduction)

continued on next page...

- poc sedimentation
p_poc_sedi_sed/(cgt_cellheight*
cgt_density)

Change of: phosphorus in particulate organic carbon in Redfield ratio

$$\frac{d}{dt} t_{\text{pocp}} =$$
$$+ \text{sedimentary pocp erosion} \\ \text{p_sed_ero_pocp}/(\text{cgt_cellheight}* \\ \text{cgt_density})$$
$$+ \frac{\text{bio resuspension of sedimentary pocp}}{\text{p_sed_biores_pocp}/(\text{cgt_cellheight} \times \text{cgt_density})}$$

+ p_dop2pocp particle formation from DOP

- p_pocp_resp respiration of POCP

- p_pocp_denit recycling of POC using nitrate (denitrification)

- p_pocp_sulf	Mineralization of POC, e-acceptor sulfate (sulfate reduction)
---------------	---

- pocp sedimentation
p_pocp_sedi_sed/(cgt_cellheight*
cgt_density)

```
- recycling of sedimentary pocp to dic and PO4 using
p_sed_pocp_sulf/(cgt_cellheight* sulfate (sulfate reduction)
cgt_density)
```

continued on next page...

Change of: nitrogen in particulate organic carbon in Redfield ratio

$$\begin{aligned} \frac{d}{dt} t_{\text{pocn}} = & \\ & + \text{sedimentary pocn erosion} \\ & p_{\text{sed_ero_pocn}} / (cgt_cellheight * \\ & cgt_density) \\ & + \text{bio resuspension of sedimentary pocn} \\ & p_{\text{sed_biores_pocn}} / (cgt_cellheight \\ & cgt_density) \\ & + p_{\text{don2pocn}} \text{ particle formation from DON} \\ & - p_{\text{pocn_resp}} \text{ respiration of POCN} \\ & - p_{\text{pocn_denit}} \text{ recycling of POCN using nitrate (denitrification)} \\ & - p_{\text{pocn_sulf}} \text{ Mineralization of POCN, e-acceptor sulfate (sulfate} \\ & \text{reduction)} \\ & - \text{pocn sedimentation} \\ & p_{\text{pocn_sedi_sed}} / (cgt_cellheight * \\ & cgt_density) \\ & - \text{recycling of sedimentary pocn to dic and NH4 using} \\ & p_{\text{sed_pocn_sulf}} / (cgt_cellheight * \text{sulfate (sulfate reduction)} \\ & cgt_density) \end{aligned}$$

end of table **Tracer equations**

Author contributions. TN, HR, BC, and MS developed and implemented the model. TN performed the model simulations. All authors contributed to writing the manuscript.

560 *Competing interests.* The authors declare that they have no conflict of interest.

Acknowledgements. Computational power was provided by the North-German Supercomputing Alliance (HLRN). Financial support by the BONUS INTEGRAL 363 project (Grant No. 03F0773A) is gratefully acknowledged. We wish to thank Bernd Schneider, and Henry Bitting for many advises and discussion. *Gregor Rehder very much helped improving the manuscript with many suggestions and careful revision.*

- Bakker, D. C. E., Pfeil, B., Landa, C. S., Metzl, N., O'Brien, K. M., Olsen, A., Smith, K., Cosca, C., Harasawa, S., Jones, S. D., Nakaoka, S., Nojiri, Y., Schuster, U., Steinhoff, T., Sweeney, C., Takahashi, T., Tilbrook, B., Wada, C., Wanninkhof, R., Alin, S. R., Balestrini, C. F., Barbero, L., Bates, N. R., Bianchi, A. A., Bonou, F., Boutin, J., Bozec, Y., Burger, E. F., Cai, W.-J., Castle, R. D., Chen, L., Chierici, M., Currie, K., Evans, W., Featherstone, C., Feely, R. A., Fransson, A., Goyet, C., Greenwood, N., Gregor, L., Hankin, S., Hardman-Mountford, N. J., Harlay, J., Hauck, J., Hoppema, M., Humphreys, M. P., Hunt, C. W., Huss, B., Ibáñez, J. S. P., Johannessen, T., Keeling, R., Kitidis, V., Körtzinger, A., Kozyr, A., Krasakopoulou, E., Kuwata, A., Landschützer, P., Lauvset, S. K., Lefèvre, N., Lo Monaco, C., Manke, A., Mathis, J. T., Merlivat, L., Millero, F. J., Monteiro, P. M. S., Munro, D. R., Murata, A., Newberger, T., Omar, A. M., Ono, T., Paterson, K., Pearce, D., Pierrot, D., Robbins, L. L., Saito, S., Salisbury, J., Schlitzer, R., Schneider, B., Schweitzer, R., Sieger, R., Skjelvan, I., Sullivan, K. F., Sutherland, S. C., Sutton, A. J., Tadokoro, K., Telszewski, M., Tuma, M., van Heuven, S. M. A. C., Vandemark, D., Ward, B., Watson, A. J., and Xu, S.: A multi-decade record of high-quality $f\text{CO}_2$ data in version 3 of the Surface Ocean CO_2 Atlas (SOCAT), *Earth System Science Data*, 8, 383–413, <https://doi.org/10.5194/essd-8-383-2016>, 2016.
- Carlson, C. A. and Hansell, D. A.: Chapter 3 - DOM Sources, Sinks, Reactivity, and Budgets, in: *Biogeochemistry of Marine Dissolved Organic Matter*, edited by Carlson, D. A. and Hansell, C. A., pp. 65 – 126, Academic Press, Boston, Second edn., <https://doi.org/10.1016/B978-0-12-405940-5.00003-0>, 2015.
- Carlson, C. A., Ducklow, H. W., Hansell, D. A., and Smith Jr., W. O.: Organic carbon partitioning during spring phytoplankton blooms in the Ross Sea polynya and the Sargasso Sea, *Limnology and Oceanography*, 43, 375–386, <https://doi.org/10.4319/lo.1998.43.3.0375>, 1998.
- Chien, C.-T., Pahlow, M., Schartau, M., and Oschlies, A.: Optimality-based non-Redfield plankton–ecosystem model (OPEM v1.1) in UVic-ESCM 2.9 – Part 2: Sensitivity analysis and model calibration, *Geoscientific Model Development*, 13, 4691–4712, <https://doi.org/10.5194/gmd-13-4691-2020>, 2020.
- Droop, M. R.: SOME THOUGHTS ON NUTRIENT LIMITATION IN ALGAE1, *Journal of Phycology*, 9, 264–272, <https://doi.org/https://doi.org/10.1111/j.1529-8817.1973.tb04092.x>, 1973.
- Eggert, A. and Schneider, B.: A nitrogen source in spring in the surface mixed-layer of the Baltic Sea: Evidence from total nitrogen and total phosphorus data, *Journal of Marine Systems*, 148, 39–47, <https://doi.org/doi.org/10.1016/j.jmarsys.2015.01.005>, 2015.
- Engel, A.: Direct relationship between CO_2 uptake and transparent exopolymer particles production in natural phytoplankton, *Journal of Plankton Research*, 24, 49–53, <https://doi.org/10.1093/plankt/24.1.49>, 2002.
- Engel, A., Thoms, S., Riebesell, U., Rochelle-Newall, E., and Zondervan, I.: Polysaccharide aggregation as a potential sink of marine dissolved organic carbon, *Nature*, 428, 929–932, <https://doi.org/10.1038/nature02453>, 2004.
- Eppley, R. W.: Temperature and phytoplankton growth, *Fish. Bull.*, 70, 1063–1085, 1972.
- Fransner, F., Gustafsson, E., Tedesco, L., Vichi, M., Hordoir, R., Roquet, F., Spilling, K., Kuznetsov, I., Eilola, K., Mörtz, C.-M., Humborg, C., and Nycander, J.: Non-Redfieldian Dynamics Explain Seasonal pCO_2 Drawdown in the Gulf of Bothnia, *Journal of Geophysical Research: Oceans*, 123, 166–188, <https://doi.org/10.1002/2017JC013019>, 2018.

- Geyer, B. and Rockel, B.: coastDat-2 COSMO-CLM Atmospheric Reconstruction [data set], https://doi.org/10.1594/WDCC/coastDat-2_COSMO-CLM, 2013.
- Griffies, S. M.: Fundamentals of Ocean Climate Models, Princeton University Press, Princeton, NJ, 2004.
- Gustafsson, E., Deutsch, B., Gustafsson, B., Humborg, C., and Mörrth, C.-M.: Carbon cycling in the Baltic Sea ? The
605 fate of allochthonous organic carbon and its impact on air-sea CO₂ exchange, *Journal of Marine Systems*, 129, 289–302, <https://doi.org/10.1016/j.jmarsys.2013.07.005>, 2014a.
- Gustafsson, E., Wällstedt, T., Humborg, C., Mörrth, C.-M., and Gustafsson, B. G.: External total alkalinity loads versus internal generation: The influence of nonriverine alkalinity sources in the Baltic Sea, *Global Biogeochemical Cycles*, 28, 1358–1370, <https://doi.org/10.1002/2014GB004888>, 2014b.
- 610 Gustafsson, E., Savchuk, O. P., Gustafsson, B. G., and Müller-Karulis, B.: Key processes in the coupled carbon, nitrogen, and phosphorus cycling of the Baltic Sea, *Biogeochemistry*, 134, 301–317, <https://doi.org/10.1007/s10533-017-0361-6>, 2017.
- Gustafsson, E., Hagens, M., Sun, X., Reed, D. C., Humborg, C., Slomp, C. P., and Gustafsson, B. G.: Sedimentary alkalinity generation and long-term alkalinity development in the Baltic Sea, *Biogeosciences*, 16, 437–456, <https://doi.org/10.5194/bg-16-437-2019>, 2019.
- 615 Hansell, D. A., Carlson, C. A., Repeta, D. J., and Schlitzer, R.: Dissolved Organic Matter in the Ocean: A Controversy Stimulates New Insights, *Oceanography*, 22, 202–211, <https://doi.org/10.5670/oceanog.2009.109>, 2009.
- HELCOM: Sources and pathways of nutrients to the Baltic Sea., *Balt. Sea Environ. Proc. No. 153*, 2018.
- Hjalmarsson, S., Wesslander, K., Anderson, L. G., Omstedt, A., Perttilä, M., and Mintrop, L.: Distribution, long-term development and mass balance calculation of total alkalinity in the Baltic Sea, *Continental Shelf Research*, 28, 593–601,
620 <https://doi.org/10.1016/j.csr.2007.11.010>, 2008.
- Ho, T.-Y., Quigg, A., Finkel, Z. V., Milligan, A. J., Wyman, K., Falkowski, P. G., and Morel, F. M. M.: The Elemental Composition of Some Marine Phytoplankton, *Journal of Phycology*, 39, 1145–1159, <https://doi.org/10.1111/j.0022-3646.2003.03-090.x>, 2003.
- Hoikkala, L., Kortelainen, P., Soinne, H., and Kuosa, H.: Dissolved organic matter in the Baltic Sea, *Journal of Marine
625 Systems*, 142, 47–61, <https://doi.org/10.1016/j.jmarsys.2014.10.005>, 2015.
- Kreus, M., Schartau, M., Engel, A., Nausch, M., and Voss, M.: Variations in the elemental ratio of organic matter in the central Baltic Sea: Part I? Linking primary production to remineralization, *Continental Shelf Research*, 100, 25–45, <https://doi.org/10.1016/j.csr.2014.06.015>, 2015.
- Kriest, I., Oschlies, A., and Khatiwala, S.: Sensitivity analysis of simple global marine biogeochemical models, *Global Biogeochemical Cycles*, 26, <https://doi.org/10.1029/2011GB004072>, 2012.
- 630 Kuznetsov, I., Neumann, T., and Burchard, H.: Model study on the ecosystem impact of a variable C:N:P ratio for cyanobacteria in the Baltic Proper, *Ecological Modelling*, 219, 107–114, <https://doi.org/10.1016/j.ecolmodel.2008.08.002>, 2008.
- Kuznetsov, I., Neumann, T., Schneider, B., and Yakushev, E.: Processes regulating pCO₂ in the surface waters of the central eastern Gotland Sea: a model study, *OCEANOLOGIA*, 53, 745–770, <https://doi.org/10.5697/oc.53-3.745>, 2011.
- 635 Larsson, U., Hajdu, S., Walve, J., and Elmgren, R.: Baltic Sea nitrogen fixation estimated from the summer increase in upper mixed layer total nitrogen, *Limnology and Oceanography*, 46, 811–820, <https://doi.org/10.4319/lo.2001.46.4.0811>, 2001.
- Leibniz Institute for Baltic Sea Research: ERGOM: Ecological Regional Ocean Model, <https://ergom.net/>, last access: 10 March 2022, 2015.

- Leipe, T., Tauber, F., Vallius, H., Virtasalo, J., Uścińowicz, S., Kowalski, N., Hille, S., Lindgren, S., and Myllyvirta, T.: Particulate organic carbon (POC) in surface sediments of the Baltic Sea, *Geo-Marine Letters*, 31, 175–188, <https://doi.org/10.1007/s00367-010-0223-x>, 2010.
- Lips, I. and Lips, U.: The Importance of *Mesodinium rubrum* at Post-Spring Bloom Nutrient and Phytoplankton Dynamics in the Vertically Stratified Baltic Sea, *Frontiers in Marine Science*, 4, <https://doi.org/10.3389/fmars.2017.00407>, 2017.
- Macias, D., Huertas, I. E., Garcia-Gorriz, E., and Stips, A.: Non-Redfieldian dynamics driven by phytoplankton phosphate frugality explain nutrient and chlorophyll patterns in model simulations for the Mediterranean Sea, *Progress in Oceanography*, 173, 37–50, <https://doi.org/10.1016/j.pocean.2019.02.005>, 2019.
- Martin, J. H., Knauer, G. A., Karl, D. M., and Broenkow, W. W.: VERTEX: carbon cycling in the northeast Pacific, *Deep Sea Research Part A. Oceanographic Research Papers*, 34, 267–285, [https://doi.org/10.1016/0198-0149\(87\)90086-0](https://doi.org/10.1016/0198-0149(87)90086-0), 1987.
- Martiny, A. C., Talarmin, A., Mouginit, C., Lee, J. A., Huang, J. S., Gellene, A. G., and Caron, D. A.: Biogeochemical interactions control a temporal succession in the elemental composition of marine communities, *Limnology and Oceanography*, 61, 531–542, <https://doi.org/10.1002/lno.10233>, 2016.
- Monod, J.: The growth of bacterial cultures, *Ann. Rev. Microbiol.*, 3, 371–394, 1949.
- Müller, J. D., Schneider, B., and Rehder, G.: Long-term alkalinity trends in the Baltic Sea and their implications for CO₂-induced acidification, *Limnology and Oceanography*, 61, 1984–2002, <https://doi.org/doi.org/10.1002/lno.10349>, 2016.
- Nausch, M., Nausch, G., Lass, H. U., Mohrholz, V., Nagel, K., Siegel, H., and Wasmund, N.: Phosphorus input by upwelling in the eastern Gotland Basin (Baltic Sea) in summer and its effects on filamentous cyanobacteria, *Estuarine, Coastal and Shelf Science*, 83, 434–442, <https://doi.org/https://doi.org/10.1016/j.ecss.2009.04.031>, 2009.
- Neumann, T.: ERGOM 1.2 model hindcast 1948–2019 [data set], https://thredds-iow.io-warnemuende.de/thredds/catalogs/projects/integral/catalog_pocNP_V04R25_3nm_agg_time.html, last access: 10 March 2022, 2021.
- Neumann, T.: Model code and boundary data for "Non-Redfield carbon model for the Baltic Sea (ERGOM version 1.2) – Implementation and Budget estimates" paper [code], <https://doi.org/10.5281/zenodo.6560174>, last access: 19 May 2022, 2022.
- Neumann, T., Fennel, W., and Kremp, C.: Experimental simulations with an ecosystem model of the Baltic Sea: A nutrient load reduction experiment, *Global Biogeochemical Cycles*, 16, 7–17–19, <https://doi.org/10.1029/2001GB001450>, 2002.
- Neumann, T., Koponen, S., Attila, J., Brockmann, C., Kallio, K., Kervinen, M., Mazeran, C., Müller, D., Philipson, P., Thulin, S., Väkevä, S., and Ylöstalo, P.: Optical model for the Baltic Sea with an explicit CDOM state variable: a case study with Model ERGOM (version 1.2), *Geoscientific Model Development*, 14, 5049–5062, <https://doi.org/10.5194/gmd-14-5049-2021>, 2021.
- Omstedt, A., Gustafsson, E., and Wesslander, K.: Modelling the uptake and release of carbon dioxide in the Baltic Sea surface water, *Continental Shelf Research*, 29, 870–885, <https://doi.org/10.1016/j.csr.2009.01.006>, 2009.
- Omstedt, A., Humborg, C., Pempkowiak, J., Perttilä, M., Rutgersson, A., Schneider, B., and Smith, B.: Biogeochemical Control of the Coupled CO₂-O₂ System of the Baltic Sea: A Review of the Results of Baltic-C, *Ambio*, 43, 49–59, <https://doi.org/10.1007/s13280-013-0485-4>, 2014.
- Pahlow, M., Chien, C.-T., Arteaga, L. A., and Oschlies, A.: Optimality-based non-Redfield plankton–ecosystem model (OPEM v1.1) in UVic-ESCM 2.9 – Part 1: Implementation and model behaviour, *Geoscientific Model Development*, 13, 4663–4690, <https://doi.org/10.5194/gmd-13-4663-2020>, 2020.

- Pfeil, B., Olsen, A., Bakker, D. C. E., Hankin, S., Koyuk, H., Kozyr, A., Malczyk, J., Manke, A., Metzl, N., Sabine, C. L., Akl, J., Alin, S. R., Bates, N., Bellerby, R. G. J., Borges, A., Boutin, J., Brown, P. J., Cai, W.-J., Chavez, F. P., Chen, A., Cosca, C., Fassbender, A. J., Feely, R. A., González-Dávila, M., Goyet, C., Hales, B., Hardman-Mountford, N., Heinze, C., Hood, M., Hoppema, M., Hunt, C. W., Hydes, D., Ishii, M., Johannessen, T., Jones, S. D., Key, R. M., Körtzinger, A., Landschützer, P., Lauvset, S. K., Lefèvre, N., Lenton, A., Laurantou, A., Merlivat, L., Midorikawa, T., Mintrop, L., Miyazaki, C., Murata, A., Nakadate, A., Nakano, Y., Nakaoka, S., Nojiri, Y., Omar, A. M., Padin, X. A., Park, G.-H., Paterson, K., Perez, F. F., Pierrot, D., Poisson, A., Ríos, A. F., Santana-Casiano, J. M., Salisbury, J., Sarma, V. V. S. S., Schlitzer, R., Schneider, B., Schuster, U., Sieger, R., Skjelvan, I., Steinhoff, T., Suzuki, T., Takahashi, T., Tedesco, K., Telszewski, M., Thomas, H., Tilbrook, B., Tjiputra, J., Vandemark, D., Veness, T., Wanninkhof, R., Watson, A. J., Weiss, R., Wong, C. S., and Yoshikawa-Inoue, H.: A uniform, quality controlled Surface Ocean CO₂ Atlas (SOCAT), *Earth System Science Data*, 5, 125–143, <https://doi.org/10.5194/essd-5-125-2013>, 2013.
- Redfield, A. C., Ketchum, B. H., and Richards, B. H.: The influence of organisms on the composition of sea water, in: *The Sea*, edited by Hill, L., vol. 2, pp. 26 – 77, Interscience, New York, 1963.
- Rehder, G., Müller, J., Bittig, H., Kahru, M., Kaitala, S., Schneider, B., Siiriä, S.-M., Tuomi, L., and Wasmund, N.: Extreme productivity patterns during the spring bloom 2018 in the central Baltic Sea suggest vertical nutrient shuttling: Unforeseen surprises for the fight against eutrophication in a warming world?, in: *All abstracts for the ICOS Science Conference 2020*, ICOS Integrated Carbon Observation System, <https://www.icos-cp.eu/sc2020/abstracts#143>, 2020.
- Schneider, B. and Müller, J. D.: *Surface Water Biogeochemistry as Derived from pCO₂ Observations*, pp. 49–92, Springer International Publishing, Cham, https://doi.org/10.1007/978-3-319-61699-5_5, 2018.
- Schneider, B., Kaitala, S., Raateoja, M., and Sadkowiak, B.: A nitrogen fixation estimate for the Baltic Sea based on continuous pCO₂ measurements on a cargo ship and total nitrogen data, *Continental Shelf Research*, 29, 1535–1540, <https://doi.org/10.1016/j.csr.2009.04.001>, 2009.
- Seifert, T., Tauber, F., and Kayser, B.: Digital topography of the Baltic Sea [data set], <https://www.io-warnemuende.de/topography-of-the-baltic-sea.html>, last access: 27 July 2020, 2008.
- Sharoni, S. and Halevy, I.: Nutrient ratios in marine particulate organic matter are predicted by the population structure of well-adapted phytoplankton, *Science Advances*, 6, eaaw9371, <https://doi.org/10.1126/sciadv.aaw9371>, 2020.
- Steele, J. H.: *The structure of marine ecosystems*, Cambridge Havard University Press, 1974.
- Szymczycha, B., Maciejewska, A., Winogradow, A., and Pempkowiak, J.: Could submarine groundwater discharge be a significant carbon source to the southern Baltic Sea?, *Oceanologia*, 56, 327–347, <https://doi.org/10.5697/oc.56-2.327>, 2014.
- Wan, Z., Jonasson, L., and Bi, H.: N/P ratio of nutrient uptake in the Baltic Sea, *Ocean Science*, 7, 693–704, <https://doi.org/10.5194/os-7-693-2011>, 2011.
- Wetz, M. S. and Wheeler, P. A.: Release of dissolved organic matter by coastal diatoms, *Limnology and Oceanography*, 52, 798–807, <https://doi.org/10.4319/lo.2007.52.2.0798>, 2007.
- Winton, M.: A Reformulated Three-Layer Sea Ice Model, *Journal of Atmospheric and Oceanic Technology*, 17, 525–531, [https://doi.org/10.1175/1520-0426\(2000\)017<0525:ARTLSI>2.0.CO;2](https://doi.org/10.1175/1520-0426(2000)017<0525:ARTLSI>2.0.CO;2), 2000.

